The Dissertation Committee for Jing Dong Certifies that this is the approved version of the following dissertation:

MOLECULAR DISSECTION OF REACTIVE OXYGEN SPECIES-MEDIATED ONCOTIC CELL DEATH

Committee:

Terrence J. Monks, Supervisor

Shawn B. Bratton, Supervisor

Serrine S. Lau

John H. Richburg

Richard E. Wilcox

Richard R. Vaillancourt

MOLECULAR DISSECTION OF REACTIVE OXYGEN SPECIES-MEDIATED ONCOTIC CELL DEATH

by

Jing Dong, B.S.

Dissertation

Presented to the Faculty of the Graduate School of

The University of Texas at Austin

in Partial Fulfillment

of the Requirements

for the Degree of

Doctor of Philosophy

The University of Texas at Austin

December 2004

Dedication

To my parents Guangyao Dong and Aimei Liu,

and my husband, Rudan Ye.

Acknowledgements

I want to express my sincere appreciation to Dr. Terrence J. Monks, my mentor, who is one of the most important people in my life. He has been very kind, supportive, and inspiring to me during my doctoral training. In my graduate studies, there are laughs and sighs, successes and failures, enthusiasm and reluctances, but Dr. Monks is always there to encourage me to achieve more. I am also grateful for Dr. Serrine S. Lau, who has been very supportive and generous to help me in my research, and always to provoke me to think beyond the superficials. I want to thank her for her guidance, training, insights, and personal care. I sincerely thank Dr. Shawn B. Bratton, supervisor for my dissertation, who has provided me with a lot of brilliant ideas and critiques, helping me to solve problems, remain focused, and assure me good research stories to write. I would like to express my sincere appreciation to all my dissertation committee members, Dr. John H. Richburg, Dr. Richard R. Vaillancourt, and Dr. Richard E. Wilcox. They have been extremely kind to help me make fast progress, and provided me with many great ideas. Many thanks to Drs. Sampath Ramachandiran and Kulbushan Tikoo, who had helped me with various laboratory techniques and shared many great ideas with me. I also want to thank everybody I've worked with in the labarotory, the assistance from the department, the college, my collaborators, and those generously provided helps and support. I also appreciate the support from SOT and GRC to travel to the annual conferences. Finally, encouragement and support for my studies from my parents and husband are so precious that without which I would not have accomplishment a Ph.D.

MOLECULAR DISSECTION OF REACTIVE OXYGEN SPECIES-MEDIATED ONCOTIC CELL DEATH

Publication No._____

Jing Dong, Ph.D.

The University of Texas at Austin, 2004

Supervisors: Terrence J. Monks and Shawn B. Bratton

Reactive oxygen species (ROS) are associated with a variety of human diseases and toxicities mediated by redox-active chemicals and/or their metabolites. One such redox active chemical, hydroquinone (HQ), is both a nephrotoxicant and a nephrocarcinogen. Sequential oxidation of HQ and addition of glutathione (GSH) leads to the formation of 2,3,5-tris-(glutathion-S-yl)hydroquinone (TGHQ). TGHQ maintains HQ's ability to redox-cycle and generate ROS, and to covalently bind to cellular molecules. Thus, TGHQ induces ROS-dependent DNA damage and cell death in renal proximal tubule epithelial cells (LLC-PK1). It is not clear how ROS generated by redox-active chemicals induce renal cell death. The molecular mechanisms of quinone-mediated nephrotoxicity therefore invite further investigation. We used TGHQ to study ROS-mediated renal cell death, and have found that TGHQ induces oncotic rather than

apoptotic cell death in LLC-PK1 cells. MAPKs are quickly and robustly activated by TGHQ in a ROS-dependent manner. Pharmacological inhibition of either extracelluar signal regulated kinase (ERK) or p38 MAPK pathways attenuates TGHQ-induced cell death in LLC-PK1 cells. TGHQ also induces ROS-dependent histone H3 phosphorylation in LLC-PK1 cells, which leads to premature chromatin condensation (PCC) and mitotic catastrophe. Our studies show that TGHQ induces epidermal growth factor receptor (EGFR) phosphorylation at multiple tyrosine residues, leading to the EGFR-dependent activation of the ERK cascade. TGHQ also induces EGFR-independent activation of the p38 MAPK cascade. Both ERK and p38 MAPK inhibition attenuates TGHQ-induced histone H3 phosphorylation in LLC-PK1 cells, indicating both ERK and p38 MAPK are associated with ROS-mediated histone H3 phosphorylation. Additionally, proteomics analysis revealed changes in the overall expression and post-translational modification of several proteins in TGHQ-treated LLC-PK1 cells. The identified proteins can be grouped according to function, as follows; antioxidants and cytoskeleton stabilizing proteins (peroxiredoxin II, peroxiredoxin III, Hsp27), membrane fusion (annexin I), nuclear shuttling (nucleophosmin/B23), and calcium binding and chaperoning (calreticulin, Hsp27, peroxiredoxins). The changes are largely due to post-translational modifications, such as phosphorylation (Hsp27) and oxidation (peroxiredoxin). These modifications likely determine cell fate. Finally, we found that in Eker rats, TGHQ induces a time-dependent increase in ERK1/2 and histone H3 phosphorylation within the outer stripe of outer medulla (OSOM) in the kidneys, confirming our findings in LLC-PK1 cells. The high constitutive *in vivo* phosphorylation of p38 MAPK obscured any changes induced by TGHQ within the OSOM. These early molecular changes likely lead to nephrotoxicity followed by excessive proliferation and amplification of genomic instability in Eker rats, and contribute to subsequent nephrocarcinogenicity. This dissertation contributes to the

understanding of the molecular mechanisms of TGHQ/ROS-induced renal cell death/nephrotoxicity. I am also of the view that this work will contribute to the future development of therapeutic strategies designed to alleviate acute renal diseases associated with ROS generation.

Table of Contents

List of Tables

List of Figures

List of Abbreviations

ASK1	apoptosis signal-regulating kinase
CYP	cytochrome p450
DAB	diaminobenzidine tetrahydrochloride
DMEM	Dulbecco's Modified Eagle Medium
DTT	dithiothreitol
EGF	epidermal growth factor
EGFR	epidermal growth factor receptor
ERK	extracellular signal-regulated kinase
FBS	fetal bovine serum
gadd	growth arrest and DNA damage
GSH	glutathione
GST	glutathione S-transferase
HEPES	4-2-hydroxyethyl-1-piperazineethanesulfonic acid
HDAT	human dopamine transporter
HQ	hydroquinone
HSERT	human serotonin transporter
Hsp27	heat shock protein 27
IR	insulin receptor
LC-MS	liquid chromatography-mass spectrometry
MALDI-TOF	matrix-assisted laser desorption/ionization-time of flight mass spectrometry
MAPK	mitogen-activated protein kinase
MDA	3,4-(±)methylenedioxyamphetamine

MDMA	3,4-(±)methylenedioxymethamphetamine
MEK	MAPK kinase
MK-2	MAPK activated protein kinase-2
MKKK	MAPK kinase kinase
Mnk1/2	MAPK-interacting kinases
MSK1	mitogen and stress activated protein kinase 1
OSOM	outer stripe of outer medulla
PARP	poly(ADP-ribose)polymerase
PCC	premature chromatin condensation
PD98059	MEK inhibitor
PDGF	platelet derived growth factor
PKC	protein kinase C
PLC-γ	phospholipase C-γ
PMSF	phenylmethylsulfonyl fluoride
PMSF	phenylmethylsulfonyl fluoride
Prx	peroxiredoxin
PTB	phosphotyrosine binding
PTP	protein tyrosine phosphatase
γ-GT	γ-glutamyl transpeptidase
RCC	renal cell carcinoma
ROS	reactive oxygen species
SRE	serum response element
Rsk2	90 kDa ribosomal S6 kinase 2
RTK	receptor tyrosine kinases
SAPK/JNK	stress activated protein kinase/c-Jun N-terminal kinases

SB202190	p38 MAPK inhibitor
SB203580	p38 MAPK inhibitor
SOD	superoxide dismutase
SH2	Src-homolgy 2
TBS	tris-buffered saline
TGHQ	2,3,5-tris-(glutathion-S-yl)hydroquinone
Tsc-2	tuberous sclerosis-2
Trx	thioredoxin
TUNEL	in situ terminal deoxynucleotidyltransferase-mediated deoxy-UTP nick end labeling assay
U0126	MEK inhibitor
5-HT	5-hydroxytryptamine
8-oxo-dG	8-oxodeoxyguanosine

Chapter 1: INTRODUCTION

I. GENERAL COMMENTS

The quality of life for human beings has been greatly improved since the industrial revolution of the eighteenth century, during which the production of chemicals has roared to an exceptional level. Nevertheless, adverse effects of these chemicals have raised many concerns and have been the subject of many studies. Scientists endeavor to protect the health of human beings by identifying toxicants, studying their properties, observing dose-response relationships, and investigating the underlying mechanisms of the toxic effects. With the rapid development of advanced molecular and cellular technologies, toxicological studies have accelerated in the past several decades. Molecular and cellular toxicology arose from traditional toxicology, and has become an innovative area of study in recent years, with some significant successes. Utilizing molecular and cellular toxicological methods, toxicologists now have a better understanding of mechanisms of toxicity than has been previously achieved. New drugs with less adverse effects are therefore being produced, prevention of diseases achieved, and human safety improved.

A lot of drugs and chemicals have adverse effects on the kidney, with a number of chemicals inducing renal diseases by generating toxic metabolites of oxygen, reactive oxygen species (ROS). Prevention and treatment of these diseases necessitates a theoretical understanding of the problem. The goal of the work described in this dissertation is to discover key mechanisms of ROS-induced nephrotoxicity and nephrocarcinogenicity, focusing at the molecular and cellular level.

II. QUINONES

A. Exposure

Quinones are named according to the parent compounds from which they are derived. Thus, benzoquinone is the simplest form of a quinone, and is named after benzene, while anthraquinones are named after anthracene. Quinones are prevalent in the environment and are ubiquitously present in the life of human beings. For example, quinones are components of a variety of natural products, endogenous biochemicals, and manufacturing intermediates (Bolton *et al.* 2000). Data on the concentration of hydroquinone in the environment are not available, but hydroquinone production in the world was 35,000 tonnes in 1992, with 16,000 tonnes produced in the USA (IPCS 1996). Benzene, which is metabolized to hydroquinone by CYP450 in the liver, is found in crude petroleum at a concentration of 4 g/l, and is produced at 14 million tonnes worldwide (IPCS 1993). Therefore, the prevalence and abundance of quinones and their derivatives assure that human beings will be exposured to quinones.

Indeed, quinones are widely used by humans. Humans first used quinones as pigments and as drugs. For example, the principal active constituents of Chinese herbal medicine rhubarb are anthroquinones. Use of the senna plant originated in the Arab world, and pigments from henna and madder were used in cosmetics, and contained derivatives of 1,4-naphthoquinone and anthraquinone. Quinones are currently used as chemical intermediates, polymerization inhibitors, antioxidizing agents, photographic chemicals, tanning agents, and as chemical reagents (IPCS 1996). Hydroquinone is also used as a food preservative, as a skin-lightening agent in cosmetics, in hair dyes, and in medicines. Occupational exposure to quinones mainly include the dyes, textile, chemical, tanning, and cosmetic industries. Quinones may also be inhaled from tobacco smoke

(IARC 1977), and automobile exhaust (Schuetzle 1983; Schuetzle *et al.* 1981). As such, hydroquinone is present in the mainstream smoke from non-filtered cigarettes, with the amount from 110-300 μg/cigarette, whereas occupational exposure to hydroquinone in manufacturing industry has been reported to be 0.13 to 0.79 mg/m^3. In addition, hydroquinone has also been found to be naturally present in many food products, such as brewed coffee, and teas. Therefore, humans may be exposed to quinones through consumption of foods, by using cosmetics, smoking, inhalation of polluted air, taking medicines, or occupationally. Fortunately, hydroquinone does not bioaccumulate in the environment, due to its rapid degradation by both photochemical and biological processes (IPCS 1996). However, exposure to quinones may cause severe adverse effects. For example, acute exposure to quinones causes irritation to the eyes, dermatitis in humans, and renal toxicity in animal studies (IPCS 1996). Chronic human exposure to quinones in human results in skin irritation and visual disturbance. More and more data support that many quinones can contribute to cancer. The toxicity and carcinogenicity of quinones are somehow dependent on their metabolism, which will be explained in the next section.

B. Metabolism

The simplest quinol/quinone, hydroquinone, is rapidly absorbed through ingestion and inhalation by animals, and is absorbed slower via dermal absorption. Hydroquinone is found in a wide range of tissues after administration, and it is oxidized to *p*-benzoquinone as well as other oxidized products. Hydroquinone and its oxidized metabolites are subsequently detoxified by glucuronidation and sulfation, but their toxicitiy can be enhanced by conjugation with glutathione (GSH) (Monks *et al.* 1985). Hydroquinone and its metabolites are excreted rapidly via the urine. In an acute study, after a single dose of hydroquinone in male Fischer-344 rats, the metabolites of

hydroquinone were principally found in the urine, including 21% as a glucuronide conjugate, 15% as a sulfate conjugate, and 13% as mercapturate conjugates (Lau *et al.* 1996). The metabolites of hydroquinone vary by species, route of administration, and duration of administration (Divincenzo *et al.* 1984; Hill *et al.* 1993; Lau *et al.* 1996; Nerland and Pierce 1990).

Hydroquinone is subject to oxidation by different isoforms of cytochrome P_{450} (1A1, 2E1, 3A4) (Hill *et al.* 1993; Lau 1997), or other enzymes such as myeloperoxidase (Subrahmanyam *et al.* 1990), and prostaglandin H synthase (Lau and Monks 1987). Benzoquinone, the oxidized form of hydroquinone, undergoes nucleophilic addition of GSH to form GSH-conjugated hydroquinone. The process of oxidation and GSH addition is repeated, leading eventually to 2,3,5-tris-conjugated hydroquinone, 2,3,5-tris-(glutathion-S-yl)hydroquinone (TGHQ) (Lau *et al.* 1988). This sequential oxidation and GSH addition is summarized in Figure 1-1. GSH conjugation was long thought of as a detoxication pathway, but GSH conjugation to a number of polyphenols, resulting in polyphenolic GSH conjugates, are actually nephrotoxicants in various animal models (Bai *et al.* 2001; Bolton *et al.* 2000; Butterworth *et al.* 1998; Lau *et al.* 1988; Monks *et al.* 1988; Monks *et al.* 2004; Monks and Lau 1997, 1998; Monks *et al.* 1985; Peters *et al.* 1996). This is because GSH conjugation to quinones frequently increases their ability to generate reactive oxygen species (ROS), which damage the cells, and also target the conjugates to specific organs (Monks and Lau 1994). Moreover, quinone-GSH conjugates maintain their electrophilicity and can covalently bind to macromolecules. These biological activities of polyphenolic GSH conjugates will be discussed in detail in the following section. After GSH conjugation, quinones are subject to futher metabolism via the mercapturic acid pathway, the first step being catalyzed by γ-glutamyl transpeptidase (γ-GT), to form cysteinyl-glycine conjugates of quinones. A second

enzyme, dipeptidase, further metabolizes the cysteinyl-glycine conjugates to the corresponding cysteinyl conjugates. Renal proximal tubule epithelial cells express high activity of both γ-GT and dipeptidase. The subsequent formation of N-acetylcysteine conjugates is the last step in the mercapturic acid pathway (Monks and Lau 1997, 1998). Each of the metabolites in the mercapturic acid pathway is highly reactive, and can generate ROS, as well as alkylate tissue macromolecules. Therefore, high activities of the enzymes of the mercapturic acid pathway in renal proximal tubule epithelial cells predisposes this tissue to the toxicity of GSH conjugates of quinones.

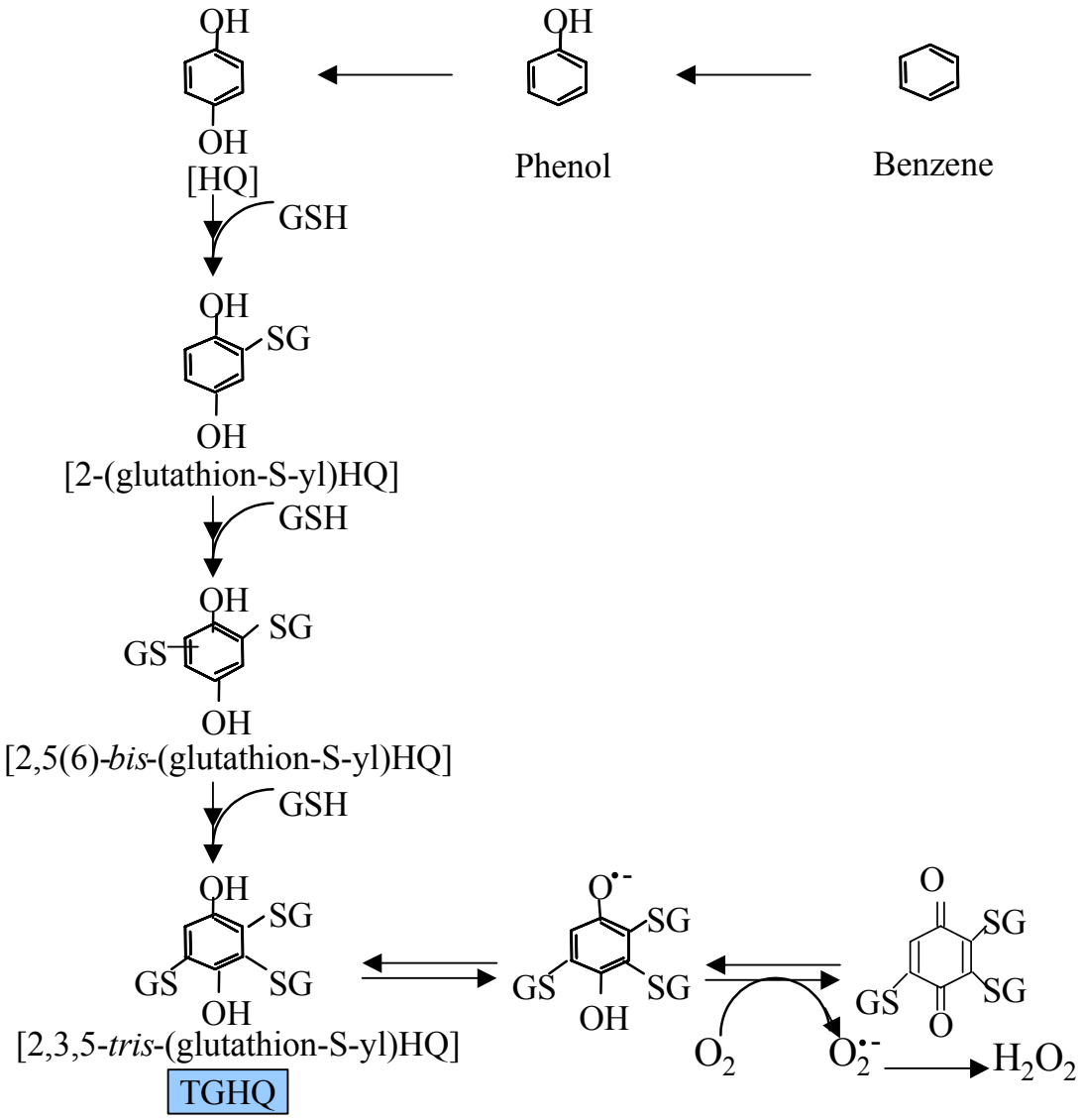

Figure 1.1. Formation of quinone-thioethers and mechanisms of ROS generation.

C. Biological and Pharmacological Properties of Quinones and their Derivatives

As summarized in the preceding section, quinones exhibit dual characteristics: they are both redox-active and electrophilic, and these two activities are closely associated (Monks and Lau 1997). Quinones may undergo either enzymatic or nonenzymatic redox cycling to generate superoxide radicals. The one-electron reduced form of a quinone, the semiquinone, may undergo oxidation to regenerate the quinone, during which an oxygen molecule gains an electron to form superoxide ($O_2^{\cdot -}$) (Monks and Lau 1997). $O_2^{\cdot -}$ subsequently generates hydrogen peroxide (H_2O_2) via spontaneous or enzyme-driven dismutation. Additionally, hydroxyl radical ($HO^{\cdot}$) is generated via reaction with Fe^{2+} and H_2O_2. $HO^{\cdot -}$ is thought to be the ROS principally responsible for the damage induced by quinones and quinone-derivatives (Monks and Lau 1997). These highly active oxygen derivatives are all called ROS, reactive oxygen species, and include $O_2^{\cdot -}$, H_2O_2, and $HO^{\cdot -}$ (Figure 1.2). Small amounts of ROS generated under physiological conditions may function as signaling factors, whereas large amount of ROS generated exogenously by chemicals or irradiation, for instance, cause deleterious effects to cellular contents. The two-electron reduction of quinones is catalyzed by NAD(P)H quinone:oxidoreductase (DT-diaphorase), and is considered a detoxication mechanism. However, due to hydroquinone's ability to redox cycle and generate semiquinone radicals and subsequent ROS, this enzyme can actually potentiate the toxicity of hydroquinone.

Quinones are also Michael acceptors and may covalently bind to a variety of cellular nucleophiles (Bolton *et al.* 2000). GSH represents the major non-protein sulfhydryl in cells, and GSH readily binds to quinones to form mono-, and multi-GSH conjugates, also known as quinone-thioethers. As noted, the addition of GSH to quinones is generally considered cytoprotective, because GSH functions as a 'sacrificial'

nucleophile to prevent binding of quinones to essential cellular proteins. But GSH addition to quinones can also increase quinone-mediated toxicity in certain target organs. This is because the conjugates maintain the properties of the parent compounds to redox cycle and to alkylate macromolecules (Monks and Lau 1997). Moreover, γ-GT and dipeptidases contribute to the formation of cysteinyl conjugates of quinones, which may enter cells by L-amino acid transporters (Monks and Lau 1997). Renal proximal tubule epithelial cells express high levels of γ-GT and dipeptidase, and are therefore targets for GSH-conjugated quinones. In summary, due to the two highly active biological properties of quinones and their derivatives, quinones and quinone-GSH conjugates may influence the essential functions of normal cells. For example, oxidation of cysteine residues of essential proteins may result in changes in their structure and function. Oxidation of lipids leads to the formation of lipid peroxide-derived malondialdehyde DNA adducts (Marnett 1999). Formation of 8-oxo-2'-deoxyguanosine is a sign of DNA oxidation and damage (Shigenaga and Ames 1991), and occurs in TGHQ-treated Eker rats (Habib *et al.* 2003). Proteins alkylated by TGHQ have been found in TGHQ-treated rats, and are localized to the S3 segment of the proximal tubule, the target of TGHQ-induced toxicity (Kleiner *et al.* 1998a). Therefore, the biological and pharmacological properties of quinones and quinone-thioethers likely determine their toxicities in humans and animals, as discussed in the following section.

(1) Dismutation of superoxide anion to hydrogen peroxide

$$2O_2^{\cdot -} + 2H^+ \xrightarrow{\text{SOD}} H_2O_2 + O_2$$

(2) The Harber-Weiss reaction

$$Fe^{3+} + O_2^{\cdot -} \longrightarrow Fe^{2+} + O_2$$
$$Fe^{2+} + H_2O_2^{\cdot -} \longrightarrow Fe^{3+} + HO^{\cdot} + HO^-$$

(3) Degradation of hydrogen peroxide

$$2\ H_2O_2 \xrightarrow{\text{catalase}} H_2O + O_2$$

Figure 1.2. ROS generation and degradation.

D. Toxicity of Quinones and Quinone-thioethers

The metabolism and biological and pharmacological properties of quinones and quinone-thioethers underlie their toxicological effects. The following discussion will focus on the various toxicities of hydroquinone as described in the literature to provide a panoramic view of hydroquinone-mediated adverse effects. Nephrotoxicity, the focus of this thesis, will be described in substantial detail, and other toxicities will also be mentioned to compare and contrast with hydroquinone-induced nephrotoxicity thereby providing a generic understanding of quinone-mediated toxicity.

1. General Toxicities of Hydroquinone:

The mammalian toxicity of hydroquinone is well-studied. Oral LD_{50} values for hydroquinone in mammals range from 300-1300 mg/kg body weight, with cats the most sensitive (LD_{50}=42-86 mg/kg body weight). Dermal LD_{50} values in rodents are approximate by >3800 mg/kg. Acute exposure to hydroquinone causes central nervous system (CNS) toxicity, depigmentation, minor irritation, sensitization, inflammatory changes, and thickening of the epidermis in skin test (IPCS 1996). Subchronic oral toxicological studies revealed nephropathy and renal cell proliferation, and CNS toxicity in Fischer-344 rats and B6C3F1 mice (IPCS 1996). Weight loss and CNS signs of toxicity were also observed in Sprague-Dawley rats after 13-week exposure to hydroquinone at 200 mg/kg body weight (IPCS 1996). Reproductive and developmental toxicities of hydroquinone were also observed (IPCS 1996). Genetic toxicities revealed numerical and structural changes to chromosomes, gene mutations, sister-chromatid exchange, and DNA damage. Chronic ingestion of hydroquinone caused dose-dependent renal tubule cell adenomas in male Fischer-344 rats, and hepatocellular adenomas in female Fisher-344 rats and male mice (Kari *et al.* 1992). The incidence of squamous cell

hyperplasia in the forestomach epithelium also increased significantly in rats. Hydroquinone demonstrates both *in vitro* and *in vivo* cytotoxic effects manifested by reduced cell counts in bone marrow and spleen, and subsequent immunosuppressive potential.

Toxicity after oral ingestion of hydroquinone by humans in the photographic industry was reported. Signs of toxicity included dark urine, vomiting, abdominal pain, brachycardia, CNS effects, coma, and even death. Ingestion of 300-500 mg hydroquinone daily for 3-5 months by a human did not induce pathological changes in blood or urine (IPCS 1996). Epidemiological studies suggest that skin creams containing hydroquinone produce leukoderma and ochronosis, irritation, and allergic contact dermatitis. Exposure to hydroquinone in the air causes eye irritation, sensitivity to light, and eye damage.

2. Nephrotoxicity

As noted earlier, GSH conjugates of polyphenols (quinone-thioethers) are nephrotoxic in Sprague Dawley and Fischer-344 rats (Bolton *et al.* 2000), and TGHQ is nephrocarcinogenic in the Eker rat (Lau *et al.* 2001a). The nephrocarcinogenicity induced by quinone-thioethers will be discussed in Section II.E. The nephrotoxicity of GSH conjugates of polyphenols is due to the relatively high activity of γ-GT and dipeptidase present in the brush border membrane of the kidney proximal tubule epithelial cells. The activity of these two enzymes leads to the formation of cysteinyl conjugates of polyphenols, which may be transported into renal cells via the L-amino acid transporter system (Monks and Lau 1997, 1998). Thus, inhibition of γ-GT activity by acivicin (AT-125) blocks quinone-thioether induced nephrotoxicity (Lau *et al.* 1988; Monks *et al.* 1988; Monks and Lau 1997, 1998). In essence, the metabolism of the GSH conjugates of polyphenols determines target-organ oriented toxicity in the kidney. Typical

nephrotoxicity by 2-bromo-bis-(glutathion-S-yl)hydroquinone in Fischer-344 rats is characterized by loss of the brush border membrane integrity (release of γ-GT and alkaline phosphatase into urine), margination of heterochromatin, loss of chromatin staining, reorganization of the endoplasmic reticulum into discrete aggregates, loss of cellular contents (glutathione-S-transferase [GST] in urine), karyorrhexis and karyolysis, DNA fragmentation, and renal cell necrosis (Monks and Lau 1998; Peters *et al.* 1997; Rivera *et al.* 1994). DNA damage induced by TGHQ in Eker rat kidneys was manifest by an increase in the 8-oxo-deoxyguanosine, an oxidized damaged nucleotide (Habib *et al.* 2003). DNA damage was found to be specifically localized within the outer stripe of outer medulla (OSOM), within the S3 segment of proximal tubule epithelial cells. These cells are most sensitive to TGHQ treatment (Monks and Lau 1998).

To study the mechamisms of polyphenolic GSH conjugate induced nephrotoxicity, we utilize an *in vitro* cell culture model system (LLC-PK1). LLC-PK1 cells are a porcine renal proximal tubule epithelial cell line, and have relatively high expression of γ-GT. GSH conjugates of polyphenols induce cell death in LLC-PK1 cells, as determined by neutral red uptake (Mertens *et al.* 1995). Thus, TGHQ induces oncotic cell death in LLC-PK1 cells (Dong *et al.* 2004; Ramachandiran *et al.* 2002), and the response is both dose- and time-dependent. Polyphenolic GSH conjugate induced cytotoxicity is associated with their ability to generate reactive oxygen species (ROS), and to cause single strand DNA damage (Jeong *et al.* 1997a; Jeong *et al.* 1996; Mertens *et al.* 1995). Cell cycle arrest induced by 2-bromo-bis-(glutathion-S-yl)hydroquinone is represented by an increase in *gadd153* expression, a growth arrest gene responding to DNA damaging agents (Jeong *et al.* 1997a; Jeong *et al.* 1996). *gadd153* induction by 2-bromo-bis-(glutathion-S-yl)hydroquinone corresponds to a direct inhibition of DNA synthesis, due to the inhibition of the DNA synthesis enzymes. As such, histone mRNAs

also decrease upon 2-bromo-bis-(glutathion-S-yl)hydroquinone treatment (Jeong *et al.* 1997b; Jeong *et al.* 1996), preventing chromatin remodeling and cell growth. Additionally, TGHQ induced activation of all three subfamilies of the mitogen activated protein kinases (MAPKs), extracellular signal-regulated protein kinase (ERK), c-Jun N-terminal kinases/stress-activated protein kinase (JNK/SAPK), and p38 MAPK (Ramachandiran *et al.* 2002). Pharmacological inhibitors of the ERK (PD-98059) and p38 MAPK (SB-202190) pathways, but not JNK (SP-600125) attenuate TGHQ-mediated oncotic cell death, yet there was no additive effects with the two inhibitors (Ramachandiran *et al.* 2002). TGHQ also increased the DNA binding activity of AP-1 and NF-κB, downstream effectors of the MAPKs, and NF-κB is likely involved in the cytoprotective effects of PD-98059 (Ramachandiran *et al.* 2002). Another downstream effector of the MAPKs is histone H3, which was phosphorylated after TGHQ treatment. Phosphorylation of histone H3 was attenuated by inhibition of the ERK pathway, using pharmacological inhibitors (Tikoo *et al.* 2001). Meanwhile, histone H3 phosphorylation by TGHQ is accompanied by an increase in chromatin condensation, and is modulated by poly(ADP)ribosylation (Tikoo *et al.* 2001). Histone H3 phosphorylation induced by DNA damage and growth arrest-inducing agents likely mediates a cellular malfunction called premature chromatin/chromosomal condensation, and leads to cell death. In summary, quinone-thioethers induce DNA damage and growth arrest, MAPKs activation, and histone H3 phosphorylation in LLC-PK1 cells, which are all associated with quinone-thioether induced renal cell death.

In contrast, cells also possess a number of signaling pathways to prevent and recover from stress-induced damage. For example, TGHQ induces early *hsp70* expression (Towndrow *et al.* 2000), a cell survival signal induced by stress and heat shock. DDM-PGE2 pretreated (24 h) or in genetic manipulated post-confluent renal cells

(Grp78 antisense), changes of total levels of Hsp27 and the subsequent phosphorylation are important in stabilizing actin and yield protective effects (Jia *et al.* 2004). Whether cells die or survive after stress depends on the balance of these death/survival signaling pathways within the cells. Theoretically, if the stress level is low, cell survival signals overwhelm the death-driven signals to protect or ensure recovery from stress-induced damage. If the stress exceeds a certain threshold, cells no longer have the capacity to compensate, and cell death signals dominate cell signaling and drive cells to die.

3. Other Quinone-thioether-mediated Target Organ Toxicities: Similarities and Differences to Nephrotoxicity

Quinones and their derivatives not only target kidneys, but also bone marrow and neural systems. For example, benzene causes a decrease in the numbers of circulating blood cells in workers occupationally exposed to benzene (Greenburg 1996). Benzene is both hematotoxic and leukemogenic in humans, and benzene causes aplastic anemia, myelodysplastic syndrome, and acute myelogenous leukemia (Snyder *et al.* 1993). The metabolism of benzene is responsible for its toxicity. Benzene is metabolized in the liver by CYP_{450} 2E1 or peroxidase(s) to form phenols, and subsequently hydroquinone and catechol, and ultimately various conjugated metabolites. Thus, a number of redox active quinol-thioethers were identified in the bone marrow of both Sprague-Dawley rats and DBS/2 mice administered a combination of hydroquinone/phenol or benzene (Bratton *et al.* 1997). Mice are more sensitive to benzene-mediated hematotoxicity than rats, partially due to different concentrations of quinone-thioethers in bone marrow (Bratton *et al.* 1997). TGHQ reproduced benzene erythrotoxicity *in vivo* (Bratton *et al.* 1997).

The molecular mechanisms behind quinone-thioether induced hematopoietic effects are due to apoptotic cell death (Bratton *et al.* 2000), but little is known about the

roles of apoptosis in benzene or benzene metabolite-induced hematotoxicity. Therefore, studies in our laboratory have attempted to define an apoptotic cell death pathway in HL-60 cells, and are exploring the mechanism of TGHQ-induced apoptosis (Bratton *et al.* 2000). In essence, TGHQ induces a decrease in cellular GSH levels independent of ROS generation, and this decrease precedes cell death (Bratton *et al.* 2000). Decreases in GSH levels likely induces apoptosis through the ceramide signaling pathway (Bratton *et al.* 2000). Ceramide induces apoptosis through the activation of caspase-3 or phosphatases. Sphingomyelin turnover is also increased by TGHQ, together with the induction of the ceramide pathway, verifying the responses of cells to decreases in GSH levels. Current studies in our laboratory are attempting to decipher the apoptotic signaling pathways involved in TGHQ-mediated apoptosis.

Another target organ of interest is the CNS. The neurotoxicity of quinone-thioethers is illustrated by the toxic effects of 3,4-(±)methylenedioxyamphetamine (MDA) and 3,4-(±)methylenedioxymethamphetamine (MDMA), the latter known as ecstasy. Ecstasy is abused in western countries, with mild to severe acute adverse effects such as convulsions, hyperthermia, rhabomyolysis, and acute liver and renal failure (Henry *et al.* 1992). The acute toxicity in rats is manifest as damage to serotonergic axonal structure and function, and increases the acute release of 5-hydroxytryptamine (5-HT), followed by a long term depletion of 5-HT in serotonergic nerve terminals, and inhibition of tryptophan hydroxylase (Stone *et al.* 1989). Long-term consumption of ecstasy induces chronic neurotoxicity in humans (Green *et al.* 2003; Obrocki *et al.* 2002).

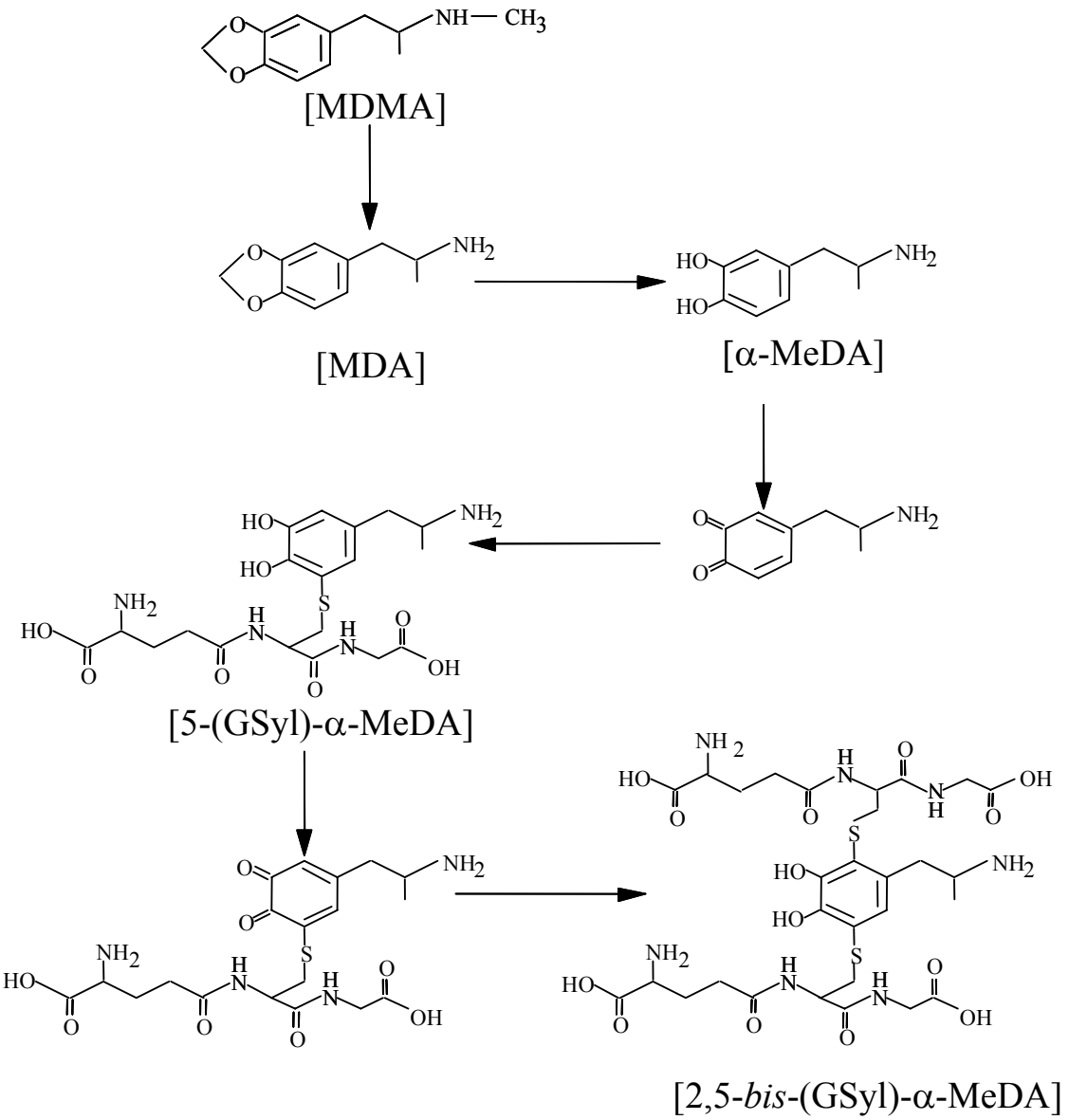

Figure 1.3. Metabolism of methylenedioxymethamphetamine (MDMA) and methylenedioxyamphetamine (MDA) to quinol-GSH conjugates.

Metabolism again plays a role in MDA and MDMA-mediated neurotoxicity, because injection of these two chemicals directly into the brain fails to produce toxic effects. CYP_{450} mediated oxidation and GSH conjugation are required for MDA and MDMA induced neurotoxicity. Very similar to hydroquinone metabolism, the metabolites of MDA and MDMA, α-MeDA and N-methyl-α-MeDA undergo sequential oxidation and addition of GSH to form 5-(glutathion-S-yl)-α-MeDA and 2,5-bis-(glutathion-S-yl)-α-MeDA (Figure 1.3), which retain the ability to redox cycle (Miller *et al.* 1997). Injection of 2,5-bis-(glutathion-S-yl)-α-MeDA into the brain reproduces similar effects as MDA and MDMA, with respect to decreases in 5-HT in the brain (Miller *et al.* 1997). Inhibition of γ-GT by acivicin (AT-125), interestingly, increases the uptake of 5-(glutathion-S-yl)-α-MeDA into the brain (Bai *et al.* 1999), which is in contrast to findings in the kidney. This is probably due to the prevalence of intact GSH transporters in the brain, which readily transport the GSH-conjugates into the brain. Inhibition of γ-GT increases the pool of GSH conjugates, therefore potentiating MDA-induced neurotoxicity (Bai *et al.* 2001). This observation is also confirmed in cell culture (Carvalho *et al.* 2002).

The molecular mechanisms by which metabolites of MDA and MDMA induced neurotoxicity are being explored. 5-(Glutathion-S-yl)-α-MeDA, 2,5-bis-(glutathion-S-yl)-α-MeDA, MDA, and MDMA all induce a concentration and time-dependent increase in ROS levels in both human serotonin transporter (hSERT) and human dopamine transporter (hDAT)-transfected cells, to a lesser extent with MDA and MDMA treated cells (Jones *et al.* 2004). Dopamine transport into the hSERT-transfected cells by the metabolites mentioned above also contributes to the metabolism-dependent neurotoxicity (Jones *et al.* 2004). Interestingly, many investigators consider MDMA-induced hyperthermia to be responsible for the enhancement of neurotoxicity, but recent findings

from our laboratory indicate that MDMA induced neurotoxicity can be dissociated from increases in body temperature (Jones, unpublished data).

In summary, quinone-thioether-induced nephrotoxicity and other target organ toxicities share some common mechanisms of actions including metabolism, ROS generation, and dependence on certain molecular mechanisms, but they also exhibit differences. For example, TGHQ induces oncotic cell death in renal epithelial cells, whereas TGHQ induces apoptotic cell death in bone marrow cells. Inhibition of γ-GT attenuates quinone-thioether-induced nephrotoxicity but potentiates neurotoxicity. Other quinone-thioethers such as GSH conjugates of 17β-estradiol, tert-butyl-4-hydroxyanisole (BHA) and its metabolite tert-butylhydroquinone (TBHQ) are mild nephrotoxic and are associated with carcinogencitiy (Monks and Lau 1997).

E. Nephrocarcinogenicity of Quinone-thioethers

Hydroquinone is ubiquitously present in natural products and in the environment, but relatively little data is available on the carcinogenicity of hydroquinone. Because hydroquinone is present in cigarette at high concentrations (155 μg per cigarette), and smoking is associated with a higher incidence of renal tumors in men (Randerath and Randerath 1993; Tavani and La Vecchia 1997), the National Cancer Institute listed hydroquinone for future study on its ability to induce carcinogenicity. The mechanism by which cigarette smoke induces carcinogenicity is probably due to the high levels of oxidants and free radicals in smoke (Church and Pryor 1985).

Hydroquinone is generally not considered mutagenic in short-term mutagenicity assays (Florin *et al.* 1980; Sakai *et al.* 1985), and not mutagenic in mouse cells *in vivo* (Gocke *et al.* 1983). However, hydroquinone causes base pair changes in the TA1535

Salmonella typhimurium test strain (Gocke *et al.* 1981), is mutagenic in TA104 and TA2637 *Salmonella* test strains (Hakura *et al.* 1996), and tested positive for mutagenicity in several Ames bacterial test strains (Hakura *et al.* 1995). Hydroquinone also induces sister chromatid exchange (Gocke *et al.* 1981; Kari *et al.* 1992; Tsutsui *et al.* 1997) catalyzes the formation of 8-oxo-dG (Leanderson and Tagesson 1990), and causes single-strand DNA breaks in hepatocytes (Walles 1992). Hydroquinone also increases the number of tubular cell adenomas in Fischer-344 rats (Kari *et al.* 1992). Nephrotoxic doses of hydroquinone induce renal cell tumors in male rats (Kari *et al.* 1992; Shibata *et al.* 1991) and mice (Shibata *et al.* 1991). Hydroquinone not only acts as an initiator by causing DNA damage, it can also act as a tumor promoter, depending on the target organ and initiation protocol used (Yamaguchi *et al.* 1989). The mechanism of hydroquinone-mediated carcinogenicity is not well characterized, and is the focus of studies in our laboratory and of others.

The acute nephrotoxicity of hydroquinone is dependent on the activity of γ-GT, which metabolizes the various GSH-conjugated hydroquinones (Lau *et al.* 1988; Monks *et al.* 1985; Peters *et al.* 1997). TGHQ is one of these metabolites and is a potent nephrotoxicant (Lau *et al.* 1988; Peters *et al.* 1997). TGHQ also causes nephrocarcinogenicity in Eker rats (Lau *et al.* 2001a). Eker rats (Eker *et al.* 1981) are derived from the Long-Evans strain, and possess a germline insertion in the tuberous sclerosis-2 (*Tsc-2*) tumor suppressor gene, which predisposes these animals to the development of renal cell carcinoma (RCC) (Lau *et al.* 2001a; Walker *et al.* 1992; Walker 2002; Yoon *et al.* 2002; Yoon *et al.* 2001). The *Tsc-2* gene has been primarily associated with the development of renal cell carcinoma (RCC) in rats, and with higher risk of development of renal tumors in humans (Walker 1998). In Eker rats, spontaneous preneoplastic lesions start to appear as early as 2-3 months, and nearly 100% of the rats

exhibit renal tumors by 1 year of age. Interestingly, these renal tumors arise from the proximal tubules (Everitt *et al.* 1992), which are the target area for TGHQ induced toxicity. Exposure to known renal carcinogens increases the incidence of renal tumors in Eker rats (Hino *et al.* 1993; Walker *et al.* 1992). Loss of the remaining normal allele of the *Tsc-2* gene underlies the development of RCC in Eker rats (Lau *et al.* 2001a; Walker *et al.* 1992; Yeung *et al.* 1995). Therefore, Eker rats provide a good model with which to investigate chemical-induced nephrocarcinogenicity.

Certain chemicals may induce carcinogenicity by first inducing toxicity, followed by excessive and sustained regeneration of cells, causing hyperlasia and finally tumor formation (Florin *et al.* 1980; Gocke *et al.* 1983; Sakai *et al.* 1985). Since TGHQ is both nephrotoxic and genotoxic (Habib *et al.* 2003; Jeong *et al.* 1999), and TGHQ induces a proliferative response after tissue damage (Peters *et al.* 1997), it is likely that TGHQ could be a carcinogenic chemical. Exposure of the supF gene to TGHQ followed by transfection and replication in either human AD293 or bacterial cells increased the mutation frequency (Jeong *et al.* 1999). TGHQ also causes the loss of heterozygosity of the *Tsc-2* gene (Lau *et al.* 2001a). Therefore, TGHQ-induced cell proliferation likely magnifies the chemical-induced DNA damage and genetic alterations, providing the opportunity for tumor initiation and progression. TGHQ or hydroquinone induces an increase in the incidence of atypical tubules and atypical hyperplasias following 4-months of treatment, and a significant increase in the number of carcinomas after 10 months treatment (Lau *et al.* 2001b). TGHQ-mediated nephrocarcinogenicity is localized to the OSOM of the Eker rat kidneys, where the acute nephrotoxicity occurs.

The *Tsc-2* gene is a tumor suppressor gene that encodes for tuberin, a protein involved in limiting tumor development. Loss of the *Tsc-2* tumor suppressor gene in TGHQ-induced tumors suggests that tuberin also plays a role in chemical-induced

nephrocarcinogenesis, but detailed mechanisms by which this gene regulates tumor formation are limited. TGHQ treatment significantly increases proliferation within the OSOM of Eker rats and the wild-type equivalents, yet only Eker rats develop renal tumors, indicating that proliferation is not sufficient for tumor development in rat kidney (Yoon *et al.* 2002). Tuberin expression is lost after long-term TGHQ treatment, and this correlates with an increase in ERK activity within the OSOM of Eker rats at 4 months, and in TGHQ-induced tumors (Yoon *et al.* 2002). Reintroduction of *Tsc-2* gene in tuberin-negative renal cells (QT-RRE) attenuates ERK activity (Yoon *et al.* 2001). QT-RRE cells are derived from quinol-thioether transformed primary renal epithelial cells from Eker rats (Yoon *et al.* 2001). In QT-RRE cells, tuberin loss is accompanied by an increase in growth signaling in tumors, such as ERK and B-Raf activity. Restoration of tuberin, achieved by transfecting *Tsc-2* cDNA back into QT-RRE cells accordingly decreased ERK and B-Raf activities (Yoon *et al.* 2001; Yoon *et al.* 2004). Additionally, cDNA microarray analysis of QT-RRE cells and of tumor tissue of Eker rats treated with TGHQ revealed alterations in a total of 80 genes, with major functions in *1)* signal transduction, *2)* stress response, tissue remodeling, and DNA repair, and *3)* electron transport and energy homeostasis (Patel *et al.* 2003). The annexin I and II proteins were further studied, and were found to be upregulated in tumor tissue and in QT-RRE cells, which likely play a role in TGHQ-induced nephrocarcinogenicity (Patel *et al.* 2003). Injection of the QT-RRE cells into nude mice generated tumors, providing further evidence that these cells are malignantly transformed (Patel *et al.* 2003).

In conclusion, TGHQ, a metabolite of hydroquinone, induces both nephrotoxicity and nephrocarcinogenicity within the chemical-targeted OSOM region of the Eker rat kidney. Nephrotoxicity, with subsequent sustained compensatory proliferation likely leads to amplification of DNA damage and enhances genomic instability. For example,

loss of heterozygosity of the *Tsc-2* gene by TGHQ treatment is associated with the generation of renal tumors. HQ is not identified in the common mutagenic tests. The "nongenotoxic" hydroquinone is therefore identified as a carcinogenetic chemical in tumor-susceptible animals following metabolism to cytotoxic and mutagenic metabolites.

III. ROS AND CELL SIGNALING

ROS play an essential role in quinone and quinone-thioether mediated renal cell death, as evidenced by the fact that catalase totally blockes ROS-induced MAPK activation, histone H3 phosphorylation, and renal cell death (unpublished data). Understanding ROS mediated signaling is a key to understanding the mechanism of quinone and quinone-thioether mediated ROS-dependent renal cell death. ROS comprise a variety of highly reactive metabolites of oxygen, including superoxide anions ($O^{\cdot-}$), hydrogen peroxide (H_2O_2), and hydroxyl radicals ($HO^{\cdot}$) (Figure 1.2). ROS are produced both endogenously, as a consequence of normal cell function, or from external sources. Physiological or sub-physiological levels of ROS play a role in signal transduction as second messengers (Forman and Torres 2002; Martindale and Holbrook 2002; Meves *et al.* 2001; Rhee 1999; Torres and Forman 2003). In contrast, the excessive generation of ROS are otherwise linked to a number of human diseases, redox-chemical induced toxicities (Bolton *et al.* 2000), and aging (Martindale and Holbrook 2002), possibly by causing severe damages to DNA, protein, and lipid.

In response to ROS-mediated cellular damage, cells possess a number of antioxidant defenses (e.g., GSH, SOD, catalase, peroxidases) to counteract ROS-mediated adverse effects. However, once ROS generation exceeds cellular antioxidant capacity, cells become subject to oxidative stress-induced damage. Therefore, cell fate is determined by the ability of cells to prevent oxidative stress and to repair cellular

damage. These cellular responses to ROS consist of signaling pathways to enhance survival and pathways to induce cell death. Additional factors, for example, cell type (different pools of signaling expression), combinatorial and/or temporal activation of the signaling pathways (Schlessinger 2000) also determine the outcome following exposure to ROS. As such, although ROS, at both low and high concentrations, induce MAPK activation, ROS induce proliferation at low doses yet cell death at high doses (Martindale and Holbrook 2002). Many signaling pathways have been identified to be activated in response to ROS, with more and more being discovered. The mechanisms by which these pathways contribute to ROS-induced renal cell death are the main focus of the current studies.

Renal proximal tubule epithelial cells are particularly sensitive to oxidative stress induced damage. The molecular mechanisms by which ROS cause injury in renal cells remain to be investigated. Studies on the initial molecular changes induced by ROS in renal cells will help to identify novel targets and therapeutic strategies. TGHQ, a quinol-thioether metabolite of HQ, contributes to HQ-mediated nephrotoxicity and nephrocarcinogenicity (Lau *et al.* 1988; Lau *et al.* 2001a; Peters *et al.* 1997). TGHQ maintains the ability to redox-cycle and to generate ROS (Towndrow *et al.* 2000; Weber *et al.* 2001). Quinol-thioethers induce rapid ROS-dependent DNA damage, growth arrest, MAPK activation, histone H3 phosphorylation, and cell death in a well-established *in vitro* model of porcine renal proximal tubule epithelial cells (LLC-PK_1) (Jeong *et al.* 1997a; Jeong *et al.* 1997b; Jeong *et al.* 1996; Mertens *et al.* 1995; Ramachandiran *et al.* 2002). TGHQ also induces ROS-dependent DNA damage (8-oxo-dG) in Eker rats (Habib *et al.* 2003). Subsequently, my research is designed to decipher the various signaling pathways that contribute to quinol-thioether-induced renal cell death/nephrotoxicity in response to oxidative stress. The findings discussed in the following chapters reveal some

of the mechanisms by which ROS induce nephrotoxicity, and provide insights for potential therapeutic intervention and prevention of HQ/ROS-mediated kidney disease. The following subsections will provide brief introductions on the concept of cell death, and cell signaling pathways that are likely involved in ROS-mediated cell death.

A. Cell Death

There are two recognized modes of cell death, oncosis and apoptosis (Majno and Joris 1995; Trump *et al.* 1997; Van Cruchten and Van Den Broeck 2002). Oncosis is a non-apoptotic cell death pathway, a passive cell death characterized by cell and organelle swelling, and loss of membrane integrity in response to various stresses. von Recklinghausen first introduced the term oncosis in 1910, derived from a Greek word meaning "swelling" (Van Cruchten and Van Den Broeck 2002). This term has subsequently been used by increased number of researches (Park *et al.* 2000; Ramachandiran *et al.* 2002; Tikoo *et al.* 2001). Oncosis was proposed to describe any type of cell death characterized by a marked cell swelling, whereas necrosis was proposed to describe post-mortal features (Majno and Joris 1995). Moreover, necrosis often occurs more frequently in the adult organism, and is the consequence of a large number of injured cells regardless of the pre-lethal changes (Majno and Joris 1995). Cell swelling during oncosis is due to damage to the cell membrane and loss of membrane integrity. Finally, cells burst and die, releasing a number of enzymes such as phospholipases, hydrolases, DNases, and RNases. These enzymes lead to the random degradation of protein, DNA and RNA. At the same time, inflammatory factors released after the cell membrane bursts cause injury to neighboring cells. Therefore, oncosis is usually observed as a zonal area of cell death. Traditionally, programmed cell death is used to describe apoptotic cell death, which encompasses active signaling pathways that

lead to cell death. However, necrotic/oncotic cell death is also involved in a number of signaling pathways, inhibition of which attenuates cell death (Ramachandiran *et al.* 2002). Therefore, programmed cell death should not be used as synonyms for either apoptosis or oncosis.

In contrast to oncotic cell death, apoptotic cell death is an active cell death pathway, characterized by cell shrinkage, cell membrane budding (while maintaining integrity), chromatin margination, and formation of apoptotic body (Trump *et al.* 1997). Various factors, including ROS, heat shock, protein synthesis inhibitors and DNA damaging agents can induce apoptosis. Apoptosis was first elaborated by Kerr in 1971 to describe a mode of hepatocyte death with morphological changes including decreased cell volume, ruffled cell membranes, condensed chromatin, and cell segregation with formation of intact vesicles. In early 1971, this mode of cell death was called shrinking necrosis, and was changed to apoptosis the next year, which in Greek refers to the falling of leaves. In the last stage of apoptotic cell death, apoptotic bodies maintaining an intact membrane and encapsulating fragmented DNA and intact organelles are formed. These apoptotic bodies are rapidly engulfed by phagocytes, without causing an inflammatory response and therefore does not adversely affect neighboring cells. However, not all apoptotic cells are recognized by phagocytes. Therefore, under certain conditions apoptotic cells can undergo secondary necrosis, or apoptotic necrosis (Majno and Joris 1995). Cells undergoing secondary necrosis share several features with necrotic cell death, with the exception of an inflammatory response. Apoptosis also occurs in normal tissues, and is an important process to control tissue development, and to maintain the appropriate number of cells within normal tissues to ensure normal tissue function. In contrast, inhibition of apoptosis occurs in tumor tissue and autoimmune disease. DNA degradation into ~180 base pair fragments, catalyzed by specific cleavage of DNA

between nucleosomes, is one of the hallmark characteristics of apoptosis (Hendzel *et al.* 1998). Another important feature of apoptosis is caspase activation (Bratton and Cohen 2001; Shi 2004). Caspases are a family of proteins that are usually present in cells as inactive precursors, procaspases. Precaspases become activated by selective and specific proteoic splicing, initiating a caspase cascade. Caspases cleave a variety of structural proteins and activate caspase-activated DNase. Mechanisms for caspase activation include a receptor-ligand binding activation of caspase 8 (Ashkenazi and Dixit 1998; Curtin and Cotter 2003; Lee *et al.* 1997b), a mitochondrial mediated activation of caspase 9 (Bratton and Cohen 2003; Gross *et al.* 1999), and an endoplasmic reticulum related activation of caspase 12 (Szegezdi *et al.* 2003). During the final stage of apoptosis caspase 3 is activated.

TGHQ induces apoptosis in hematopoeic cells (Bratton *et al.* 2000), whereas the nature of cell death pathways in acute renal failure caused by ROS-generating chemicals such as TGHQ is unknown. Whether TGHQ induces oncotic or apoptotic renal cell death will be investigated in Chapter 3.

B. EGFR

The epidermal growth factor (EGF) receptor (EGFR) is activated by ROS in different cellular systems. The EGFR is one family of the growth factor receptor proteins (e.g., EGFR, insulin receptor [IR], platelet derived growth factor [PDGF] receptor). These receptors possess intrinsic tyrosine kinase activity, and are thus called receptor tyrosine kinases (RTKs). RTKs play an important role in a variety of cellular functions, including proliferation/differentiation, migration, metabolism, and survival. The EGFR family consists of four RTKs, EGFR, ErbB2, ErbB3, and ErbB4 (Schlessinger 2000). EGFR is a 170 kDa protein, and consists of several domains (Jorissen *et al.* 2003). The

N-terminal of the EGFR is the extracelluar portion (ectodomain) that contains the ligand binding domain (L1 & L2) rich of glycosylation (IgG like), and the cysteine-rich domain (CR1 & CR2). Juxtamembrane domains (JM) are located within the double layer membrane. The C-terminal domain (CT) of the EGFR contains tyrosine residues that are phosphorylated after ligand-receptor binding, and the tyrosine kinase domain.

1. EGFR Activation and Regulation

Upon ligand (EGF or TGF-α) binding, the EGFR ectodomain dimerizes to form a 2:2 complex (Kim *et al.* 2002; Lemmon *et al.* 1997). Dimerization of the EGFR leads to an autophosphorylation of EGFR, and these phospho-tyrosine sites provide a platform for the binding of a variety of signaling proteins, either directly or indirectly (Schlessinger 2000). EGFR phospho-tyrosine residues are recognized by proteins containing Src-homolgy (SH2) and phosphotyrosine binding (PTB) domains, such as Grb2, Shc and PLC-γ (Schlessinger 2000). The activation of the Ras/MAPK pathway, for example, occurs through phospho-tyrosine→(SH2)Grb2(SH3)→Sos→Ras→Raf→MEK→ERK. Sos is a guanine nucleotide exchange factor, activating Ras via an exchange of GDP to GTP on Ras. The signaling proteins that bind EGFR are listed in Table 1.1, and they lead to the activation of different signaling pathways. Activation of EGFR is tightly regulated by compensatory inhibitory mechanisms. The most commonly observed mechanism of EGFR down-regulation involves the activation of protein kinase C (PKC), which subsequently induces phosphorylation of serine and threonine residues on EGFR, resulting in less tyrosine kinase activity and ligand binding to receptors (Cochet *et al.* 1984). Another mechanism of EGFR down-regulation involves endocytosis and degradation of the receptors, mediated by the binding of Cbl to EGFR (Joazeiro *et al.*

1999). Finally, dephosphorylation of EGFR by phosphatases is another potential mechanism for EGFR deactivation.

2. ROS and EGFR

The EGFR is regulated by ROS, and EGFR itself also induces generation of ROS. There are several possible mechanisms by which ROS mediate EGFR activation. For instance, ROS may mimic EGF:EGFR interaction via modification of cysteine residues on EGFR (Chen *et al.* 1998). ROS may also inactivate phosphatases, thereby inhibiting dephosphorylation of the EGFR (Knebel *et al.* 1996). Finally, ROS inhibit the internalization and degradation of EGFR, thereby enhancing the activation of the EGFR (Ravid *et al.* 2002). On the other hand, EGF (500 ng/ml) also induces a transient increase in the intracellular levels of ROS in A431 human epidermoid carcinoma cells (Bae *et al.* 1997). This phenomenon explains the stimulatory effects of H_2O_2 on glucose transport and lipid synthesis in adipocytes (Mukherjee *et al.* 1978). MAPK activation occurs via EGFR activation in many cell systems. Since TGHQ is redox-active, and causes ROS-dependent MAPK activation, it is likely that quinol-thioether-mediated MAPK activation occurs through the activation of the EGFR. This hypothesis has been tested and is discussed in Chapter 3.

Table 1.1. List of potential binding proteins for EGFR.

Name	**Domain**	**Binding Residue(s)**	**Downstream Effector**	**Key Function**
Src kinases	SH2	pY845, pY1101	ERK,	tyrosine kinase
Shp	SH2	PY1173	kinases	protein tyrosine phosphatase
PLCγ	SH2	pY992, pY1173	PKC	calcium regulation, ERK activation
Grb2	SH2, SH3	pY1068, pY1086	Ras	adaptor protein
Nck	SH2, SH3	N/A	Ser/Thr kinases	adaptor protein
Crk	SH2, SH3	N/A	Ras	adaptor protein
Shc	SH2, PTB	pY1148, pY1173	Ras	adaptor protein
Cbl	PTB	pY1045	Receptor tyrosine kinases	ubiquitin ligase for EGFR degradation
Dok	PTB	pY1086 pY1148	N/A	cell growth, proliferation, differentiation

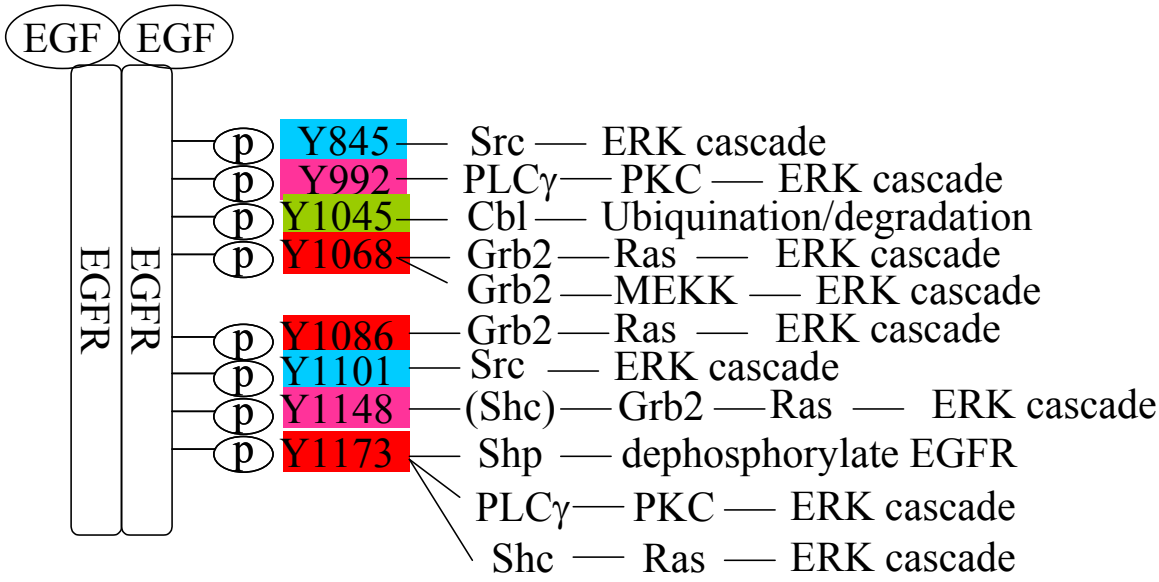

Figure 1.4. Potential phospho-EGFR tyrosine residues and the subsequent signaling cascades.

EGFR tyrosine residues are labeled with different colors according to their binding partners: red, major phospho-tyrosine residues; pink, minor phospho-tyrosine residues; blue, Src kinase binding sites; green, binding site for the EGFR downregulation.

C. MAPKs

1. ROS and MAPKs

Following EGFR activation, the MAPK pathways are activated. Many studies have shown that ROS lead to the activation of MAPKs (Guyton *et al.* 1996; Ramachandiran *et al.* 2002; Wang *et al.* 1998). Prevention of ROS accumulation by antioxidants blocks MAPK activation in various systems. The mechanisms by which exogenous or endogenous ROS activate the MAPKs are not well known, but several mechanisms have been proposed. ROS likely activate the ERK pathway through the activation of EGFR. Alternatively, Ras, an upstream activator of the ERKs could also be activated directly by oxidation of a cysteine residue that resides close to the guanine nucleotide binding site, leading to the subsequent activation of the ERK cascade (Lander *et al.* 1995). Activation of the p38 MAPK and JNK pathways is probably involved in ROS-dependent dissociation of the MKKKs from inactivating regulators (Fanger *et al.* 1998; Saitoh *et al.* 1998). Ask1 is a MKKK for p38 MAPK and JNK, and is associated with reduced thioredoxin (Trx), which negatively regulates the activity of Ask1. ROS cause oxidation of Trx and subsequent dissociation from Ask1, leading to JNK activation (Saitoh *et al.* 1998). 14-3-3 is also found being associated with MKK1, 2, or 3 (Fanger *et al.* 1998).

2. MAPK Cascades

The MAPKs are a family of evolutionary conserved serine/threonine kinases that require phosphorylation of a tyrosine and threonine motif (TxY). This motif is localized in the activation loop and is phosphorylated by a cascade of upstream kinases (Cobb 1999; Torres and Forman 2003). This cascade of kinases is called a MAPK module, and

includes MAPK kinase kinase (MKKK), MAPK kinase (MKK or MEK), and MAPK (See Figure 1.4). MAPKKKs activate MAPKKs, and MAPKKs subsequently activate MAPKs. Overlap between these cascades may occur, but the activation of MAPKs by MAPKKs has relatively higher fidelity. There are four main subfamilies of MAPKs, and they are ERK1/2 (TEY), JNKs (TPY), p38 MAPKs (TGY), and ERK5 (TEY), the last one also refered to as Big MAPK. Each subfamily also has different isoforms, such as ERK1/2, JNK1/2/3, and p38 MAPKα, β1, β2, δ, γ. There is preferential activation of different isoforms by upstream kinase, for example, MKK4 preferentially phosphorylates Y182 of JNK, while MKK7 only phosphorylates T180 of JNK (Wada *et al.* 2001); MKK6, but not MKK3 selectivity activates p38β2, and both MKK3 and MKK6 can activate p38α and p38γ (Enslen *et al.* 1998).

3. ERKs

MAPKs are one of the most important signaling pathways that are activated by mitogenic factors, UV irradiation, oxidative stress, and many others. The ERK cascade is traditionally regarded as mitogenic, and is associated with cell proliferation or differentiation. In contrast, the stress-activated protein kinases (SAPKs), including both JNK and p38 MAPK, are more related to various stresses, and may lead to cell death. Oxidative stress induces intensive activation of ERK1/2, likely via the activation of growth factor receptors, because interference with the activities of these receptors attenuates ERK activation in response to oxidative stress (Knebel *et al.* 1996; Sachsenmaier *et al.* 1994; Zanella *et al.* 1996; Zhougang and Schnellmann 2004). EGFR activation leads to ERK activation through several different signaling pathways. The most well known pathway involves the activation of ERK1/2 by MEK1/2, which is activated by MKKK1 (c-Raf), which is activated by Ras, a binding partner of EGFR

through adaptor proteins, such as Grb2 and Shc. Upon translocation into the nucleus, ERK1/2 activates Rsk2 (Frodin and Gammeltoft 1999), phospholipase A2, Msk1, and a number of transcription factors (Sos, Elk-1, Ets1, Myc, Sap1a, STAT). ERKs are also constantly overexpressed in many tumors, and are current targets for cancer treatment. For instance, PD184352, a pharmacological inhibitor with *in vivo* activity is currently being developed as an anti-cancer drug by Pfizer (Delaney *et al.* 2002). Recent research has revealed that the ERK cascade is also activated by a variety of stresses and is associated with cell death. Thus, *(i)* ERK1/2 inhibition by pharmacological inhibitors protects renal epithelial cells from ROS-induced cell death (Ramachandiran *et al.* 2002), *(ii)* ERK activation is coupled to vanadate-induced oncotic cell death of vascular smooth muscle cells (Daum *et al.* 1998); and ERK1/2 activation is coupled to H_2O_2-induced cell death of *(iii)* oligodendrocytes (Bhat and Zhang 1999); in *(iv)* T cells (van den Brink *et al.* 1999) *(v)* and in pleural mesothelial cells (Jimenez *et al.* 1997).

4. p38 MAPKs

The p38 MAPK pathway is activated by various environmental stresses, including heat, osmotic and oxidative stresses, ionizing radiation and ischemia-induced vasoactive stresses, and inflammatory factors (New and Han 1998). The p38 MAPK pathway, in most studies, is involved in apoptosis, cell motility, transcription and chromatin remodeling. Different p38 MAPK isoforms are activated preferentially by upstream kinases (Chan-Hui and Weaver 1998; Enslen *et al.* 1998). The α and β isoforms of p38 MAPK are the major isoforms studied in cells, and are responsible for activation of MAPK activated protein kinase-2/3 (MAPKAPK-2/3, or MK-2/3) and heat shock protein 25/27 (Hsp25/27). α, γ and δ isoforms of p38 MAPK activate ATF2. Moreover, p38 isoforms have opposite effects on AP-1 dependent transcription through regulation of c-

Jun (Pramanik *et al.* 2003). Inhibitors of the p38 MAPK belong to the category of pyridinyl imidazole derivatives, which bind and inhibit p38 MAPK activation. However, only p38 α and β isoforms are sensitive to these inhibitors, while the other two isoforms are insensitive to these inhibitors (Lee *et al.* 1999).

The differential expression, activation, and substrate specificity of different p38 MAPK isoforms likely result in their various functions in different tissues. For example, p38γ is primarily expressed in skeletal muscle, and p38δ is expressed in lung, kidney, endocrine organs, and small intestine (Hu *et al.* 1999). p38 MAPK activated transcription factors include ATF2, Stat1, Max, MEF-2, Elk-1, CHOP, and CREB. The roles of p38 MAPK in apoptosis are controversial, with evidences supporting pro-apoptotic, anti-apoptotic, and no functions of p38 MAPK in oxidative injury in different systems (Martindale and Holbrook 2002). To the best of our knowledge, the role of p38 MAPK in oncotic cell death has not been well defined, and is discussed in this dissertation.

5. JNKs

The JNK subfamily includes JNK1,2,3, with JNK3 selectively expressed in brain (Davis 2000). JNKs may be activated by heat shock, osmotic stress, pro-inflammatory factors, ischemia, and UV irradiation (Hoeflich *et al.* 1999; Irving and Bamford 2002; Pombo *et al.* 1994). JNK activation often leads to apoptosis, but under certain conditions, it also promotes cell survival (Irving and Bamford 2002), and is involved in tumorogenesis and inflammation. JNKs are activated by MKK4/7, which may be activated by MKKK1 to 4, ASK1, or MLKs. The transcription factors activated by JNKs include c-Jun, ATF-2, Bcl-2, IRS-1, Elk-1, p53, Myc, DPC4, NFAT4.

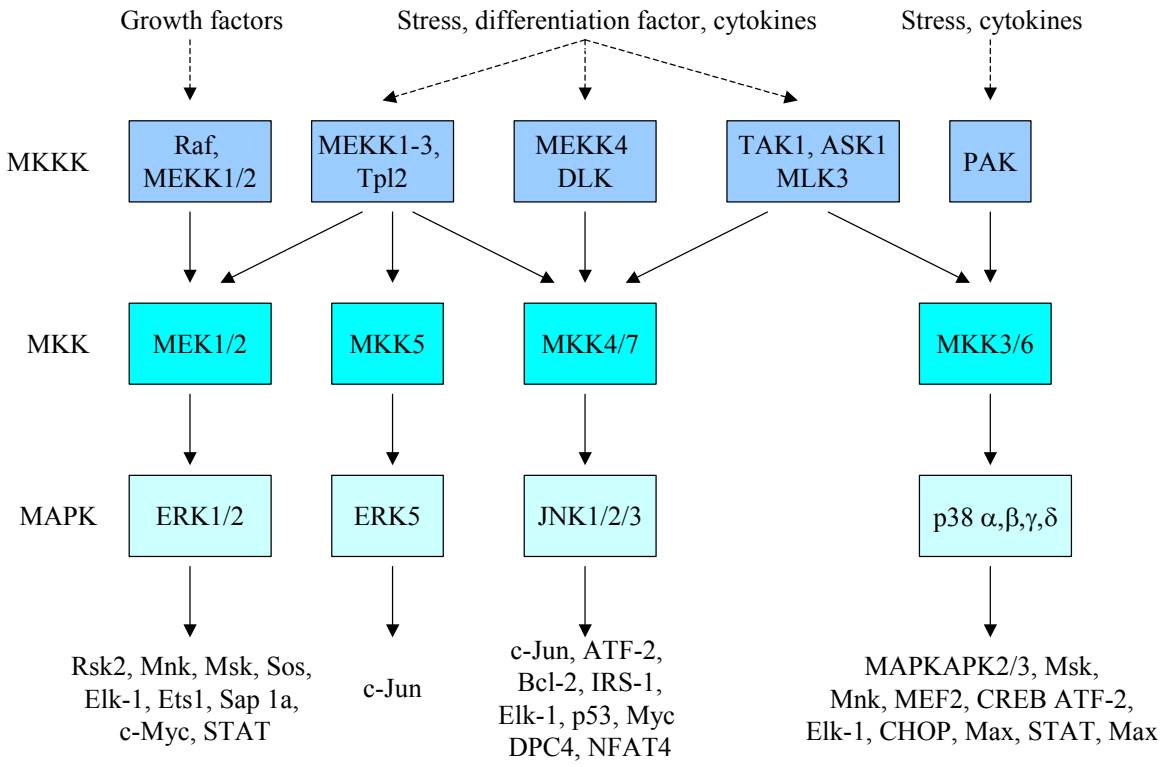

Figure 1.5. The MAPK cascades.

6. Nuclear Translocation of MAPKs and Downstream Effectors

Upon activation, MAPKs translocate from cytoplasm into nucleus to act on downstream transcription factors. As evidence, ERK2 is phosphorylated and is actively imported into the nucleus in a dimeric form, or by diffusion (Adachi *et al.* 1999, 2000; Fukuda *et al.* 1997). ERK2 is dephosphorylated and binds to MEK1 in the nucleus to exit the nucleus, because MEK1 possesses a nuclear export sequence and can facilitate a CRM1-dependent ERK2 export from the nucleus. Leptomysin B, an inhibitor of nuclear export, blocks the nuclear export of ERK2 (Adachi *et al.* 1999, 2000; Fukuda *et al.* 1997). The transcriptional factors targeted by MAPKs include AP-1, CREB, ATF-2, c-Jun, Elk1, Sos, Ets1, Sap1a, c-Myc, STAT. For example, ERKs translocate into the nucleus and phosphorylate/activate Elk-1. Elk1 then binds to the serum response element (SRE) in the promoter element of c-fos gene, activating transcription. AP-1 is a homo- or hetero-dimer of Jun/Fos and ATF families of transcription factors. AP-1 activation increases the transcription of the c-jun and c-fos genes. The induction of a particular gene is complicated, and usually requires more than one transcription factor, and is most likely involves multiple MAPK signaling pathways. In addition to transcription factors, MAPKs also activate kinases such as MAPKAPK1 (Rsk1) (Tan *et al.* 1996), MAPKAPK2/3 (MK-2/3) (Freshney *et al.* 1994; McLaughlin *et al.* 1996), MAPK-interacting kinases (Mnk1/2), and mitogen- and stress-activated protein kinase (Msk) (Deak *et al.* 1998). Except for Msk1, which is localized within the nucleus, all the above kinases are localized in the cytoplasm, and translocate into the nucleus upon activation.

7. Specificity and Regulation of MAPK Activation

The fidelity and specificity of MAPK activation is controlled by scaffold proteins which prevent cross-talk between pathways (Morrison and Davis 2003; Yoshioka 2004). Ste5p is a MAPK scaffold protein in yeast, but no mammalian counterpart of Ste5p has been found. Several other scaffold proteins in mammalian cells have been found to act as a MAPK scaffold, such as MP1, the beta-arrestins, and the JNK-inhibitory proteins (JIPs) (Perry and Lefkowitz 2002; Schaeffer *et al.* 1998; Yasuda *et al.* 1999). Similar to the regulation of EGFR activation, the duration and intensity of MAPK activation is tightly controlled by both positive and negative regulators, such as kinases and phosphatases. The serine/threonine phosphatase PP2a and tyrosine phosphatases can dephosphorylate/inactivate MAPKs. Another family of dual specificity phosphatases called MAPK phosphatases (MKP) can also inactivate MAPKs (Camps *et al.* 2000).

Previous studies in our laboratory have revealed that ERK1/2, p38 MAPK and JNK1/2 are all activated by TGHQ treatment, and are all ROS-dependent in renal proximal tubule epithelial cells (Ramachandiran *et al.* 2002). Inhibition of both ERK and the p38 MAPK pathway, but not the JNK pathway, attenuates TGHQ-induced cell death. Therefore, MAPKs are important in TGHQ-mediated cytotoxicity. A goal of my studies was therefore to determine exactly how MAPKs are activated by TGHQ, and their roles in TGHQ-induced renal cell death. One role of MAPKs is probably to phosphorylate histone H3 via the activation of histone kinases, which could lead to cell death. This hypothesis has proposed as part of this dissertation.

D. Histone H3 Phosphorylation and Cell Death

The eukaryotic genome has enormous length, and therefore requires packaging into a stable structure to prevent damage. During mitosis, correct modification of this higher-order structure allows selective access to genetic information. This higher-order structure is called chromatin, and contains the entire genome and associated proteins. Chromatin is comprised of nucleosomes, which consist of 146 base pairs of DNA wrapped in 1.75 turns around core histones, an octamer formed from two copies each of histone H2A, H2B, H3, and H4, and a linker histone H1. Histones are small basic proteins with a relatively high proportion of lysine and arginine residues, positively charged amino acids. These positive charges assisting in histone binding tightly to negatively charged DNA. At the same time, the location of the N-terminal tails of histones outside of the nucleosomal structure permits their covalent post-translational modification, including phosphorylation, acetylation, methylation, ubiquination, and ADP-ribosylation (Honda *et al.* 1975; Jump *et al.* 1979; Levinger and Varshavsky 1982; Mahadevan *et al.* 1991; Paulson and Taylor 1982; Rea *et al.* 2000), all of which may lead to chromatin remodeling. The combinatorial pattern of histone N-terminal modifications results in a unique identity for each nucleosome that the cell recognizes as a readable code (Nowak and Corces 2004), called the "histone code hypothesis" (Strahl and Allis 2000). Acetylation and methylation of different lysine and arginine residues in histone H3 and H4 are linked to either transcriptional active or repressive states of gene expression (Fischle *et al.* 2003). In contrast, histone H3 phosphorylation is linked to chromosome condensation during mitosis and meiosis, or it can act as a transcriptional activator (Nowak and Corces 2004; Sassone-Corsi *et al.* 1999; Thomson *et al.* 1999; Wei *et al.* 1998). Two phosphorylation residues, S10 and S28 are present in the N-terminus of histone H3. The T11 residue of histone H3 may also be phosphorylated during mitosis

(Preuss *et al.* 2003). S10 phosphorylation of histone H3 is associated with chromosome condensation and mitosis (Strahl and Allis 2000; Wei *et al.* 1998). Histone H3 phosphorylation at Ser10 is also associated with transcriptional activation of c-*fos* and c-*jun* (Sassone-Corsi *et al.* 1999; Thomson *et al.* 1999). Various stimuli, including growth factor, okadaic acid, and stresses, may lead to histone H3 phosphorylation, but likely via the activation of different signaling pathways. Phosphorylation of H3 at S10 is also linked to acetylation of histone at lysine 14 (Lo *et al.* 2000). The S28 residue of histone H3 is phosphorylated at an early stage of mitosis, and is associated with mitotic chromosome condensation (Goto *et al.* 1999).

TGHQ induces oncotic cell death in LLC-PK1 cells, yet the signal transduction pathways involved in this process remain unclear. After TGHQ treatment, there is a rapid and intensive time-dependent histone H3 phosphorylation, along with chromatin condensation, observed morphologicaly (Tikoo *et al.* 2001). For dividing cells, the timing of the initiation of DNA replication (S-phase entry) is rigidly controlled by multiple mechanisms, to prevent excessive DNA replications, as well as to prevent the initiation of mitosis before DNA replication is complete. Entry into mitosis before cells have the correct number of copies of DNA is called “mitotic catastrophe”, and occurs in yeast (Novak and Tyson 1997). Studies have cited this term to describe similar observations of morphological and molecular changes in mammalian systems (Castedo *et al.* 2004; Tikoo *et al.* 2001). Thus, TGHQ generated ROS induce DNA damage and consequent stress signaling pathway activation, whereas histone H3 phosphorylation drives cells into premature chromatin condensation (PCC) and subsequent mitotic catastrophe. The mechanisms coupling TGHQ-generated ROS with histone H3 phosphorylation are unclear. Because some phosphatase inhibitors are also able to induce PCC (Coco-Martin and Begg 1997), protein kinases therefore likely play an important role in this process.

Several kinases have been implicated as potential histone H3 kinases. Msk1 has been described as a potential histone H3 kinase (Thomson *et al.* 1999), and Rsk-2 is another potential histone H3 kinase, which is reported to be responsible for EGF induced phosphorylation of H3 (Sassone-Corsi *et al.* 1999). In addition, Msk1 is activated by both ERK and p38 MAPK (Deak *et al.* 1998), and Rsk2 is activated by ERK. Because phosphorylation of histone H3 at Ser10 and Ser28 is linked to chromatin condensation and early gene expression (c-fos, c-jun), and inhibition of the MAPK pathways lead to attenuation of inducible histone H3 phosphorylation (Tikoo *et al.* 2001; Zhong *et al.* 2001; Zhong *et al.* 2000), histone H3 phosphorylation is linked to MAPK activation. Poly(ADP-ribose)polymerase (PARP) can also cause post-translational modification of histone H3 to remodel chromatin structures (D'Amours *et al.* 1999). PARP is involved in histone shuttling and nucleosomal unfolding (Realini and Althaus 1992), and possibly contributes to histone H3 phosphorylation. Inhibitors of PARP protect against hydrogen peroxide-induced cell death (Chatterjee *et al.* 1999), or shift the mode of cell death from oncotic to apoptotic cell death in oxidant exposed endothelial cells (Walisser and Thies 1999). Interestingly, TGHQ-induced histone H3 phosphorylation is inhibited by the PARP inhibitor, 3-aminobenzamide (Tikoo *et al.* 2001).

TGHQ-induced changes in chromatin structure are preceded by an increase in phosphorylation of histone H3 and a decrease in phosphorylation of histone H2A (Tikoo *et al.* 2001). Dephosphorylation of histone H2A is probably associated with the exit from the cell cycle or cell cycle arrest upon TGHQ treatment (Jeong *et al.* 1997b). TGHQ induces a rapid DNA damage and growth arrest in LLC-PK1 cells that is accompanied by the activation of the growth arrest and DNA damage-inducible gadd153 gene and down-regulation of histone gene expression (Jeong *et al.* 1996; Monks and Lau 1998). Therefore, the dephosphorylation of histone H2A and phosphorylation of histone H3 may

disrupt the interaction between chromatin from the nuclear matrix, further contributing to chromatin condensation (Tikoo *et al.* 2001). TGHQ also induces an initial cell cycle arrest, followed by override of the cell cycle checkpoint, which indicates that cells enter mitosis in an "unprepared" state. Thus, ROS and DNA damage-inducible histone H3 phosphorylation occurs within the content of an overall state of growth arrest and possibly contributes to ROS-induced renal cell death.

E. Other ROS-regulated Signaling Pathways

Since TGHQ can generate ROS both intracellularly and extracellularly, and TGHQ-induced cell death is ROS-dependent, oxidative stress induced responses must be important upon TGHQ treatment. We have found that EGFR, MAPKs, and histone H3 are all regulated by ROS, and there remain some other pathways to be revealed that are targeted by ROS. A proteomics study has revealed novel TGHQ-induced changes in several proteins, including Hsp27 and peroxiredoxins (Prxs), both of which were found to be modified followed TGHQ treatment. These data will be discussed in Chapter 4.

1. Heat Shock Protein 27

Hsp27 belongs to the small heat shock protein family (sHsp), which is constitutively expressed in virtually all organisms and with a molecular weight ranging from 15-42 kDa (Ehrnsperger *et al.* 1998). sHsps can undergo oligomerization to form oligomeric complexes of up to 1 MDa. sHsps seem to play roles in different cellular processes, such as heat resistance (Knauf *et al.* 1994), RNA stabilization (Nover *et al.* 1983), interaction with the cytoskeleton (Miron *et al.* 1991; Nicholl and Quinlan 1994), and apoptosis (Arrigo 1998; Mehlen *et al.* 1996b). sHsps also act as chaperones to prevent aggregation of unfolded proteins, by facilitating refolding of denatured or

malfolded proteins (Ehrnsperger *et al.* 1997; Horwitz 1992; Jakob *et al.* 1993; Lee *et al.* 1997a; Merck *et al.* 1993).

Both mouse Hsp25 and human Hsp27 are responsive to cellular stress. Heat shock increases both the expression and phosphorylation of Hsp27 and Hsp25, with phosphorylation more rapid (minutes) than induction of expression (hours) (Landry *et al.* 1991). Since the kinetics of phosphorylation versus induction of expression are distinct, the acute effects mediated by ROS can be solely designated as post-translational. There are several residues in Hsp27 that can be phosphorylated, including S15, S78, and S82 (Gaestel *et al.* 1991; Landry *et al.* 1992). Additionally, both S15 and S82 are evolutionary conserved phosphorylation residues, whereas S78 is not (Ehrnsperger *et al.* 1998). Stress-induced phosphorylation of Hsp27 occurs subsequent to the activation of the p38 MAPK cascade, and MAPKAPK2/3 are direct upstream kinases for Hsp27 phosphorylation (Guay *et al.* 1997; Ludwig *et al.* 1996; Rouse *et al.* 1994; Stokoe *et al.* 1992). Hsp27 may also be phosphorylated by other classes of kinases, such as cGMP-dependent protein kinase, casein kinase, cAMP-dependent protein kinase, PKC, and Akt (Butt *et al.* 2001; Rane *et al.* 2003). Upregulation of Hsp27 within certain cells is capable of protecting cells from stress (Arrigo 1998; Baek *et al.* 2000; Landry *et al.* 1989; Lee *et al.* 2004; Mehlen *et al.* 1993; Park *et al.* 1998). Hsp25 overexpression also down-regulates ERK2 expression, and the suppression of ERK2 is involved in cytoprotection against irradiation-induced damage (Cho *et al.* 2002).

There are two types of modification for Hsp27, phosphorylation and S-thiolation (Summarized in Firgure 1.5). Phosphorylation of Hsp27 is known to lead to changes in the oligomeric organization of Hsp27, either resulting in smaller (Kato *et al.* 1994; Lavoie *et al.* 1995). Small oligomers and monomers are likely responsible for the stabilization of actin filaments (Benndorf *et al.* 1994; Lavoie *et al.* 1993a; Lavoie *et al.*

1993b). In contrast, large oligomers protect cells against various stresses (Ehrnsperger *et al.* 1997; Lee *et al.* 1997a; Mehlen *et al.* 1997; Preville *et al.* 1998). The influence of the changes in Hsp27 structures on its chaperoning activity has been characterized (Rogalla *et al.* 1999). Using mutants that mimic Hsp27 phosphorylation (S15D, S78+82D, and S15+78+82D), constitutive phosphorylation of Hsp27 at all three residues was found to decrease the chaperone function of Hsp27 (Rogalla *et al.* 1999). Unphosphorylated Hsp27 forms an oligomeric complex, whereas phosphorylated Hsp27 forms quaternary structures. The loss of the chaperone function of Hsp27 must be due to its altered oligomerization post phosphorylation. Interestingly, transfection of mutants (S15D or S78+82D) into L929 cells decreases TNF-α– and H_2O_2-induced cell death, but transfection of mutant (S15+78+82D) cannot decrease stress-induced cell death (Rogalla *et al.* 1999). This indicates that partial blocking of Hsp27 phosphorylation does not decrease the chaperoning function of Hsp27, and therefore the mutant transfections grant the cells an overall increase in large Hsp27 oligomers, with subsequent cytoprotective effects. These data suggest that a higher degree of oligomerization of Hsp27 is necessary for its full protective effects (chaperone functions), which is abolished when the three serine residues are all phosphorylated. Furthermore, phosphorylation of S82 of Hsp27 is located at the beginning of the second β-strand (β2) of Hsp27, which might influence the interaction between β2 and β6 of two different monomers, resulting in smaller oligomers.

Besides phosphorylation, S-thiolation of Hsp27 also regulates its multimeric aggregate size, independently of phosphorylation (Eaton *et al.* 2002). During oxidative stress, a cysteine residue in rat cardiac Hsp27 is S-thiolated, and this modification, without phosphorylation, disaggregates multimeric Hsp27. These two independent mechanisms (phosphorylation and S-thiolation) ensure dissociation of large oligomeric Hsp27 into small oligomers or monomers, indicating that this process is necessary during

cellular stress. Therefore, Hsp27 may have multiple functions in different forms. Under non-stressful conditions, Hsp27 functions as a chaperone to assist in protein folding, whereas during stress, Hsp27 phosphorylation leads to breakdown of large Hsp27 oligomers into small oligomers and monomers, which subsequently bind to the cytoskeleton (actin, desmin, or membrane proteins) (Barbato *et al.* 1996; Bennardini *et al.* 1992).

Overexpression of nonphosphorylatable mutants of sHsps in attachment-independent cells (Ehrlich ascites tumor cells and Raf transformed NIH 3T3 cell) confers stress-resistance, whereas in attachment-dependent cells (hamster fibroblast CCL39 cells) these mutants fail to confer stress-resistance (Lavoie *et al.* 1995). This is possibly due to the multiple functions of Hsp27 and post-translationaly modified Hsp27 in different cells, as discussed above. The observation that mutant Hsp27 (S15+78+82D) did not protect cells from the cytotoxic effects of H_2O_2, menadione, and TNF-α is in agreement with the finding that nonphosphorylatable mutants of Hsp25 (S15A, S86A) and Hsp27 (S15+78+82A) form large oligomers and protect against oxidative stress in NIH 3T3-Ras and L929 cells (Mehlen *et al.* 1997; Preville *et al.* 1998). Therefore, the presence of large oligomers of Hsp27 and their chaperoning function may be important in protecting cells against ROS-induced cytotoxicity. These studies, while shedding light on the role of phosphorylated Hsp27 in stress-induced cell death, also serve to highlight the complexity within the Hsp27 stress response. Moreover, Hsp27 is associated with Akt (Konishi *et al.* 1997; Rane *et al.* 2003), and controls apoptosis by regulating Akt activation (Rane *et al.* 2003). Phosphorylation of Hsp27 at S82 both *in vitro* and in intact cells dissociates Hsp27 from Akt. The association between Hsp27 and S82 is also needed for the activity of Akt in neutrophils (Rane *et al.* 2003), which could be due to loss of the chaperoning function of Hsp27 upon phosphorylation. Inactivated Akt, in sequestration with Hsp27,

enhances the constitutive neutrophil apoptosis, and this process is reversed by introduction of constitutively active Akt. These observations are supported by other studies that found that Hsp27 inhibits apoptosis through inactivation of caspase 3, caspase 9, and cytochrome C (Bruey *et al.* 2000; Garrido *et al.* 1999; Pandey *et al.* 2000; Paul *et al.* 2002). Whether unphosphorylated Hsp27 oligermers bind to other signaling factors, especially those contributing to ROS-induced damage, would be interesting to investigate.

The ability of sHsps to protect against oxidative stress is also reported to be dependent on their abilities to increase intracellular concentration of GSH (Mehlen *et al.* 1996a), and to maintain the reduced form of GSH during oxidative stress. The chaperoning function of Hsp27 is also likely involved in the regulation of intracellular GSH levels and initiating oxidative stress, thus contributing to its protective effects. In support of this view, mutant Hsp27 (S15+78+82D) overexpressed in NIH 3T3-Ras cells is not able to increase intracellular GSH levels (Gao and Lenard 1995). Exactly how the chaperoning function of sHsps protect cells against cellular stress is unknown. However, one model proposes that sHsps actually bind to unfolded proteins and facilitate their transfer to ATP-dependent chaperones, such as Hsp70, which subsequently refold the malfolded proteins (Ehrnsperger *et al.* 1997), or direct the bound proteins for ubiquination and degradation (Parcellier *et al.* 2003b). Phosphorylation of sHsps releases the unfolded proteins, which cannot then be transfered to Hsp70 to be refolded, or degraded. On the other hand, sHsps could translocate from the cytoplasm to nucleus under stress in different cellular systems (Arrigo *et al.* 1988; Preville *et al.* 1998; Rossi and Lindquist 1989). Phosphorylation of sHsps could facilitate this stress-dependent nuclear translocation, which is probably also associated with the chaperoning functions of sHsps in the nucleus, since overexpression of Hsp27 in cells increases their recovery

from nuclear protein aggregation (Kampinga *et al.* 1994). Thus, phosphorylation of Hsp27 induces a transition from large oligomers to the smaller tetrameric rod-like particles, which are more easily translocated into the nucleus. Phosphatases in the nucleus may dephosphorylate Hsp27 and stimulate the formation of large oligomers that possess chaperoning functions.

Finally, sHsps also contribute to the stabilization of intracellular actin filaments and contribute to the regulation of the organization of the cytoskeleton (Lavoie *et al.* 1993a; Lavoie *et al.* 1993b; Lavoie *et al.* 1995). In contrast to the chaperoning function of sHsps that requires large oligomers, the actin stabilizing function of sHsps requires small oligomers or monomers of Hsp27 (Benndorf *et al.* 1994). Hsp27 binding to actin and regulation of the polymer dynamics of the cytoskeleton may allow Hsp27 to intervene during stressful events, and to provide cytoprotection (Huot *et al.* 1996; Landry and Huot 1995; Wang and Spector 1996). Nevertheless, Hsp27 phosphorylation also leads to F-actin polymerization, which is associated with misassembly of focal adhesions that is responsible for the induction of membrane blebbing mediated by various stressful agents (Huot *et al.* 1998). The appropriate timing and location of Hsp27 phosphorylation possibly determines whether Hsp27 is cytoprotective or deterious. In conclusion, many factors determine the roles of Hsp27 and its modification, including different cellular systems, stimuli, modifications of Hsp27, cellular locations, and timing, which in combination contribute to the observed contradictory roles of Hsp27.

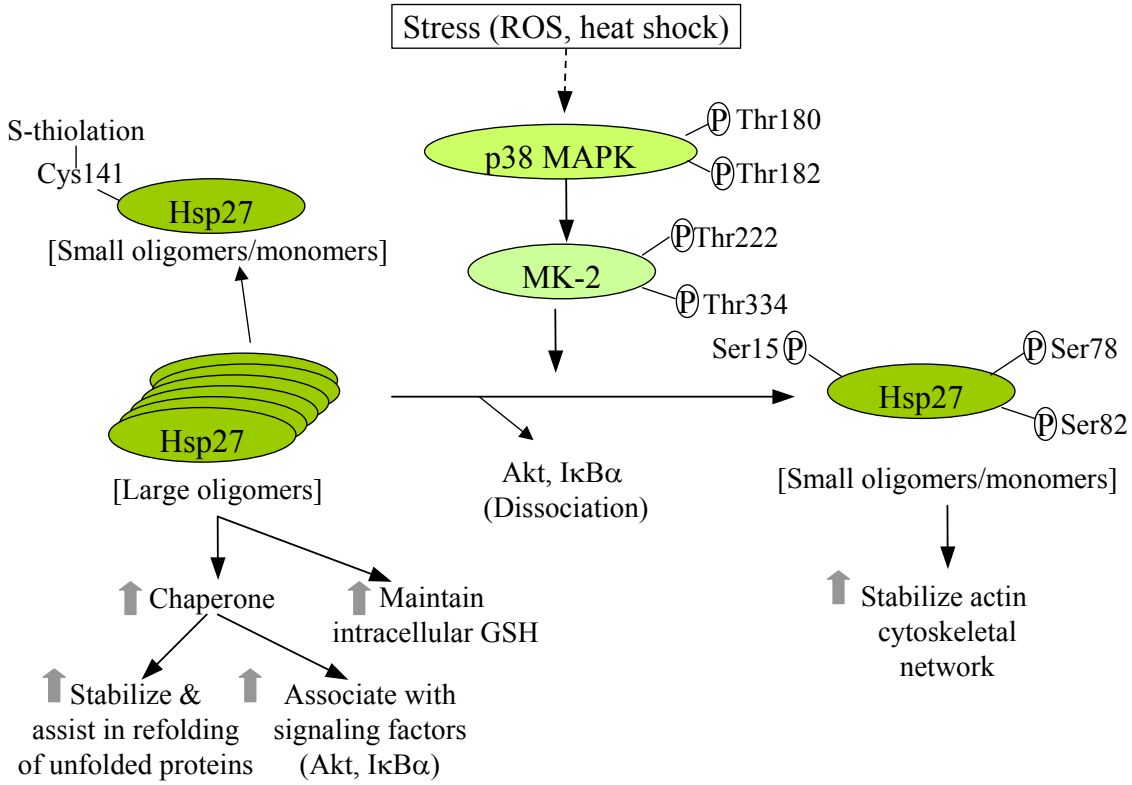

Figure 1.6 Roles for Hsp27 and the consequences of post-translational modifications (phosphorylation or S-thiolation).

Stress such as ROS and heat shock induce the activation of the p38 MAPK cascade, leading to Hsp27 phosphorylation (S15, S78, S82). Unphosphorylated Hsp27 (large oligomers) is associated with its chaperoning function and maintainence of intracellular GSH concentration in response to stress. In contrast, phosphorylated Hsp27 (small oligomers/monomers) assist in stabilizing the actin cytoskeletal network. S-thiolation on the Hsp27 cysteine residue (Cys141) by ROS also induces a break down of large oligomers into smaller oligomers and monomers, which have a similar function as phosphorylated Hsp27.

2. Peroxiredoxins

As discussed above, ROS possibly function as second messenger molecules, generated through a receptor-dependent pathway (Bae *et al.* 1997; Sundaresan *et al.* 1995; Ushio-Fukai *et al.* 1999). But ROS are too simple structurally to be specifically recognized by other signaling factors/proteins. Therefore, ROS possibly function as second messenger by oxidizing other proteins on their cysteine residues. Only certain proteins possess cysteine residues that are susceptible to H_2O_2 (Kim *et al.* 2000). Thus, cysteine residues form cysteine thiolate anion ($Cys\text{-}S^-$) when nearby positively charged amino acid residues are available for interaction with the negatively charged thiolate anion group (Kim *et al.* 2000). Proteins with these low p*K*a cysteine residues are readily oxidized by H_2O_2, and the reaction is reversible by thiol donors such as GSH and Trx. Examples of such proteins include protein tyrosine phosphatase (PTP), and peroxiredoxins (Prx). In this session we will focus on discussing Prxs.

There are several enzymes which can eliminate intracellular ROS, such as SOD, catalase, glutathione peroxidase, and Prx. Prx is a family of peroxidases that use Trx to reduce H_2O_2 and alkylhydroperoxidates (Chae *et al.* 1994b; Rhee *et al.* 2001). Prx have received considerable attention in recent years as a new family of thiol-specific antioxidant proteins. Prxs are ubiquitously expressed in a wide range of organisms, and are abundantly expressed in cells. The peroxidase function of Prxs actually overlap with glutathione peroxidases and catalase, but exhibit moderate catalytic efficiencies when compared to these other two enzymes. Therefore, the peroxidase function of Prxs is questionable. Nonetheless, the high abundance of Prxs in cells makes their presence as a peroxidase important. Recently, a range of other roles have been described for Prx family

members, including the modulation of cytokine-induced H_2O_2 levels, and interacting with MAPKs (Butterfield *et al.* 1999; Rogalla *et al.* 1999).

There are six known mammalian Prxs, with Prx1-4 having two conserved cysteine residues (2-Cys Prxs), and Prx6 having only one conserved cysteine residue involved in their peroxidase activity (1-Cys Prx) (Kang *et al.* 1998b; Kim *et al.* 1988; Lim *et al.* 1994). Prx5 also possesses two cysteine residues, yet the cysteine residue in the N-terminus is not conserved. All Prxs contain a reactive cysteine in a conserved region near the N-terminus, and this catalytic residue forms cysteine-sulfenic acid as a reaction intermediate during the reduction of peroxide (Claiborne *et al.* 2001). Prx1-4 contain an additional cysteine residue at a conserved position near the C-terminus, while Prx5 contains an additional cysteine residue in the less conserved C-terminus, and Prx6 contains only one cysteine residue. The cysteine residue in the N-terminus of Prx1-4 is separated from the cysteine residue in the C-terminus by 120-123 amino acids, and the sequences surrounding each of these cysteine residues are also highly conserved. Prxs exist as homodimers, with the two monomers arranged in a head-to-tail manner (Chae *et al.* 1994c; Choi *et al.* 1998; Hirotsu *et al.* 1999). The subcellular localization of the Prxs basically covers all the locations ROS are produced, and Prxs are able to translocate in response to stimuli, as demonstrated for Trx (Nakamura *et al.* 1997). For instance, Prx1 and 2 exist in cytosol, Prx3 exists in mitochondria, Prx4 is a secreted protein, Prx6 is present in the plasma membrane, and Prx5 is found in mitochondria, peroxisomes, and cytosol (Fujii and Ikeda 2002).

The catalytic mechanism of Prxs has been established (Rhee *et al.* 2003) (Figure 1.7). The N-terminal cysteine residue is oxidized by ROS to cysteine sulfenic acid (Cys-SOH), which is not stable. The Cys-SOH then reacts with the C-terminal cysteine residue of the second subunit of the homodimer to form an intermolecular disulfide. The disulfide

is then reduced by Trx (Chae *et al.* 1994a). Because the formation of the disulfide is a slow process, the sulfenic intermediate is occasionally hyperoxidized into sulfinic acid (Cys-SO_2H) and sulfonic acid (Cys-SO_3H), which results in loss of Prx function (Chae *et al.* 1994a; Rabilloud *et al.* 2002; Yang *et al.* 2002) (Figure 1.7). Proteins that contain hyperoxidized cysteine residues are identified in 2-dimensional polyacrylamide gels as the satellite spots with more acidic pIs corresponding to the unoxidized form of the protein (Rabilloud *et al.* 2002). Thus, after ROS treatment (tert-butyl hydroperoxide [BHP], or glucose oxidase), a satellite spot with a more acidic pI was found in addition to the spot with more basic pI, both identified as Prx2 or Prx3 (Rabilloud *et al.* 2002). LC-MS/MS confirmed the modification of Prx2 as oxidation, and this oxidation was reversed in an ROS-free medium (Rabilloud *et al.* 2002). The reversible oxidation is also confirmed by immunoblots using specific antibodies to the sulfonylated Prx peptides (Woo *et al.* 2003b). The sensitivity of 2-Cys Prxs to inactivation by hyperoxidation is not a limitation of the Prxs catalytic mechanism, but rather an evolutionary selection for eukaryotes (Wood *et al.* 2003). Interestingly, Prx1 and 2 may also be phosphorylated specifically at the T90 residue by several Cdks, including Cdc2 kinase (Chang *et al.* 2002), and this phosphorylation causes a decrease in Prx activity. Cdc2 kinase is inactivated by low dose of TGHQ treatment (100 μM), but this inhibitory effect is overriden at high doses of TGHQ treatment (200-400 μM) (Ramachandiran, unpublished data). Cdc2 activation is linked to cell cycle progress into mitosis, and is closely related to chromatin remodeling and condensation. Therefore, ROS generation by TGHQ likely regulate Prxs through both direct oxidation and indirect phosphorylation by the activation of Cdc2 kinase.

Other functions of Prxs in addition to its peroxidase activity have recently been discovered. For example, overexpression of Prxs in a variety of cells reduces intracellular

levels of ROS, and blocks apoptosis, indicating Prxs serve as anti-oxidants and as a signaling molecule (Jin *et al.* 1997; Kang *et al.* 1998a; Kang *et al.* 1998b; Nonn *et al.* 2003; Zhang *et al.* 1997). *In vivo*, 2-Cys Prxs are required for Myc-mediated transformation and apoptosis (Mu *et al.* 2002; Wonsey *et al.* 2002), and can regulate NF-κB activation (Jin *et al.* 1997; Kang *et al.* 1998b). Because H_2O_2 a cellular damaging agent as well as a second messenger in signaling pathways, the question arises as to what precisely determines the cellular responses to ROS. We know that the amount of ROS determines responses, and Prxs can function as an intracellular switch for the consequences of ROS. Since Prxs are ubiquitously expressed in cells, and are reversibly oxidized by ROS, they are the ideal candidates as a molecular switch for the different effects of ROS. Prxs are present in the cells in large amounts, and ensure that ambient levels of peroxides are maintained at very low levels to ensure no inappropriate signaling is triggered by ROS. In contrast, a burst of exposure of cells to ROS inactivates Prxs rapidly, and these ROS could then act as second messengers by interacting with other proteins, such as phosphatases (Wood *et al.* 2003).

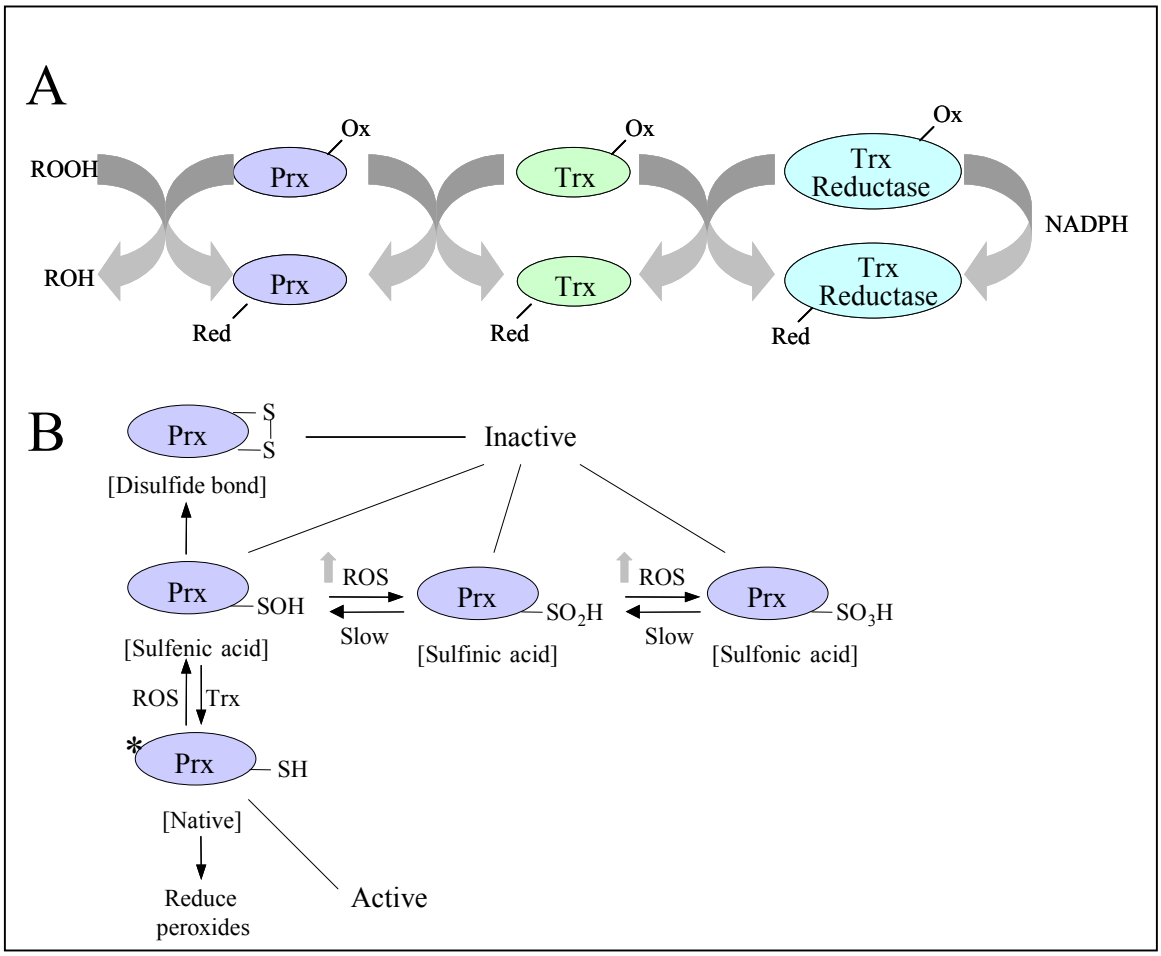

Figure 1.7 The peroxidase reaction of Prx and the oxidation of Prx.

A. The reduction of peroxides by Prx. Prx is subsequently reduced by the Trx and Trx reductase system. **B.** Oxidation of Prx cysteine residues to sulfenic (SOH), sulfinic (SO_2H), or sulfonic (SO_3H) acids. Only the reduced form of Prx (SH) is active as a peroxidase. The cysteinyl sulfenic acid or disulfide is easily reduced by Trx, whereas reduction of the cysteinyl sulfinic or sulfonic acids is relatively slow and requires an unknown reductase(s).

F. Inhibitors of Signaling Pathways

Pharmacological inhibitors have been widely used in the studies on signal transductions. Most of the inhibitors are ATP-competitive, except PD98059, PD184352 U0126, and Li^+ (Cohen 1999). PD98059 binds to unphosphorylated rather than phosphorylated MKK1 (also called MEK1), and prevents its activation by upstream kinase MKKK1 (Alessi *et al.* 1995). At a concentration of 50 μM, PD98059 prevents activation of the classical MAPK cascade in cell-based assays but does not inhibit other kinases (Davies *et al.* 2000). PD98059 also prevent the activation of ERK5, another MAPK family member. The concentration needed to inhibit ERK5 activation was comparable to that to inhibit MEK1 (Davies *et al.* 2000). PD98059 is also known to inhibit cyclo-oxygenases 1 and 2, which are required for production of prostaglandins and leukotrienes (Borsch-Haubold *et al.* 1998). Another MEK1 inhibitor that functions similar to PD98059 is U0126, and it does not inhibit COX1&2 yet is more potent than PD98059 (Davies *et al.* 2000). PD184352 is another potent MEK1 inhibitor, and is applicable *in vivo* (Delaney *et al.* 2002). SB202190 and SB203580 are two pyridinyl imidazoles that inhibit the activity of p38 MAPK α and β isoforms, but not δ and γ isoforms (Davies *et al.* 2000). SB202190 has specificity similar to that of SB203580, which has high degree of specificity toward other protein kinases, including a number of closely related MAPK family members (Cuenda *et al.* 1995). However, Raf, PDK1 and LCK are inhibited by SB203580, but less potently than p38 MAPK (Davies *et al.* 2000). AG1478 (tyrphostin, 4-[3-chloroanilino]-6,7-dimethoxyquinazoline) is a potent ATP-dependent inhibitor of EGFR (Levitzki and Gazit 1995). At a concentration of 0.25 mM, AG1478 blocks EGF-mediated cell cycle progression, proliferation and Src kinase activation (Levitzki and Gazit 1995). Pharmacological inhibitors are beneficial because

they can be used simply and rapidly for various researches, and they don't cause artificial up- or down-regulation of signaling pathways by genetic manupulation of kinases. But there are concerns on the specificity of these inhibitors, which should be taken into consideration during experimental designs.

IV. DISSERTATION AIMS

Because of the ubiquity of quinones and quinone-derivatives and subsequent constant human exposure, we performed studies to elucidate the mechanisms by which quinones and quinone metabolites produce their adverse effects. GSH conjugation to hydroquinone accounts for hydroquinone's nephrotoxicity and nephrocarcinogenicity. In particular, TGHQ is even more reactive than hydroquinone. The renal selectivity of polyphenolic GSH conjugates is due to the high activity of enzymes which further metabolize GSH-conjugates of quinones and which faciliate the uptake of the metabolites into target cells. Due to the abilities of quinol-thioethers to redox cycle and alkylate macromolecules, two coupled properties, these chemicals or their metabolites are extremely toxic to cells. It is most likely that the nephrotoxicity and/or nephrocarcinogenicity induced by GSH conjugates of quinones is due to their reactive biological properties. Thus, TGHQ is metabolized by γ-GT and dipeptidase to generate a cysteine conjugate of hydroquinone, which can be transported into cells by the L-amino acid transporter. TGHQ generates ROS both exogenously and endogenously, providing a good example to study the mechanisms of nephrotoxicity and nephrocarcinogenicity induced by similar chemicals.

The molecular mechanisms of quinone-thioether induced acute nephrotoxicity and nephrocarcinogenicity are not clear. Although substantial studies have been performed to

understand ROS-mediated signaling pathways within cell systems and in animal models, relatively less is understood on the molecular mechanisms by which ROS-generating chemicals mediate acute toxicity and carcinogenicity. In this dissertation, I have endeavored to define the molecular mechanisms of TGHQ-mediated nephrotoxicity and nephrocarcinogenicity, by understanding ROS and alkylation mediated adverse effects in renal cells. There are two types of cell death, oncotic and apoptotic cell death. The first goal of my study was to define the type of renal cell death induced by TGHQ. Previous studies have found that TGHQ induces DNA damage, growth arrest, and rapid cell death in LLC-PK1 cells. TGHQ also induces DNA damage (8-oxo-dG), acute nephrotoxicity, and nephrocarcinogenicity in rats. Multiple signaling pathways are activated by TGHQ treatment, and MAPKs are all activated by TGHQ, rapidly and intensively in renal cells. Histone H3 is phosphorylated by TGHQ treatment, a response linked to ERK pathway activation. Histone H3 phosphorylation under oxidative stress likely causes premature chromatin condensation and mitotic catastrophe, leading to cell death. However, relatively less is known of how MAPKs are activated, and a systematic understanding of the signaling pathways activated in association with histone H3 phosphorylation is needed. The first Specific Aim of this dissertation is to find out how MAPKs are activated, and how MAPKs are linked to histone H3 phosphorylation and cell death.

p38 MAPK is responsive to oxidative stress, and has differential functions in different cell systems. TGHQ induces a rapid activation of p38 MAPK, and the activation is linked to TGHQ-mediated renal cell death. However, what is the role or mechanism of action of p38 MAPK in TGHQ-induced renal cell death? One mechanism of p38 MAPK-mediated renal cell death, as stated, is probably through the activation of histone kinase(s), which phosphorylate histone H3 to induce premature chromatin condensation and mitotic catastrophe. However, there are many substrates for p38 MAPK, some of

which are kinases, and some are transcription factors. But since TGHQ-mediated cell death is rapid (60% live cells following a 2 h treatment with 200 μM of TGHQ), the molecular changes must largely be due to post-translational modifications. In addtion to histone kinases, there could be other key kinases downstream of the p38 MAPK cascades that are activated and contribute to the determination of cell fate during oxidative stress. A proteomics study revealed changes in Hsp27, a downstream effector of p38 MAPK, after TGHQ treatment. Therefore, further investigations into the roles of p38 MAPK signaling pathways involved in TGHQ-mediated cell death are included in this dissertation.

Oxidative stress tends to influence a combination of signaling pathways in different cells, a network of signaling pathways that is fairly complicated and which likely involves substantial cross-talk. For example, H_2O_2 can inhibit phosphatases, and therefore indirectly "activate" a number of kinases. ROS may also oxidize thiol-containing molecules, such as GSH, Trxs, and Prxs, which are the first defense against oxidative stress. Extensive ROS generation causes depletion or loss of functions of these anti-oxidant proteins, which leads to the activation of a number of signaling pathways. In addition, alkylation of macromolecules by quinones or quinone-thioethers may also lead to signaling activation. Due to the complex nature of the oxidative-response system, and the development of new techniques for high throughput screening for cellular responses to stimuli, I intend to use these techniques to discover meaningful and novel targets during TGHQ-induced renal cell death. The results I acquire will persuit have a new and generic view of the most dramatic signaling changes induced by TGHQ. Subsequent studies to confirm these results, and analysis of the association of these signaling pathways compared to previous findings, may assist in providing a better understanding of the mechanisms of TGHQ-mediated renal cell death.

TGHQ induces renal tumor in Eker rats, likely acting as an initiator. Eker rats possess a germ-line insertion in one allele of the *Tsc-2* gene, which predisposes these animals to the development of renal tumors. Repeated doses of TGHQ cause nephrotoxicity in the OSOM region of the kidneys, and subsequent excessive proliferation, which likely enhances the DNA damage caused by TGHQ treatment, leading to tumor formation. Loss of heterozygosity was found in TGHQ treated Eker rats, confirming that genetic instability is amplified by the compensatory proliferation of renal tubule cells after toxicity. Studies have linked tumor formation to loss of tuberin function following chronic administration of TGHQ. DNA damage was found following acute treatment of Eker rats with TGHQ, evidenced by the formation of 8-oxo-dG. TGHQ also upregulates Raf and ERK activities in TGHQ transformed QT-RRE cells. Because nephrotoxicity precedes nephrocarcinogenicity, and the toxicity-induced cellular responses contribute to the ultimate tumor formation, studies on the early molecular mechanisms of nephrotoxicity leading to nephrocarcinogenicity are important. Therefore, the last Specific Aim of this dissertation was designed to examine the early molecular changes that occur in TGHQ-treated Eker rats, focusing on the MAPKs and histone H3 phosphorylation, targets identified by *in vitro* studies. These studies, hopefully, will shed light on the molecular mechanisms possibly involved in later nephrocarcinogenicity.

In summary, this dissertation focuses on deciphering the signaling pathways involved in quinol-thioether-mediated renal cell death, and attempts to contribute to an understanding of the nephrotoxicity and nephrocarcinogenicity induced by ROS generating or alkylating chemicals. A significant number of chemicals are known to cause renal disease and toxicity, a majority of them being redox-active and generating ROS. Therefore, I hope that the studies and discussion in this dissertation will provide

important information on the mechanisms of ROS induced renal disease, and contribute to future therapeutic intervention and prevention of ROS-related renal disease.

Chapter 2: MATERIALS AND METHODS

I. MATERIALS

A. Chemicals and Reagents

2,3,5-Tris-(glutathion-S-yl)hydroquinone (TGHQ) was freshly synthesized and purified according to established protocols (Lau *et al.* 1988), and used at >98% purity. PD98059, SB202190, SB203580, U0126 were purchased from CalBiochem (San Diego, CA). AG1478 was obtained from Biomol Biomolecules (Plymouth Meeting, PA). FuGENE 6 Reagent for transfection was purchased from Roche Molecular Biochemicals (Indianapolis, IN). Plasmid DNA purification kit was purchased from QIAGEN (Valencia, CA). Annexin V-PI apoptosis detection kit was purchased from Beckman Coulter, Inc. (Fullerton, CA). Antibiotics were all purchased from Invitrogen (Carlsbad, CA). Antibodies were purchased from either Cell Signaling Technology, Inc. (Beverly, MA), Upstate Biotech. Inc. (Lake Placid, NY), Santa Cruz Biotechnology (Santa Cruz, CA), Stressgen (Victoria, BC, Canada), or BioSource International, Inc. (Camarillo, CA). Prx3 antibody was generously provided by Dr. Garth Powis (University of Arizona Cancer Center, AZ). ABC immunostaining kits were purchased from Santa Cruz Biotechnology (Santa Cruz, CA). All other chemicals were from Sigma (St. Louis, MO) or Fisher Scientific (Houston, TX), and of the highest grades available.

B. Plasmids

The plasmids pcDNA3 containing a cDNA of wild type p38 MAPK, or dominant negative mutant p38 MAPK were kindly provided by Dr. Roger Davis (University of Massachusetts, Worcester, MA). Plasmids pcDNA3.1 containing mutated Hsp27s that

mimics the phosphorylated Hsp27 (S15, S78, S82 mutated to D15, D78, D82), or unphosphorylated Hsp27 (S15, S78, S82 mutated to A15, A78, A82) were generously provided by Dr. Michael J. Welsh (University of Michigan, Ann Arbor, MI). Plasmids pcDNA3, pcDNA3.1 were both purchased from Invitrogen (Carlsbad, CA).

II. METHODS

A. TGHQ Purification

TGHQ was freshly synthesized and purified according to established protocols (Lau *et al.* 1988). Briefly, 200 mM of GSH in 50 mL water was added drop wise to 1,4-benzoquinone (200 mM in 50 mL water) with stirring. The mixture was stirred at room temperature for additional 30 min, and was extracted twice with 3 volumes of ethyl acetate (HPLC grade) to remove residual 1,4-benzoquinone and hydroquinone formed by reduction. The organics in the aqueous phase extract were removed with a roto-evaporator. The extraction was then frozen on dry ice in acetone, and lyophilized. The resulting crystals were dissolved in 1% acetic acid, and injected onto a Beckman Ultrasphere ODS reverse phase column. Fractions of TGHQ were collected, pooled, frozen, and lyophilized. The purity of TGHQ was examined by HPLC, and had identical HPLC retention times and exhibited characteristic UV absorption spectra when compared to previously synthesized authentic standards.

B. Cell Culture and Treatment Regimen

LLC-PK_1 cells (American Type Culture Collection, Rockville, MD), a renal proximal tubule epithelial cell line derived from the New Hampshire Mini-Pig, were maintained in Dulbecco's modified Eagle's medium (DMEM) containing 10% fetal

bovine serum (FBS) at 37°C in a humidified incubator, with 5% carbon dioxide. Cells were plated in 24-well, 12-well, 6-well plates, or in 100 mm dishes, as needed, and grown to 70-80% confluence before treatment. Cells were then washed once, and treated with various agents in DMEM containing 25 mM HEPES. Cells were washed three times with DMEM containing 25 mM HEPES to terminate treatment, and subject to various analyses.

C. Experimental Protocols

1. Neutral Red Assay

To determine the viability of LLC-PK_1 cells after challenge with various agents, Neutral Red uptake was determined as previously described (Mertens *et al.* 1995). Briefly, cells were plated in 24-well plates at a density of 5×10^4 cells/well, and used upon reaching 70% confluence. Cells were washed once and treated with various agents in DMEM containing 25 mM HEPES. After treatment, cells were washed three times, and incubated with neutral red (0.25 mg/mL) dissolved in DMEM with HEPES at 37°C in the incubator for 1 h, followed by one wash in DMEM with HEPES, and then in washing/fixation solution (1% formaldehyde and 1% calcium in water). Neutral red was extracted by 1 ml extraction solvent (1% acetic acid in 50% ethanol), and was measured with a spectrophotometer at λ=540 nm. The absorbance of treated samples was compared to that of control samples, and expressed as % of control.

2. Apoptosis by In Situ Terminal Deoxynucleotidyltransferase-Mediated Deoxy-UTP Nick End Labeling Assay (TUNEL)

LLC-PK1 cells were plated on sterilized square cover slides in 6-well plates at a density of 3×10^5 cells/well and grown for 48 h to 60-70% confluency. The cells were

then washed once and incubated with TGHQ (200 μM) for 2 h or gliotoxin (100 ng/mL) for 30 min followed by TNF-α (30 ng/mL) for 2 h in DMEM with 25 mM HEPES (pH 7.4). Apoptosis was detected using the ApopTag kit (Intergen, Purchase, NY). Cells were fixed in 10% neutral buffered formalin for 10 min at room temperature, and ethanol-acetic acid (2:1) for 5 min at -20^{o}C, and then incubated in 2% hydrogen peroxide for 5 min followed by equilibration buffer for 2 min. The TdT enzyme solution (50 μL) was incubated with the cells at 37^{o}C for 60 min in a humid environment, and then washed in stop-wash buffer at 37^{o}C for 30 min, with gentle agitation. Cells were subsequently incubated with 50 μL anti-digoxigenin peroxidase enzyme at 37^{o}C for 45 min followed by 50 μL of DAB solution for 10 min in dark. The cover slides were then counterstained in methyl green for 1-5 min and dehydrated in 100% butanol and Hemo-de fixative solutions. Finally the cover slides were mounted on rectangular slides for microscopic examination. Images were taken with a Kodak DC120 digital camera and processed with Adobe Photoshop 6.0 software.

3. Apoptosis by Caspase 3 Activity Assay

LLC-PK1 cells were plated in 6-well plates at a density of 3×10^5 cells/well and treated as described above. Apoptosis was assessed by measuring caspase 3 activity (Caspase 3 Activity Assay Kit, Roche Molecular Biochemicals, Indianapolis, IN). Briefly, cells were lysed in lysis buffer containing 10 mM dithiothreitol (DTT) on ice for 30 min. Microtiter plates were coated with anti-caspase 3 coating buffer for 1 h at 37^{o}C and blocked in blocking solution for 30 min at room temperature. After three washings of the plate with incubation buffer, the lysates were added to the plates and incubated at 37^{o}C for 1 h. Plates were then washed carefully and incubated with substrate solution containing 50 mM Ac-DEVD-AFC at 37^{o}C for 2 h. Ac-DEVD-AFC is cleaved by

caspase 3 in the cell lysates, and the liberated fluorescent AFC was quantified with a Bio-Tek FL600 microplate fluorescence reader and KC4 software (V2.5) (Bio-Tek Instruments, Inc., Winooski, Vermont) at 505 nm.

4. Western Blot Analysis

Cells were plated in 100 mm dishes at a density of 1×10^6 cells/dish, or 6-well plates at a density of 3×10^5 cells/well and grown for 36 h (70-80% confluent) before treatment. Cells were washed in ice cold PBS twice, and lysed with 1 × lysis buffer (Cell Signaling Technology, Inc., Beverly, MA.), containing 20 mM Tris-HCl (pH 7.5), 150 mM NaCl, 1 mM Na_2EDTA, 1 mM EGTA, 1% Triton, 2.5 mM sodium pyrophosphate, 1 mM β-glycerophosphate, 1 mM Na_3VO_4, 1 μg/mL leupeptin, and 1 mM PMSF. Cell lysates were centrifuged at 10000 × g for 10 min, and supernatants were stored at -80°C. Rat tissues (OSOM) were homogenized and lysed in RIPA buffer (1 × PBS, 1% Nonidet P-40, 0.5% sodium deoxycholate, 0.1% SDS, 1 mM PMSF, 1 cocktail protease inhibitors from Roche, 1 mM $NaVO_4$, 10 mM β-glycerophosphate, 5 mM sodium pyrophosphate, 50 mM NaF). Aliquots of 2-50 μg of lysates were separated by 7-15% SDS-PAGE, or PAGE without SDS (non-denaturing condition), and transferred to nitrocellulose membranes. The membranes were blocked in 5% non-fat dry milk (Bio-Rad, Hercules, CA) in tris-buffered saline (TBS) with 0.1% Tween-20 (TBST) for 1 h and then incubated with primary antibodies overnight at 4°C or for 1 h at room temperature in blocking solution. Secondary antibodies, goat anti-rabbit, goat anti-mouse, or bovine anti-goat IgGs conjugated with HRP were diluted to 1:2000 in blocking solution (5% non-fat dry milk in TBS containing 0.1% Tween20), and incubated with the membranes for 1 h at room temperature. Blots were finally developed with the ECL (enhanced chemiluminescence), and exposed to Hyperfilm (Amersham Pharmacia Biotech, UK).

5. Immunoprecipitation

Cells were plated in 100 mm dishes at a density of 1×10^6 cells/dish, and treated when reaching 70% confluence. Cells were washed in ice cold PBS twice, and lysed as described for the western blot analysis. Total cell lysate (200 μL) was precleared by incubation with 1 μg of normal IgG (same species as primary antibody) and 20 μL of protein A/G agarose (Santa Cruz Tech., Santa Cruz, CA) on ice for 30 min, followed by centrifugation at 1000 × g for 30 sec at 4°C. Primary antibody (1-10 μg) was added to the lysate, and incubated overnight at 4°C. Protein A/G agarose (20 μL) was added to the cell lysate and incubated at 4°C for 1 h with gentle rocking. The mixture was centrifuged at 1000 × g for 30 sec at 4°C, and supernatant was discarded. The pellet was washed with RIPA buffer (Santa Cruz Tech., Santa Cruz, CA) for 4 times, with centrifugation after each wash. The pellet was resuspended in 20 μL of 2 × loading buffer (Bio-Rad Laboratories, Hercules, CA) containing 5% reducing agent (β-mercapturic acid) was boiled for 3 min. Samples were loaded onto SDS-PAGE, and subjected to Western blot analysis.

6. Immunohistochemistry

Paraffin sections (4 μm) were incubated at 65˚C overnight, and then deparaffinized and rehydrated in xylene, 100% ethanol and 95% ethanol separately. The sections were then incubated in 0.5% hydrogen peroxide for 10 min to quench endogenous peroxidase activity. The slides were then heated at 100°C for 10 min in 10 mM sodium citrate buffer (pH 6.0) to unmask antigens. Subsequently, the slides were incubated with primary antibodies [phospho-p42/44 MAPK (polyclonal, 1:50), phospho-p38 MAPK (monoclonal, 1:50), phospho-JNK/SAPK (polyclonal, 1:50), and phospho-histone H3 (Ser10) (monoclonal, 1:50)] at 4°C overnight. The slides were then incubated

with secondary antibodies (goat anti-rabbit IgG, biotin-conjugated; or goat anti-mouse, biotin-conjugated) at room temperature for 30 min. An ABC staining kit was used to probe the proteins of interest. Briefly, the slides were incubated with AB enzyme reagents provided by the ABC staining kit for 30 min at room temperature, and then washed in PBS for 3 times at 5 min each, and then incubated with peroxide substrate solution (DAB, substrate, in substrate buffer) for 5 to 10 min. Finally, the slides were washed in double distilled water, counterstained with hematoxylin, and observed by light microscopy. Images were taken with a Kodak DC120 digital camera and processed with Adobe Photoshop 6.0 software.

7. Immunocytochemistry

LLC-PK_1 cells were plated on sterile square cover slides in 6-well plates until reaching 70-80% confluency. Cells were then treated, rinsed in PBS twice, and fixed with 100% methanol (–20^{o}C) for 10 min. Cells were then washed three times for 5 min each with 1 mL TBS containing 0.1% Triton X-100 (TBS/Triton) and then rinsed with TBS at room temperature. Subsequently, cells were blocked with blocking solution containing 5% goat serum and 1% BSA in TBS/Triton at room temperature for 1 h and washed for 5 min with TBS. Subsequently, cells were incubated with primary antibodies in 3% BSA in TBS at room temperature, washed twice with TBS/Triton, and once with TBS, and then incubated with biotinylated secondary antibodies in 3% BSA in TBS at room temperature for 1 h. Cells on the cover slips were washed three times for 5 min each in TBS/Triton and once with TBS. Hydrogen peroxide (0.6%, room temperature, 10 min) was used to quench the endogenous peroxidases, and cells were washed for 5 min with TBS/Triton, once with TBS, and then incubated with ABC reagent for 1 h at room temperature. After two washes in TBS, cells were then incubated with 1 mL DAB reagent for 10 min at

room temperature, and then rinsed with DDI H_2O. Cover slips were then counterstained in hematoxylin, washed, and mounted onto rectangle slides with VectaMount (Vector Laboratories, Burlingame, CA), and observed under light microscope. For IgG control slides, only secondary antibody was incubated with the cells in the absence of primary antibody.

8. Transformation and Plasmid DNA Purification

Plasmids (2 μg) were mixed and incubated with 50 μL of competent cells (DH5α, Invitrogen, Carlsbad, CA, or XL1-Blue, Stratagene, La Jolla, CA) on ice for 30 min, followed by being subject to heat shock in a 42^{o}C water bath for 90 sec. The cells were then incubated in 1 mL LB medium with selective antibiotics for 45 min at room temperature with rocking. The above cells (50 μL) were subsequently spread onto LB-Agar plates containing antibiotics, and incubated at 37^{o}C for 18 h. Colonies were selected and dropped into 25 ml LB medium with antibiotics, and incubated at 37^{o}C for 8 h with shaking (2500 rpm). The above cells (20 mL) were transferred to a 1 L LB medium with antibiotics, and incubated at 37^{o}C for 18 h with shaking (2500 rpm).

Plasmid DNAs were purified by MegaPrep plasmid DNA purification kits (Qiagen, Valencia, CA). Briefly, cells were centrifuged at 6000 × g for 10 min at 4^{o}C, and resuspended in 50 mL of buffer P1 containing freshly added RNase. Buffer P2 (50 mL) was added gently to the bottle, and mixed gently but thoroughly 4-6 times, and incubated for 5 min at room temperature. Pre-chilled buffer P3 (50 mL) was added and mixed gently by inverting 4-6 times, followed by incubation on ice for 30 min. The mixture was centrifuged at 20000 × g for 30 min at 4^{o}C, and supernatant was transferred to another tube, and re-centrifuged at 20000 × g for 15 min at 4^{o}C. Supernatant was transferred to a pre-equilibrated QIAGEN tip 2500 (by applying 35 mL buffer QBT). The

tip was washed with 200 mL of QC buffer. Plasmid DNA was eluted with 35 mL of QF buffer, and was precipitated in isopropanol, and centrifuged at 15000 × g for 30 min at 4°C. The pellet was washed with 7 mL of 70% ethanol at room temperature, and re-centrifuged at 15000 × g for 10 min at 4°C. Supernatant was removed, and the pellet was air dried for 10-20 min, followed by dissolvation in TE buffer (pH 8.0). DNA was quantified by spectrophotometry at λ=260 nm, and purity was assured by the ratio of A260/A280.

9. Transfection

LLC-PK_1 cells were seeded in 6-well plates or 24-well plates, and grown for 16 h, followed by transient transfection with native p38 MAPK, dominant negative mutant p38 MAPK expressing vector (pcDNA3-p38, pcDNA3-DNp38), and empty vectors (pcDNA3), using FuGENE 6 Reagent according to the manufacturer's instructions. Cells were incubated with a mixture of DMEM medium, tranfection reagent, and vectors at 37°C for 4 h, and then DMEM medium, containing 10% FBS, was added to each well, and incubated for 48 h before treatment.

10. Metabolic Labeling of Cells and Histone Extraction for Phosphorylation Studies

To determine the effects of TGHQ-induced oxidative stress on histone phosphorylation, LLC-PK_1 cells were labeled with 40 μCi/mL of [^{32}P]-orthophosphoric acid in DMEM with 25 mM HEPES for 4 h. Radioactivity was removed and cells were treated in DMEM containing 25 mM HEPES. Cells were washed in ice-cold low salt buffer (LSB; 10 mM Tris-HCl pH7.4, 10 mM NaCl, 2.5 mM EDTA) and then lysed in lysis buffer (LSB containing 0.25 mM sucrose, 1% Triton-X-100). Histones were extracted with 0.25 M HCl and precipitated in 20% trichloroacetic acid. The precipitate

was washed twice, once with 0.25 M HCl containing acetone and then with acetone only. Proteins were separated on a 13.5% SDS polyacrylamide gel by electrophoresis. After electrophoresis, the proteins were stained with Coomassie Blue, dried, and then exposed to Kodak XAR film.

11. 2-Dimensional Gel Electrophoresis

LLC-PK1 cells (1×10^6) were treated, washed in phosphate buffered saline (PBS), centrifuged, and resuspended in 100 μL of a modified RIPA buffer containing 50 mM Tris-HCl, pH 7.5, 150 mM NaCl, 1% NP-40, 0.5% sodium deoxycholate, 0.5% Triton X-100, and 10 mM EDTA. The cells were subjected to freezing and thawing three times, followed by sonication (3 x 15s). Cell lysates were then centrifuged at 14,000×*g* for 15 min at 4 °C. To remove DNA and RNA, proteins was treated with DNase and RNase, followed by overnight acetone precipitation at –20°C. The protein pellet (150 μg) was resuspended in 185 μL of rehydration buffer, and incubated at room temperature for 1 h for complete protein solubilization. The protein mixture was centrifuged at 15,000×*g* for 30 min at ambient temperature, and the supernatant was loaded onto an 11 cm focusing tray. 2-D SDS-PAGE was performed using Bio-Rad PROTEAN IEF Cell (Hercules, CA). A pre-cast IPG dry strip (pH 3-10) was layered onto the protein mixture (150 μg/sample) with the gel side down, and covered with mineral oil. After rehydration for 12 h at 50 V, the focusing was carried out automatically with the following program: 250 V for 15 min, from 250 V to 5,000 V for 2.5 h, and a final focusing step at 8000 V for 55000 VH. Focused IPG strips were equilibrated in 5 mL of equilibration solution (150 mM Tris-HCl, pH 8.8, 6 M urea, 30% v/v glycerol, 2% SDS with 2.5% DTT added for the first 10 min and 2% iodoacetamide added for the last 10 min). SDS-PAGE was carried out using a pre-cast Criterion 8-16% gradient gel in Criterion Cell, at 20 V for 10

min and then at 200 V for 45 - 55 min. Gels were then fixed in 10% methanol-7% acetic acid for 40 min, stained with SYPRO Ruby protein stains (Bio-Rad) overnight, and then destained in 10% methanol-7% acetic acid for 1 h. Images of stained 2-D gels were taken on a Vistra FluorImager SI (Amersham Phamacia Biotech, Piscataway, NJ), and analyzed using PDQUEST software package (Bio-Rad).

12. MALDI-TOF and PSD

2-D images were visualized by at least 2 individuals. Spots were analyzed quantitatively using Kodak 1D Image Analysis Software as well as by PDQUEST 7.0 software (Bio-Rad). Spots with altered densities were manually cut out of the gel, subject to in-gel tryptic digestion, and analyzed on a Voyager DePRO^{TM} MALDI-TOF MS system (Applied Biosystems, Foster City, CA). The samples were mixed with matrix at 1:1 ratio on a 100-well steel MALDI target for analysis, with 1 mL total volume. The α-cyano-4-hydroxy cinnamic acid matrix was prepared at 2 mg/mL in 50% ACN/0.3% trifluoroacetic acid solvent. Samples were analyzed in the positive ion mode with delayed extraction. The co-crystallized target spot was ionized with a UV nitrogen laser (337 nm) at 20 Hz, accelerated at 20 kV and analyzed in the reflector mode. Each sample mass spectrum is the average of 200 laser shots. Instrumental parameters used were as follows: bin size – 0.5 nsec, delay time – 100 nsecs, mass range – 800-3200 Da, low mass gate 750 Da, grid – 78.4% of accelerating voltage, guide wire – 0.005% of accelerating voltage. Automated database search was performed on the Proteomic Solution 1 data station (Applied Biosystems, Foster City, CA). Peptide mass lists were filtered to remove trypsin autolysis peaks. The mass list for each sample was entered in the search program, MS-Fit 3.3.1, in the Protein Prospector suite. The Swiss-PROT database was searched using a 15 ppm peptide mass tolerance for tryptic digest and a maximum of 3 missed

cleavages and carbamidomethylation of the cysteines. The search was performed for all species with unrestricted pI and molecular weight. The protein represented by the highest scoring match is reported and peptide sequences assigned according to the best match. Following the analysis of each sample by peptide mass mapping, one ion from each MS spectrum was subjected to Post Source Decay (PSD) analysis in order to further confirm the protein identification by peptide sequencing. The PSD spectra of each ion was acquired in automated mode and is a composite of several segments of spectrum each acquired at a different PSD mirror ratio (each mirror ratio focusing a certain m/z region). The mirror ratios ranged from 1.000 to 0.03 with the actual number of mirror ratios depending on the mass of the ion fragmented. Each segment of the spectrum was the average of 250 laser shots. For MALDI-PSD spectra, the raw data was smoothed and the mass list exported to the MS-Tag peptide fragmentation database search engine in the Protein Prospector suite. Similar parameters were used *vide infra*, except that the parent ion mass tolerance was 20 ppm and the fragment ion tolerance was 800 ppm. The protein identified in each case as the highest scoring match was identical to that identified in the peptide mass mapping analysis. Since the two methods use different data sets and independent database searches, the resulting identification has a very high confidence level.

13. Animal Treatment and Tissue Preparation

Frozen kidney tissues derived from male Eker rats (*Tsc-2*$^{EK/+}$) were from previous *in vivo* studies (Habib *et al.* 2003). Briefly, male Eker rats (*Tsc-2*$^{EK/+}$) were obtained from the University of Texas MD Anderson Cancer Center, Smithville, TX. Animals were treated with a single dose of TGHQ (7.5 μmol/kg in PBS, pH 7.4 *i.v.*). Control animals were administered phosphate buffered saline (PBS) only. Animals were euthanized at 0,

0.5, 1, 2, 4, 8, 12, 24, 48 and 72 hours following TGHQ treatment. Kidneys were removed and dissected longitudinally. Half of the kidney was preserved in 10% formalin in PBS, 0.01 M, pH 7.4. The outer stripe of the outer medulla (OSOM) was excised from the remaining kidney sections and immediately snap frozen in liquid nitrogen.

III. STATISTICAL ANALYSIS

All data are expressed as mean ± standard deviation. Analysis of variance with a post-hoc Student Newman Kuel's test was used to compare the mean values, and $p<0.05$ was considered to be significant.

Chapter 3: EGFR-DEPENDENT ERK ACTIVATION AND EGFR-INDEPENDENT P38 MAPK ACTIVATION CONTRIBUTE TO TGHQ-INDUCED ONCOTIC RENAL CELL DEATH

I. INTRODUCTION AND RATIONALE

Oxidative stress is known to activate mitogen activated protein kinases (MAPKs) (Cobb 1999; Martindale and Holbrook 2002). The MAPK family is comprised of three major subgroups, extracellular signal-regulated protein kinase (ERK), c-Jun N-terminal kinases/stress-activated protein kinase (JNK/SAPK), and p38 MAPK (Cobb 1999). ERKs behave mainly as mitogen-activated proliferation/differentiation factors, whereas JNK/SAPK and p38 MAPK are mainly stress-activated proteins related to apoptotic cell death. The MAPKs are all rapidly activated by TGHQ in LLC-PK_1 cells, and inhibition of ERK1/2 activation with PD98059 or inhibition of p38 MAPK activation with SB202190 attenuates cell death induced by TGHQ (Ramachandiran *et al.* 2002). In contrast, the JNK inhibitor SP600125 has no effect on TGHQ-induced cell death (Ramachandiran *et al.* 2002). Upon activation, following phosphorylation of tyrosine and threonine residues, MAPKs subsequently activate a variety of substrates, the majority of which are transcription factors. However, one indirect downstream target of the MAPKs is histone H3, which becomes phosphorylated following TGHQ-induced ERK activation (Tikoo *et al.* 2001). ERK1/2 activation may contribute to both cell proliferation and cell death in a variety of cells. In a few cases, activated ERK1/2 may act as a cell death-inducing factor. Thus, ERK activation is related to vanadate-induced oncotic cell death of vascular smooth muscle cells (Daum *et al.* 1998), to H_2O_2-induced cell death of oligodendrocytes (Bhat and Zhang 1999), of T cells (van den Brink *et al.* 1999) and of

pleural mesothelial cells (Jimenez *et al.* 1997). Therefore, the inappropriate phosphorylation of histone H3 by ERK1/2 may lead to premature chromatin condensation (PCC) and cell death in LLC-PK_1 cells (Tikoo *et al.* 2001). p38 MAPK and JNK1/2 are more responsive to cell stress than ERK1/2 including stress induced by inflammatory cytokines, heat shock, and ROS (Paul *et al.* 1997). Interestingly, in certain cell systems, p38 MAPK and JNK1/2 can be activated in an EGFR-dependent manner (Chen *et al.* 2001; Kanda *et al.* 2001).

The events that couple ROS generation to MAPKs activation in TGHQ-treated LLC-PK_1 cells are unknown. Oxidants can activate growth factor-linked signaling pathways (Meves *et al.* 2001), but the initial events of this activation are not clear. Two possible mechanisms may exist: (i) oxidants mimic epidermal growth factor (EGF)-EGF receptor (EGFR) interactions by modification of the cysteine residues on the receptors (Chen *et al.* 1998); or (ii) oxidants inactivate phosphatases, thereby inhibiting dephosphorylation of the EGFR (Knebel *et al.* 1996). The EGFR, platelet derived growth factor (PDGF) receptor, and T-cell receptor complexes are all activated following oxidative stress, and are coupled to the subsequent activation of ERKs (Guyton *et al.* 1998; Meves *et al.* 2001; Sachsenmaier *et al.* 1994). Binding of EGF to the EGFR induces the dimerization, autophosphorylation and transactivation of the tyrosine kinase activity of EGFR, providing a variety of binding sites for a series of proteins, thereby initiating the activation of downstream signaling pathways. For example, phospho-tyrosine 992 (pY992) within the EGFR provides a binding motif for phospholipase C-γ (PLC-γ), initiating downstream signaling, including protein kinase C (PKC) activation and subsequent ERK activation (Emlet *et al.* 1997). Phospho-tyrosine 1068 (pY1068) within the EGFR provides a binding motif for Grb2/SH2 domain binding, which also leads to ERK activation (Rojas *et al.* 1996). Phospho-tyrosine 1173 (pY1173) represents

a motif for PLC-γ and Shc, both of which can initiate activation of the ERK cascade (Sorkin *et al.* 1992). Interestingly, pY1068, pY1148, and pY1173 are essential for EGFR internalization and degradation, as well as for tyrosine kinase activity (Helin and Beguinot 1991). Additional phospho-tyrosine sites on the EGFR (pY845, pY1148, pY1086, pY1101) permit the differential activation of a number of other proteins in response to EGF stimulation (Biscardi *et al.* 1999; Bishayee *et al.* 1999; Levkowitz *et al.* 1999; Sakaguchi *et al.* 1998; Sieg *et al.* 2000). Although all MAPKs appear to be EGFR-dependent in different cellular systems (Chen *et al.* 2001; Kanda *et al.* 2001), whether TGHQ mediated MAPK activation occurs through EGFR activation, and which tyrosine phosphorylation site(s) are targeted by TGHQ remain unclear.

Following TGHQ-induced MAPK activation, histone H3 is phosphorylated in LLC-PK1 cells (Tikoo *et al.* 2001). Because histone H3 phosphorylation is usually associated with mitosis, inappropriate histone H3 phosphorylation may provide a signal that conflicts with the cell cycle arrest induced by TGHQ (Jeong *et al.* 1997a), resulting in PCC and subsequent oncotic cell death. Both ERK1/2 and p38 MAPK have the potential to induce histone H3 phosphorylation by activating downstream histone kinases (Tikoo *et al.* 2001). Another downstream signaling factor of p38 MAPK is MAPKAP kinase-2 (MK-2), which can phosphorylate heat shock protein 27 (Hsp27). Hsp27 is a chaperone protein that regulates actin stabilization (Landry and Huot 1995) and apoptosis (Parcellier *et al.* 2003a). Both histone H3 and Hsp27 have the potential to remodel chromosome structure, and to possibly contribute to TGHQ-induced PCC and oncotic cell death. The present study was therefore designed to determine how MAPKs are activated by TGHQ, and the role of MAPK activation in TGHQ-induced oncotic cell death.

II. RESULTS

A. TGHQ induced oncotic renal cell death

TGHQ induces oncotic cell death of LLC-PK1 cells (Ramachandiran *et al.* 2002). We further determined whether TGHQ induces apoptosis in LLC-PK1 cells, as measured by caspase 3 activity and TUNEL assays (Figure 3.1). Cell death at different doses of TGHQ (50 μM to 400 μM) and at different exposure times (5 min to 24 h) to TGHQ, were examined, but no indication of apoptosis was ever found. The data shown in Figure 3.1 indicate no apoptotic cell death in TGHQ (200 μM, 2h) treated and untreated LLC-PK1 cells, whereas cells treated with TNF-α (30 ng/ml) for 2 h revealed significant amounts of apoptosis, as evidenced by both caspase 3 activation and DNA fragmentation (TUNEL staining). Apoptotic and oncotic cell death are distinguished by both morphological and biochemical changes. For example, apoptosis is characterized by cell shrinkage, formation of apoptotic body, DNA fragmentation, and activation of caspases, whereas oncotic cell death is usually accompanied by cell and organelle swelling, loss of membrane integrity, and diffuse chromatin condensation and margination. From microscopic observations, TGHQ-induced cell death of LLC-PK1 cells is manifest by chromatin condensation and cell swelling. The evidence for TGHQ-mediated oncotic cell death rather than apoptotic cell death is reinforced by biochemical assays, including assays for caspase 3 activity measurement, and DNA damage staining (TUNEL assay). The combined data reveal that TGHQ induces oncotic rather than apoptotic cell death in renal proximal tubule epithelial cells.

B. TGHQ but not EGF Induces Histone H3 Phosphorylation:

TGHQ induces the rapid phosphorylation of both ERK1/2 (Figure 3.2) and histone H3 (Figure 3.3) in renal proximal tubule epithelial cells (LLC-PK_1), in a ROS-dependent manner (Tikoo *et al.* 2001). EGF, a ligand for the EGFR, also induces the rapid phosphorylation of ERK1/2 in LLC-PK_1 cells (Figure 3.2), but fails to induce histone H3 phosphorylation within 24 hours (Figure 3.3). H_2O_2 induces ERK1/2 phosphorylation (Figure 3.2) and histone H3 phosphorylation (data not shown) in a manner similar to TGHQ, confirming the ROS-dependent manner of TGHQ-induced histone H3 phosphorylation. The data therefore imply that the consequences of ERK1/2 activation in LLC-PK_1 cells are different in TGHQ or EGF-treated cells, and that the activation of the ERK pathway alone is probably insufficient for histone H3 phosphorylation and cell death. Differences in the kinetics of ERK1/2 activation may also be crucial for the subsequent phosphorylation of histone H3.

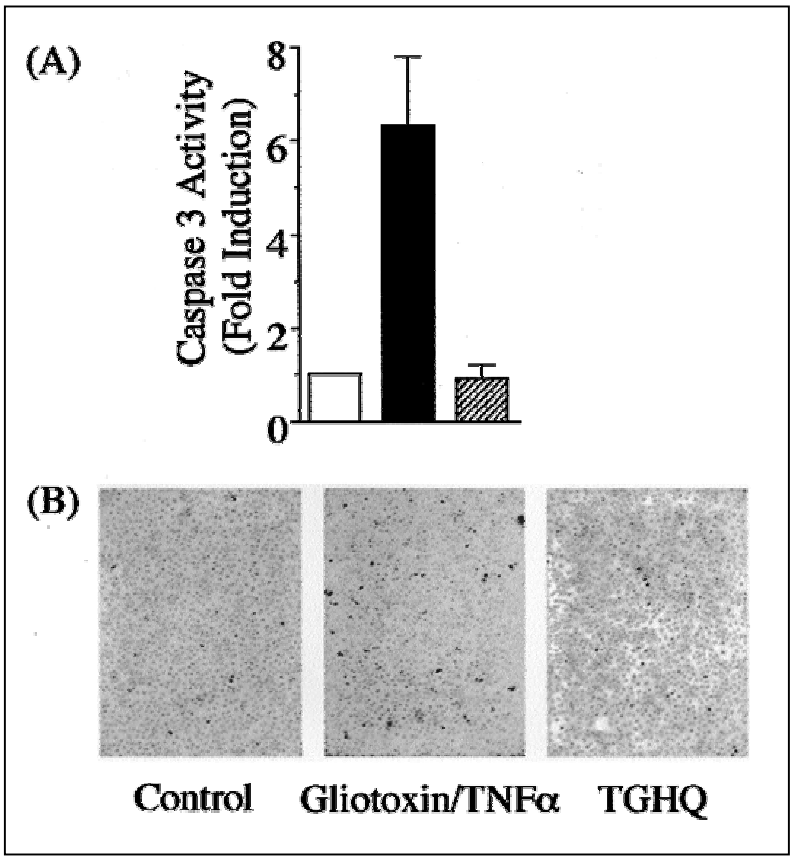

Figure 3.1. TGHQ does not induce apoptosis in LLC-PK1 cells.

(A) Biochemical assessment of apoptosis was performed with a caspase 3 assay kit as described in methods. LLC-PK1 cells were treated with TGHQ (200 μM; hatched bar) for 2 h, or gliotoxin (100 ng/mL) for 0.5 h followed by TNF-α (30 ng/mL) for 2 h (black bar). Means of each sample were compared by T-test (n=3), and $p<0.05$ is considered statistically significant. ***(B)*** Histological assessment of apoptosis was monitored by the TUNEL assay as described in the Materials and Methods. Apoptotic cells stain dark brown, whereas normal cells counter stain with methyl green. Data shown here represent 3 independent experiments.

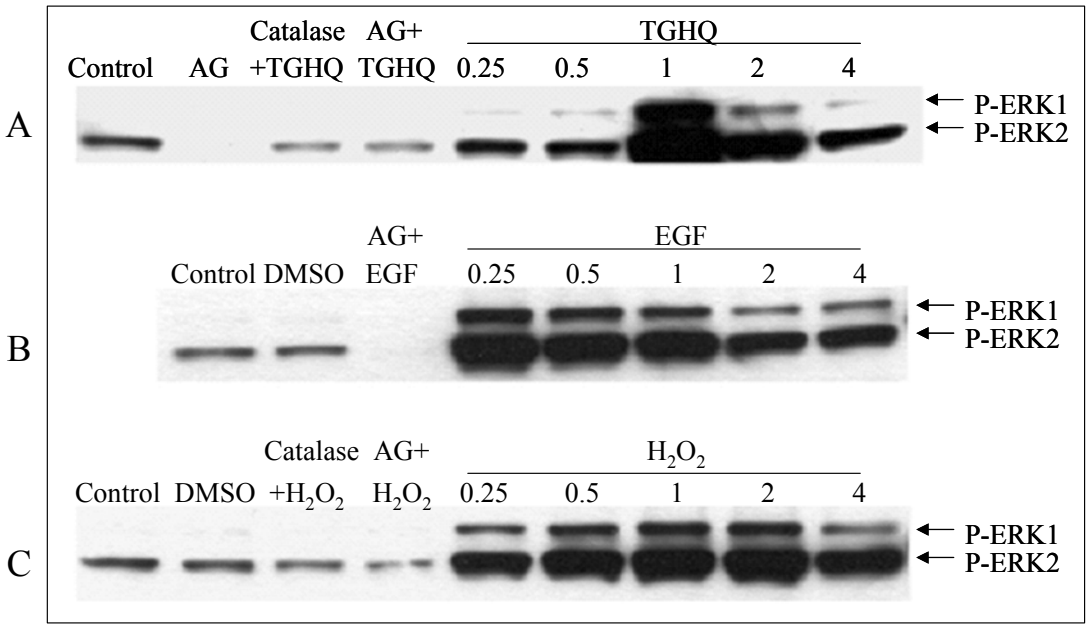

Figure 3.2. TGHQ, EGF and H_2O_2 all induce EGFR-dependent ERK1/2 phosphorylation, but with varying kinetics.

LLC-PK1 cells were treated with TGHQ (200 μM), H_2O_2 (88.2 μM) or EGF (50 ng/mL) for different periods of time (0, 0.25. 0.5, 1, 2, 4 h). Some cells were pretreated with AG1478 (0.25 μM) for 1 h, followed by treatment with TGHQ (1 h), H_2O_2 (1 h), or EGF (15 min). DMSO treated samples represent the solvent control for AG1478. Catalase was used at a concentration of 10 U/mL in DDI H_2O, and was co-administered with the various agents. Whole cell lysates were extracted and electrophoretically resolved on a 10% SDS-PAGE gel, followed by Western blot analysis. A. EGF treated cells; B. TGHQ treated cells. C. H_2O_2 treated cells. Numbers shown represent hours of treatment. Total ERK levels did not change during the treatment time (data not shown).

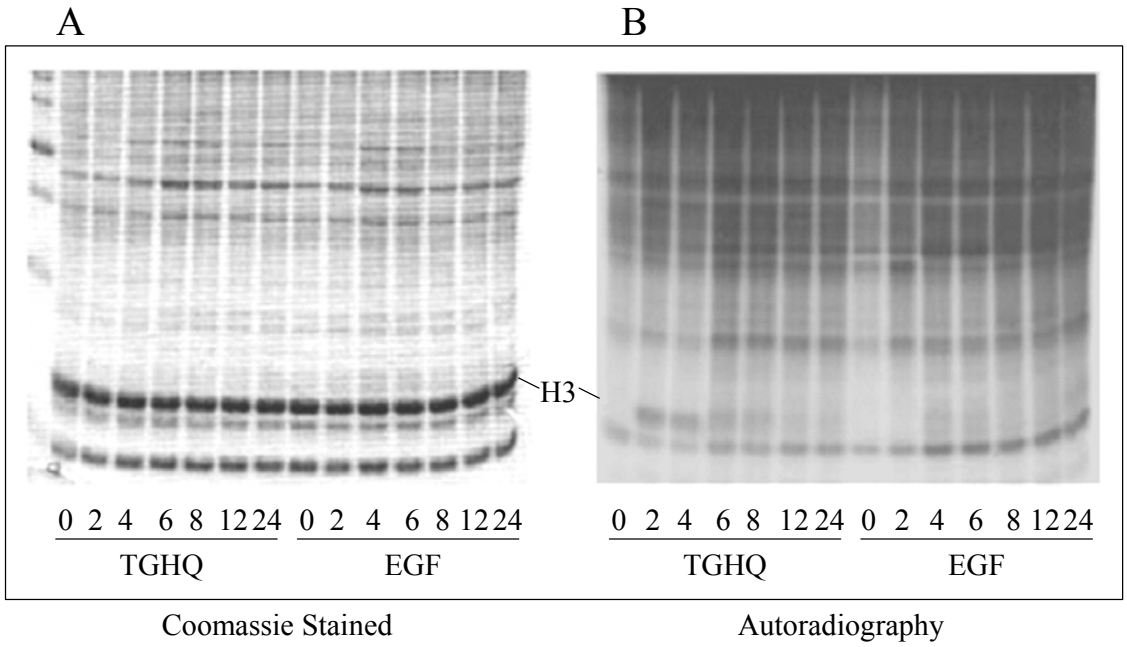

Figure 3.3. TGHQ, but not EGF, induces histone H3 phosphorylation in renal epithelial cells.

[^{32}P]-Labeled LLC-PK1 cells were treated with TGHQ (400 μM) or EGF (50 ng/mL) for different periods of time (0, 2, 4, 6, 8, 12, 24 h). Histones were extracted and electrophoretically resolved on a 13.5% SDS polyacrylamide gel. A. Coomassie stained gel; B. Autoradiography. Numbers shown represent hours of treatment.

C. EGFR Tyrosine Phosphorylation Induced by EGF, TGHQ, and H2O2:

To determine whether the differences in the downstream consequences of ERK1/2 activation arise as a consequence of the differential interaction between EGF or TGHQ and the EGFR, we compared the effects of EGF and TGHQ on the pattern of EGFR phosphorylation. Because TGHQ induces ERK1/2 activation in a ROS-dependent manner, the effects of H_2O_2 were also compared with TGHQ and EGF. The dose of H_2O_2 (88.2 μM) was selected based upon the dose at which it induced the same level of loss in cell viability as TGHQ (200 μM) following 2 h of treatment (Figure 3.4). EGF (50 ng/ml) induced rapid ERK1/2 phosphorylation (Figure 3.2), without subsequent loss of cell viability (Figure 3.4). Time-response curves for TGHQ and H_2O_2 are shown in figure 3.4.

Phosphorylation of EGFR at Y992, Y1068, Y1086, Y1148, and Y1173 was specifically investigated, because phosphorylation at any of these sites could result in MAPK/ERK activation, but through different downstream signaling events (Scheme 1). EGF, as a competent ligand for the EGFR, is able to bind to the EGFR, cause dimerization and autophosphorylation of the EGFR, and tyrosine kinase transactivation at all the pY sites examined (Figure 3.5). TGHQ induced rapid and intensive EGFR phosphorylation at Y992 and Y1068, and weaker EGFR phosphorylation at Y1086 and Y1148, but not at Y1173 (Figure 3.5). In contrast, H_2O_2 induced significant amounts of EGFR phosphorylation only at Y992, and trace amounts of EGFR phosphorylation at Y1086 and Y1148 (Figure 3.5). EGF-induced EGFR phosphorylation reached maximal levels as early as 15 min, whereas both TGHQ and H_2O_2-induced EGFR phosphorylation peaked at 1 h (Figure 3.5). Differences in the patterns and kinetics of EGFR phosphorylation among TGHQ, EGF and H_2O_2 (Scheme 1) likely determine the activation of the subsequent downstream signaling pathways engaged subsequent to

EGFR phosphorylation. The pattern of TGHQ-induced EGFR phosphorylation is also different from that seen with H_2O_2, suggesting a ROS-independent component to TGHQ-induced EGFR phosphorylation. EGF-mediated EGFR phosphorylation is followed by decreases in total EGFR levels (Figure 3.5) probably due to the rapid internalization and degradation of the activated receptor required to desensitize the system (Levkowitz *et al.* 1998; Ravid *et al.* 2002; Waterman and Yarden 2001).

D. TGHQ, EGF, and H_2O_2-mediated ERK1/2 Phosphorylation is EGFR Dependent, whereas TGHQ and H_2O_2-induced p38 MAPK and JNK1/2 Phosphorylation are EGFR Independent:

TGHQ, EGF, and H_2O_2 all induced ERK1/2 phosphorylation very rapidly (Figure 3.2). However, the kinetics of ERK1/2 phosphorylation by each of these agents varied. EGF induced extremely rapid and relatively sustained ERK1/2 phosphorylation, peaking at 15 min, whereas TGHQ induced a slower, less sustained but more intense ERK1/2 phosphorylation, reaching a maximum at 1 h. H_2O_2-induced ERK1/2 phosphorylation was more rapid and more sustained than TGHQ, consistent with its effects on EGFR tyrosine phosphorylation at Y992. H_2O_2 induces phosphorylation of relatively fewer tyrosine residues in the EGFR, but more intensive ERK1/2 phosphorylation, perhaps implying the presence of additional tyrosine phosphorylation sites on EGFR for H_2O_2. Whether differences in the kinetics of both EGFR and ERK1/2 phosphorylation by EGF, TGHQ, or H_2O_2 contribute to the different effects on the downstream targets is not clear at present and requires further investigation.

An EGFR antagonist, AG1478, totally blocked constitutive ERK1/2 phosphorylation in untreated cells (Figure 3.2). AG1478 also completely blocked EGF induced ERK1/2 phosphorylation (Figure 3.2), while it reduced TGHQ and H_2O_2 induced

ERK1/2 phosphorylation to levels significantly lower than those seen in untreated cells (Figure 3.2). The mechanism of ERK1/2 activation by either EGF or TGHQ/H_2O_2 are likely different. EGF is an EGFR ligand, causing dimerization and autophosphorylation of EGFR, and subsequent ERK1/2 activation. In contrast, TGHQ/H_2O_2 probably stimulate EGFR phosphorylation by either modifying the cysteine residues or mimicking EGF-EGFR interactions, or by inactivating phosphatases, thereby inhibiting dephosphorylation of the EGFR, or by inducing cytokine release from the cells to activate the EGFR. Thus, residual ERK1/2 phosphorylation may be a consequence of the inhibition of phosphatase(s). DMSO, the solvent for AG1478, had no effect on ERK1/2 phosphorylation. Thus, ERK1/2 phosphorylation caused by TGHQ, EGF, and H_2O_2 appears to be EGFR dependent. We subsequently determined whether p38 MAPK and JNK1/2 phosphorylation requires EGFR activation. TGHQ and H_2O_2, induced phosphorylation of p38 MAPK and JNK1/2 (Figure 3.6), but EGF did not (data not shown). AG1478 failed to block either TGHQ or H_2O_2 induced p38 MAPK and JNK1/2 phosphorylation, indicating that both TGHQ and H_2O_2 induced p38 MAPK and JNK1/2 phosphorylation is in an EGFR independent manner.

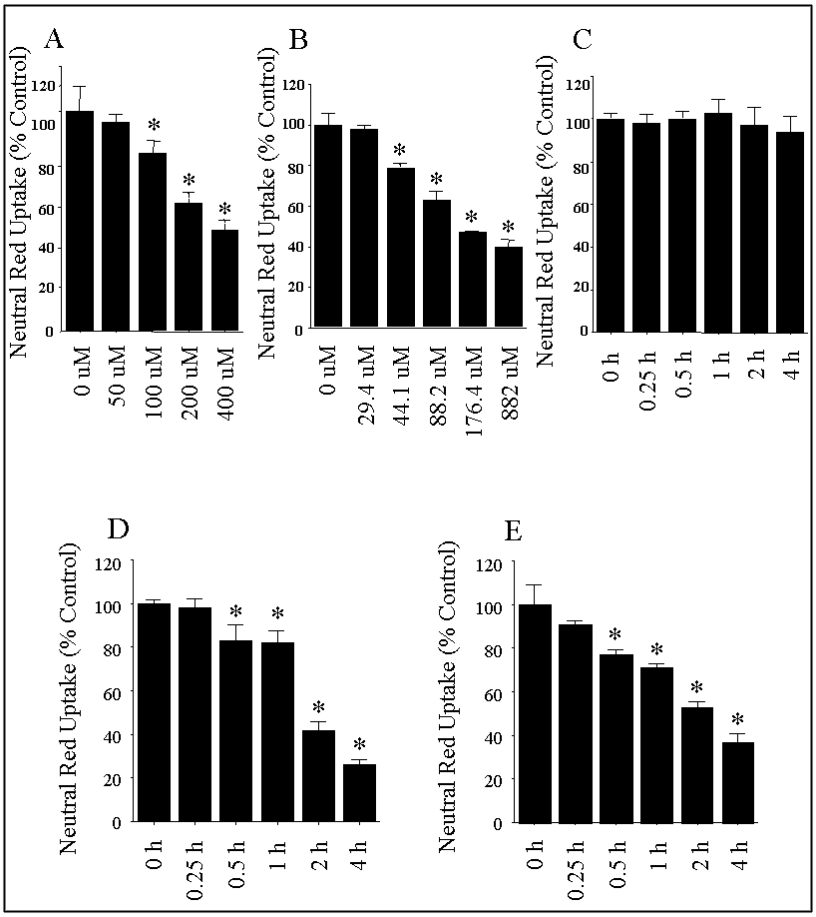

Figure 3.4. Cell viability in TGHQ, H_2O_2, and EGF treated cells at different concentrations and different time points.

Cell viability was determined by measuring lysosomal neutral red uptake by live cells. Neutral Red uptake compared to untreated cells (% of control) represents cell viability after treatment. LLC-PK1 cells were treated with different concentrations of A. TGHQ (50, 100, 200, 400 μM), or B. H_2O_2 (0, 29.4, 44.1, 88.2, 176.4, 882.0 μM) for 2 h in DMEM+HEPES. C. LLC-PK1 cells were treated with EGF (50 ng/ml) for 0, 0.25. 0.5, 1, 2, 4 h and neutral red uptake measured. D & E. Neutral Red uptake in LLC-PK1 cells treated with TGHQ (200 μM) or H_2O_2 (88.2 μM), respectively, for different time periods (0, 0.25, 0.5, 1, 2, 4 h). Data represent the mean ± standard deviation (n≥3). *: $p<0.05$.

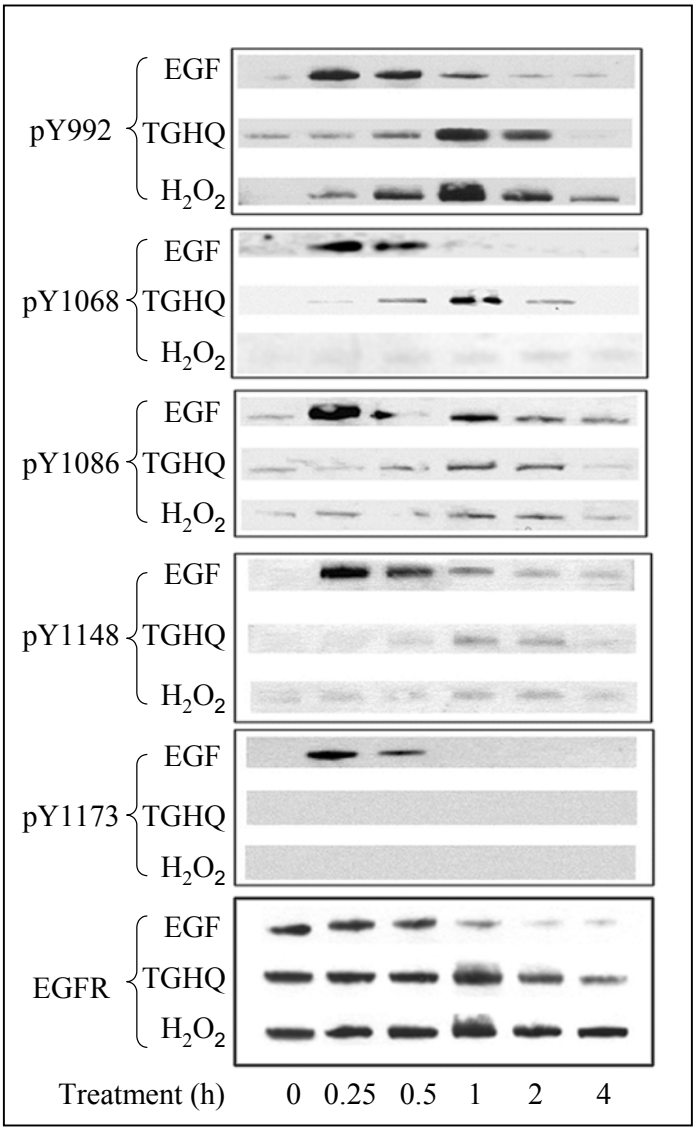

Figure 3.5. Differential EGFR tyrosine phosphorylation induced by TGHQ, EGF and H_2O_2.

LLC-PK1 cells were treated with TGHQ (200 μM), H_2O_2 (88.2 μM) or EGF (50 ng/ml) for different periods of time (0, 0.25. 0.5, 1, 2, 4 h). Whole cell lysates were extracted and equal amount of proteins were electrophoretically resolved on a 10% SDS-PAGE gel. Western blot analysis was performed as described. Representative blots of EGFR tyrosine phosphorylation at Y992, at Y1068, at Y1086, at Y1148, at Y1173, and total EGFR are shown in the microphotographs. Total EGFR levels and EGFR tyrosine phosphorylation sites were examined in EGF-, TGHQ-, and H2O2-treated cells.

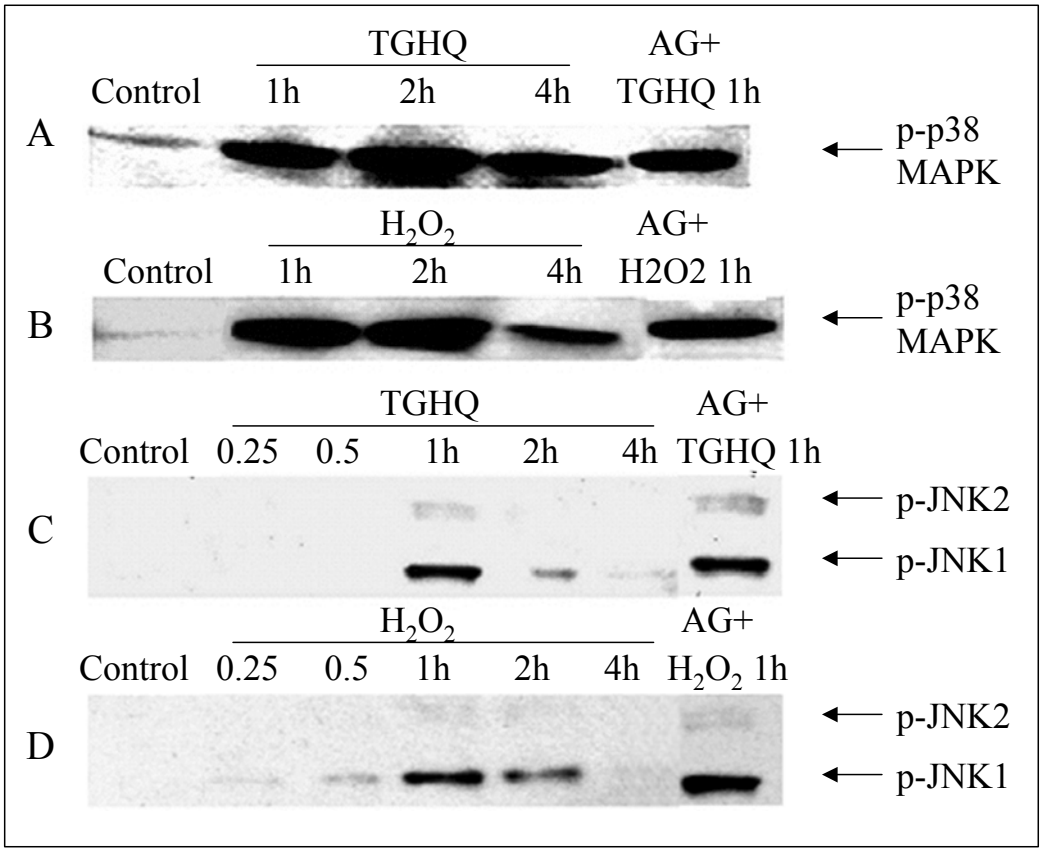

Figure 3.6. TGHQ and H2O2 induced EGFR-independent p38 MAPK and JNK1/2 phosphorylation.

LLC-PK1 cells were treated with TGHQ (200 μM), H_2O_2 (88.2 μM) or EGF (50 ng/ml), and/or with AG1478 (0.25 μM). Whole cell lysates were extracted and electrophoretically resolved on a 10% SDS-PAGE gel and examined by Western blot analysis. A & B. p38 MAPK phosphorylation. C & D. JNK1/2 phosphorylation. A & C. LLC-PK1 cells treated with TGHQ at various time (0, 1, 2, 4 h), or pretreated with AG1478 for 1 h, and co-treated with TGHQ for 1 h. B & D. LLC-PK1 cells treated with H_2O_2 at various time (0, 1, 2, 4 h), or pretreated with AG1478 for 1 h, and co-treated with H_2O_2 for 1 h. Results from EGF-treated cells are not shown because neither p38 MAPK nor JNK1/2 phosphorylation was observed in cells treated with EGF. Total p38 MAPK or JNK1/2 expression levels did not change within the observed time (data not shown).

E. Histone H3 is phosphorylated via both ERK and p38 MAPK Pathways:

TGHQ induced the activation of all three subfamilies of MAPKs (Figure 3.2 & 3.6), among which ERK1/2 and p38 MAPK could potentially induce histone H3 phosphorylation (Tikoo *et al.* 2001). To determine whether TGHQ-induced histone H3 phosphorylation occurs through ERK1/2 and p38 MAPK pathways, we used PD98059, an ERK1/2 pathway inhibitor, SB202190, a p38 MAPK pathway inhibitor, and AG1478, an EGFR inhibitor. Cells were pretreated with each of the inhibitors, and were subsequently exposed to TGHQ. Treatment of LLC-PK1 cells with either inhibitor alone had no effect on histone H3 phosphorylation (Figure 3.7). Histone H3 phosphorylation was significantly increased by TGHQ treatment (400 μM, 1 h), and both PD98059 and SB202190 attenuated TGHQ-induced histone H3 phosphorylation, PD98059 being more effective than SB202190 (Figure 3.7). The data imply that histone H3 phosphorylation likely occurs through the activation of both ERK and p38 MAPK pathways. The combination of the two inhibitors had no additive effects against TGHQ-induced cell death (Ramachandiran *et al.* 2002). Equal loading of the extract is illustrated in the Coomassie stained gel. Surprisingly, AG1478, an inhibitor of EGFR, decreased histone H3 phosphorylation to a less significant extent compared with either ERK or p38 MAPK pathway inhibitors (Figure 3.7). AG1478 did not alter cell death induced by TGHQ treatment, which matches its absence of effect on histone H3 phosphorylation induced by TGHQ (data not shown).

F. TGHQ-Induced Phosphorylation of MK-2 and Hsp27 is p38 MAPK-Dependent:

One downstream target of p38 MAPK is the mitogen activated protein kinase activated protein kinase (MAPKAP kinase-2, or MK-2), which is known to

phosphorylate Hsp27. MK-2 was phosphorylated by TGHQ (200 μM, 1 h) at both phosphoserine residues: Thr222 and Thr334 (Figure 3.8). Both SB202190 and SB203580 are inhibitors of the p38 MAPK pathway, and pretreatment of LLC-PK_1 cells with each of these inhibitors for 1 h significantly decreased or completely blocked TGHQ-induced MK-2 phosphorylation at Thr222 and Thr334 respectively, indicating that MK-2 activation occurs via the p38 MAPK pathway (Figure 3.8). Equal loading was confirmed by Western blot analysis for actin on the same blots after stripping (Figure 3.8).

We subsequently investigated whether Hsp27 phosphorylation occurs through the p38 MAPK pathway. Hsp27 is a chaperone protein that regulates actin polymerization and subcellular localization in response to ROS generation (Martindale and Holbrook 2002). Interestingly, in an independent study using 2-dimensional electrophoresis, followed by matrix-assisted laser desorption/ionisation-time of flight mass spectrometry (MALDI-TOF) peptide mass mapping and post source decay (PSD), we found that TGHQ altered the relative intensity of three spots, each identified as Hsp27, in LLC-PK_1 cells, such that the more intense spot migrated with a more acidic pI. We confirmed that the shift in pI was due to the phosphorylation of Hsp27 at three serine residues (Ser15, Ser78, Ser82), using phospho-specific antibodies for phosphorylated Hsp27 by Western blot analysis (Figure 3.9). The phosphorylation of Hsp27 at all three sites increased as early as 15 min following treatment of cells with TGHQ, and reached a peak between 1 h and 2 h. Total levels of Hsp27 did not change during the period of treatment (Figure 3.9). Phosphorylation of Hsp27 was similarly attenuated or blocked by inhibition of the p38 MAPK pathway (by SB202190, SB203580), but not by inhibition of the ERK pathway (PD98059) (Figure 3.10). In fact, PD98059 appeared to slightly enhance TGHQ-induced phosphorylation of Hsp27 at Ser78 (Figure 3.10). The overall expression of Hsp27 did not change in all samples examined (Figure 3.10).

To confirm the effects of pharmacological inhibitors of the p38 MAPK pathway on TGHQ-induced Hsp27 phosphorylation, LLC-PK_1 cells were transfected with dominant negative mutant p38 MAPK expressing vectors (pcDNA3-DNp38), or empty vectors pcDNA3, or native p38 MAPK expressing vectors (pcDNA3-p38). In untransfected, pcDNA3-transfected, or native p38-transfected cells, TGHQ was capable of inducing intensive p38 MAPK phosphorylation. Indeed, in pcDNA3-p38-transfected cells, phosphorylation of p38 MAPK was higher than in untreated cells, and TGHQ induced even more p38 MAPK phosphorylation in these cells (Figure 3.11), probably due to the significantly increased levels of p38 MAPK in these cells. In contrast, in DNp38-transfected cells, TGHQ failed to induce p38 MAPK phosphorylation (Figure 3.11). Consistent with these findings, only in DNp38-transfected cells did TGHQ fail to induce MK-2 (both Thr222 and Thr334) and Hsp27 (Ser15, Ser78, Ser82) phosphorylation (Figure 3.11). Again, total Hsp27 expression levels were similar in all samples. The data therefore confirm that phosphorylation of both MK-2 and Hsp27 occurs via the p38 MAPK pathway, and that Hsp27 phosphorylation is independent of the ERK pathway.

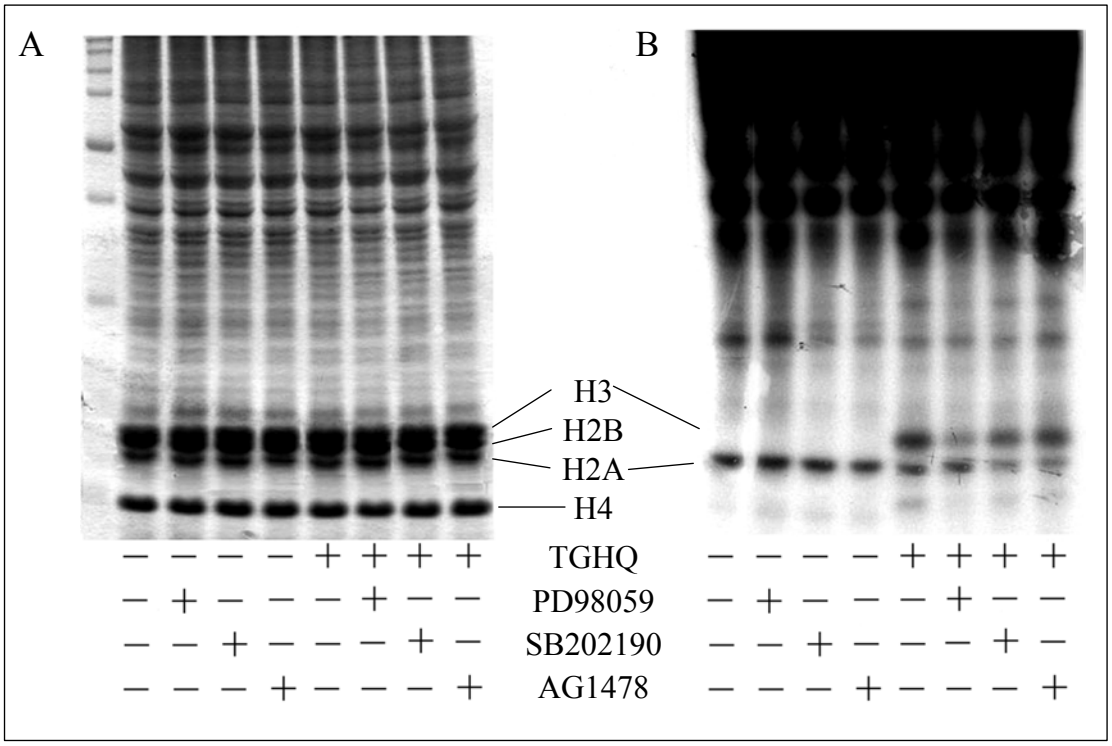

Figure 3.7. TGHQ-induced histone H3 phosphorylation is associated with both ERK and p38 MAPK pathways.

[^{32}P]-Labeled LLC-PK1 cells were treated with TGHQ (400 μM) for 1 h, or pretreated with each inhibitor (PD98059, 50 μM; SB202190, 50 μM; AG1478, 0.25 μM) for 1 h, and co-treated with TGHQ (400 μM) for an additional hour. Histones were extracted and electrophoretically resolved on a 13.5% SDS polyacrylamide gel. A. Coomassie stained gel; B. Autoradiography.

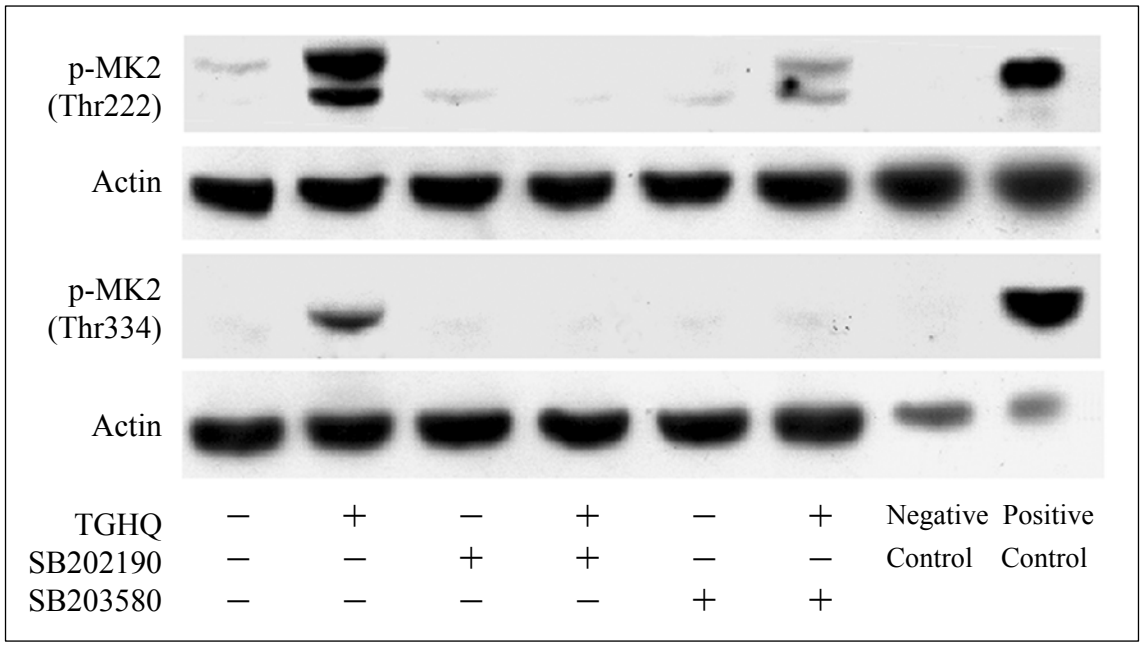

Figure 3.8. TGHQ induced MK-2 phosphorylation, dependent on p38 MAPK activation.

LLC-PK1 cells were treated with TGHQ (200 μM) for 1 h, or pretreated with inhibitors (SB202190, 50 μM; SB203580, 50 μM) for 1 h, and co-treated with TGHQ (200 μM) for an additional hour. Cells were lysed and loaded to 10% SDS-PAGE gel at equal amount of protein, and analyzed by Western blot analysis. Phospho-MK-2 at Thr222 and Thr334 were examined. Western on actin denotes equal loading of the proteins for each sample. Negative and positive controls were provided by the vendor to confirm MK-2 phosphorylation at these two sites.

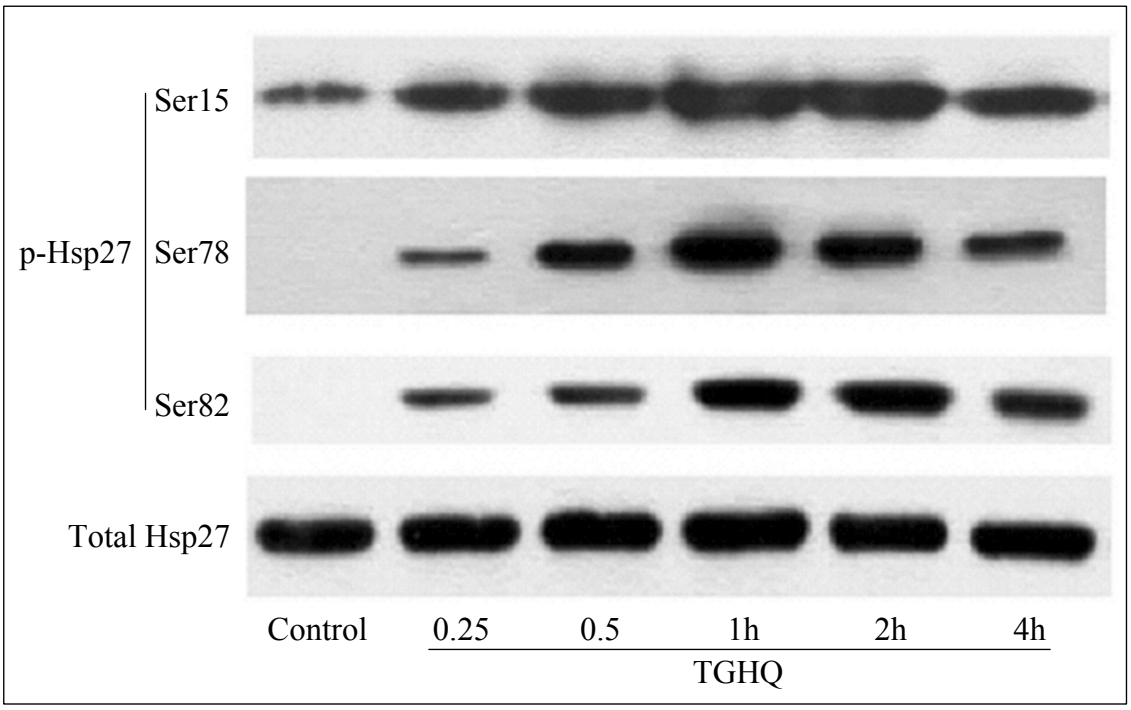

Figure 3.9. TGHQ induced Hsp27 phosphorylation at Ser15, Ser78 and Ser82, occurring in the absence of changes in Hsp27 expression.

LLC-PK1 cells were treated with TGHQ (200 μM) for 0, 0.25, 0.5, 1, 2, 4 h. Whole cell lysates were extracted and electrophoretically resolved on a 10% SDS-PAGE gel, followed by Western blot analysis using phospho-specific antibodies for Hsp27 with phosphorylation each at Ser15, Ser78, or Ser82. Total Hsp27 expression level was examined and no changes were revealed.

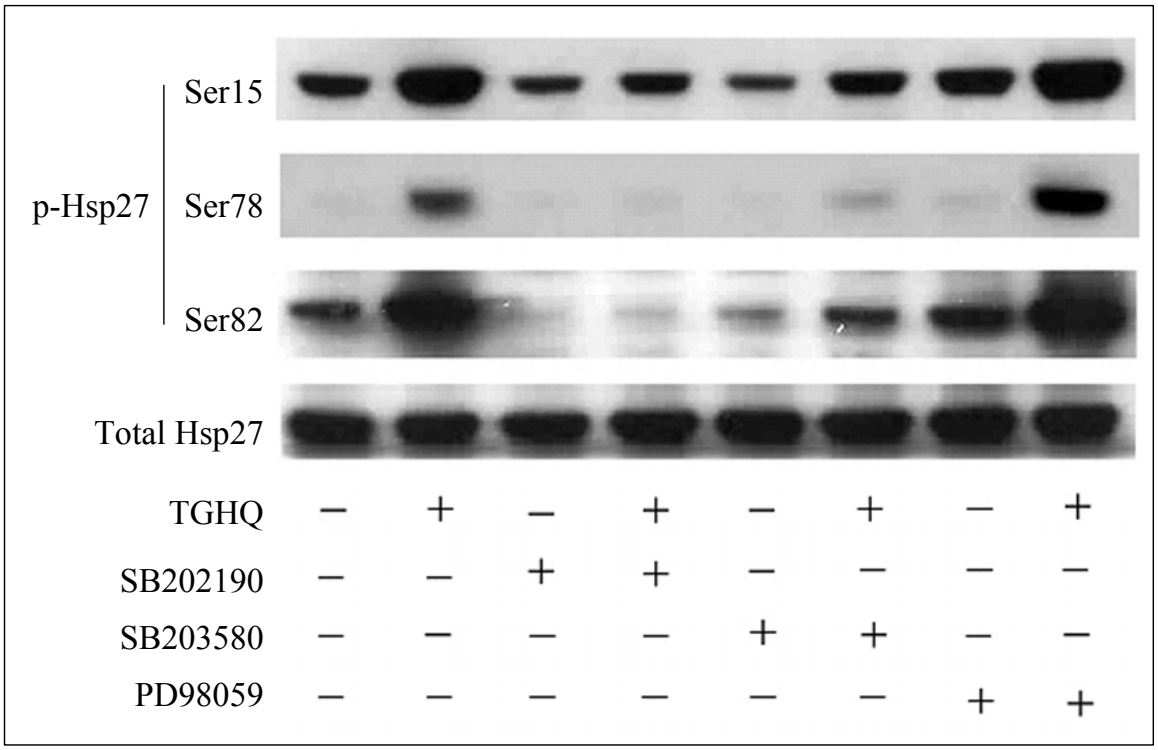

Figure 3.10. TGHQ induced Hsp27 phosphorylation is dependent on p38 MAPK activation.

LLC-PK1 cells were treated with TGHQ (200 μM) for 1 h, or pretreated with inhibitors (SB202190, 50 μM; SB203580, 50 μM) for 1 h, and co-treated with TGHQ (200 μM) for an additional hour. Cells were lysed and loaded onto 10% SDS-PAGE gels at equal amounts of protein, and analyzed by Western blot analysis. Hsp27 phosphorylation at Ser15, Ser78, and Ser82 induced by TGHQ was examined using phospho-specific antibodies. PD98059 (50 μM, 1 h pretreatment), an inhibitor of ERK pathway was used to examine whether Hsp27 phosphorylation is through the ERK pathway. Total Hsp27 expression levels did not change in all samples examined.

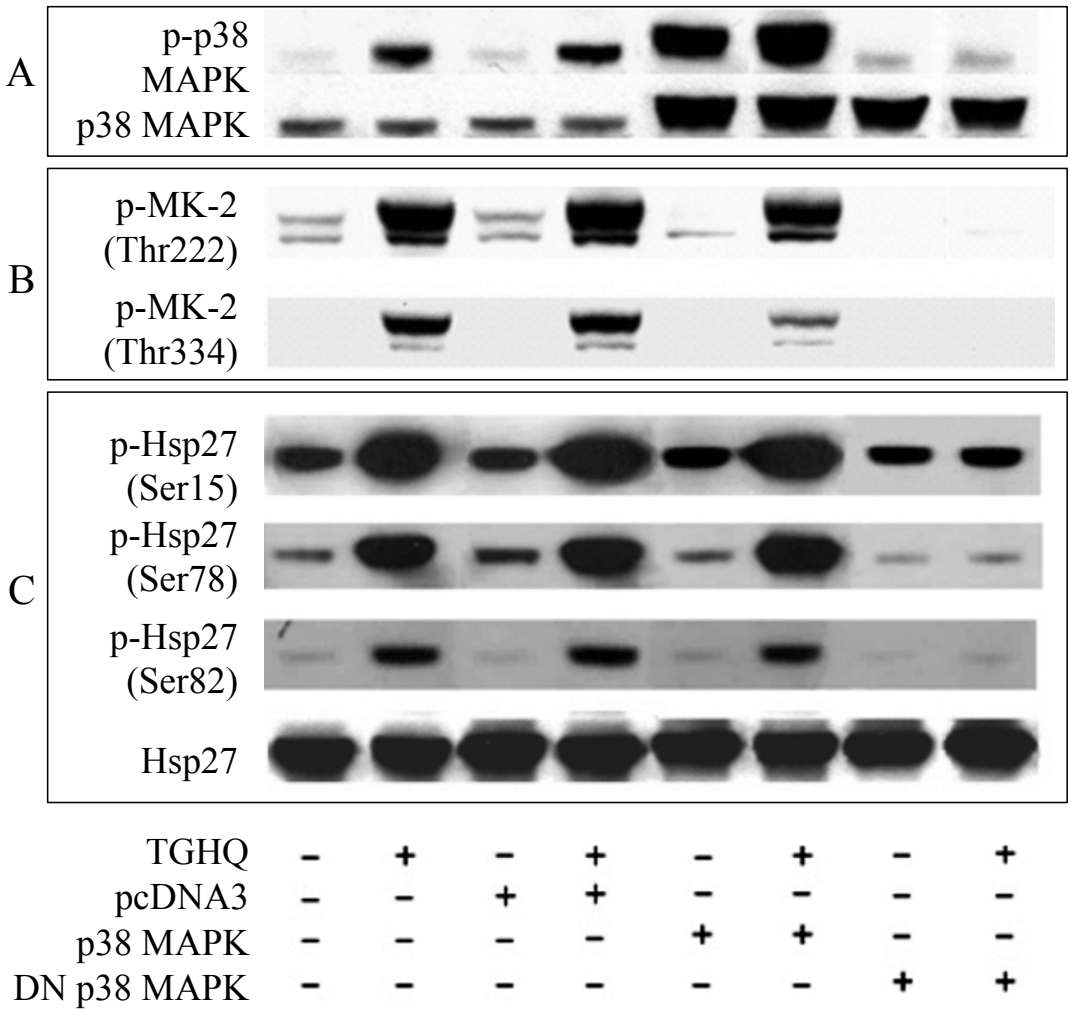

Figure 3.11 LLC-PK$_1$ cells transfected with a dominant negative mutant of p38 MAPK expressing vector fail to respond to TGHQ-induced responses.

LLC-PK1 cells were transfected with pcDNA3 (empty vector), pcDNA3 vector expressing native p38 MAPK (p38), or pcDNA3 vector expressing dominant negative mutant p38 MAPK (DNp38) as described in Methods. Transfected cells or untransfected cells were treated with TGHQ (200 μM) for 1 h, and cell lysates were separated by 10% SDS-PAGE gels, followed by Western blot analysis using phospho-specific antibodies for p38 MAPK, MK-2, and Hsp27. Total p38 MAPK expression levels was higher in p38 and DNp38 MAPK expressing vector transfected cells. Total Hsp27 expression levels were examined and no changes were revealed.

III. DISCUSSION

ROS are well known inducers of apoptosis, but can also induce oncosis under specific conditions, such as during ischemia reperfusion injury and hypoxia-induced ung cell death. The chromatin condensation and morphological changes that occur during TGHQ-induced renal cell death are indicative of oncotic cell death (Tikoo *et al.* 2001). To determine whether TGHQ, a ROS generating chemical, induces apoptosis in renal proximal tubule epithelial cells, I used various methods to detect apoptosis in TGHQ-treated LLC-PK1 cells. No apoptosis was detected at several different consentrations and exposure times to TGHQ. In contrast, TNFα induced substantial apoptotic cell death in LLC-PK1 cells. Therefore, TGHQ induces oncotic rather than apoptotic cell death in LLC-PK1 cells. It is well known that apoptosis is a genetically programmed mode of cell death, and which can be manipulated. In contrast, fewer studies have attempted to manipulate oncotic cell death, which appears also to engage various signaling pathways. Our studies on the signaling pathways activated during TGHQ-mediated oncotic cell death may eventually permit the manipulation of this deleterious and inflammatory type of cell death. At the least, manipulation of these signaling pathways such that the renal epithelial cells are driven from oncotic to apoptotic mode of cell death may better limit the adverse effects on adjacent cells and promote tissue survival.

Although we confirmed that TGHQ induces MAPKs phosphorylation robustly and in a time-dependent fashion (Figure 3.2 & 3.6), the upstream and downstream targets during TGHQ-mediated activation of the MAPK pathway remained unclear. Because MAPKs activation is EGFR–dependent in most cells, we examined whether TGHQ-induced MAPK activation in LLC-PK_1 cells also occurs through the EGFR. TGHQ induced histone H3 phosphorylation rapidly in LLC-PK_1 cells, whereas EGF did not

induce histone H3 phosphorylation, for at least 24 h (Figure 3.3). Histone H3 phosphorylation induced by TGHQ is ROS-dependent, and is associated with TGHQ-induced oncotic cell death (Tikoo *et al.* 2001). TGHQ, H_2O_2, and EGF all induced ERK1/2 phosphorylation in an EGFR-dependent manner, since AG1478, an inhibitor of EGFR, blocked ERK1/2 phosphorylation induced by each agent (Figure 3.2). In contrast, TGHQ and H_2O_2-induced p38 MAPK and JNK1/2 activation were EGFR-independent (Figure 3.6), and EGF failed to induce p38 MAPK or JNK1/2 phosphorylation in LLC-PK_1 cells. Since pharmacological inhibitors of the p38 MAPK and ERK, but not the JNK pathway decrease histone H3 phosphorylation (Figure 3.7), and protect LLC-PK1 cells from TGHQ-induced cell death (Ramachandiran et al. 2002), we conclude that both p38 MAPK and ERK pathways contribute to TGHQ-induced histone H3 phosphorylation and cell death. Thus, in contrast to the general concept that p38 MAPK is an inflammation/apoptosis-related kinase, p38 MAPK also participates in ROS-induced oncotic renal proximal tubule epithelial cell death.

Several tyrosine residues on the EGFR that are prone to autophosphorylation have been identified, including three major sites (Y1068, Y1148, and Y1173), and two minor ones (Y992 and Y1086) (Biscardi *et al.* 1999). Upon phosphorylation, these residues promote the binding of a number of downstream signaling proteins that possess SH2 domains, such as Shc, PLC-γ, Grb2, and SHP1, or PTB domain, such as Shc, c-Cbl. Binding of these molecules to the EGFR results in the activation of multiple signaling pathways that enhance DNA synthesis and promote cell division. Interestingly, TGHQ, H_2O_2, and EGF induce differential phosphorylation of EGFR tyrosine residues and subsequent different kinetics of MAPK activation in LLC-PK_1 cells (Figure 3.2 & 3.5). EGF, the endogenous ligand of the EGFR, induces rapid (<15 min) EGFR tyrosine phosphorylation at all residues examined (Y992, 1068, 1086, 1148, 1173) (Figure 3.5,

and summarized in 3.12). In contrast, TGHQ induced much slower (1 h) EGFR tyrosine phosphorylation, and only at residues Y992 and Y1068. Surprisingly, H_2O_2 only induced significant EGFR tyrosine phosphorylation at Y992, but H_2O_2-mediated ERK1/2 phosphorylation was dependent on EGFR activation (Figure 3.2). Additional, as yet unidentified phosphorylation site(s) may exist on the EGFR that are responsive to H_2O_2. One possibility is through the activation of the Src kinase. Src kinase binds to phosphorylated EGFR tyrosine residues at either 845 or 1101, and Src kinase can also phosphorylate EGFR at both residues (Sato *et al.* 2003; Tice *et al.* 1999). Interestingly, phosphorylation of EGFR tyrosine residue 1068, but no 992, recruits Grb2 binding to EGFR, which provides binding of C-Cbl binding and lead to degradation of EGFR (Jiang *et al.* 2003). Both TGHQ and H_2O_2 induced weaker EGFR tyrosine phosphorylation at residues Y1086 and Y1148, compared to EGF (Figure 3.5). Phosphorylation of Y1068, Y1148, and Y1173 can lead to the degradation of the EGFR, but they are also required for maximum kinase activity (Helin and Beguinot 1991). Absence or weak phosphorylation of EGFR Y1173 in TGHQ and H_2O_2-treated cells may prolong the activation of EGFR by these two agents. Moreover, H_2O_2 poorly phosphorylates the EGFR at Y1045, the major docking site for the ubiquitin ligase c-Cbl (Ravid *et al.* 2002). Consequently, H_2O_2 activated EGFR fails to recruit c-Cbl and does not undergo ubiquination and endocytosis(Ravid *et al.* 2002).

Since TGHQ generates ROS in LLC-PK_1 cells (Monks and Lau 1998), it is likely that there exist(s) common EGFR phosphorylation site(s) for both TGHQ and H_2O_2. Src phosphorylation sites, Y845 and Y1101, could represent additional phosphorylation targets of TGHQ and H_2O_2. Differential EGFR tyrosine phosphorylation profiles induced by different agents will likely contribute to the differential recruitment of signaling factors to the EGFR, resulting in different cellular responses (Schlessinger 2000). Based

on this view, TGHQ, EGF, or H_2O_2-induced EGFR tyrosine phosphorylation likely results in the recruitment of different signaling proteins to the EGFR that determines the differences in the cellular response. Additionally, AG1478 blocked TGHQ, H_2O_2 and EGF induced EGFR Y992 phosphorylation (data not shown), verifying its ability to block EGFR phosphorylation. However, AG1478 does not decrease histone H3 phosphorylation to a significant degree (Figure 3.7), neither does it protect cells from TGHQ-induced cell death (data not shown). We conclude that although AG1478 blocks ERK1/2 activation, it could also interfere with other signaling pathways, compromising its effects on cell death. The specificity of the pharmacological inhibitors should also be examined in our cell system to ensure their blocking of the designated signaling pathway.

Oxidative stress induces the phosphorylation of heat shock protein 27 (Hsp27), and both oligomerization and phosphorylation of Hsp27 may play an important role in the regulation of actin dynamics in response to growth factors and stress (Garrido 2002). Overexpression of Hsp27 prevents kidney ischemia/reperfusion-induced functional injury (Park *et al.* 2002). Because SB202190, an inhibitor of the p38 MAPK pathway, protects LLC-PK_1 cells against TGHQ-induced cell death (Ramachandiran *et al.* 2002), TGHQ-induced p38 MAPK-mediated Hsp27 phosphorylation might contribute to ROS-induced cell death. In support of this view, MK-$2^{-/-}$ mice are protected from ischemic brain injury (Wang *et al.* 2002), indicating that the p38 MAPK pathway is involved in ROS-induced cell death. Although Hsp27 overexpression or induction is associated with cytoprotection, the role of Hsp27 phosphorylation in ROS-induced renal cell death is unclear. Hsp27 serves as a molecular chaperone that associates with certain proteins, such as actin, Akt (Rane *et al.* 2003), and IκBα (Parcellier *et al.* 2003a), to stabilize and regulate their activation/deactivation. Inappropriate phosphorylation of Hsp27 might therefore convert Hsp27 from a cytoprotective to a death-inducing protein (Huot *et al.* 1998). TGHQ-

induced phosphorylation of MK-2 and Hsp27 is totally blocked by the p38 MAPK pathway inhibitors, SB202190 or SB203580 (Figure 3.9), or by transfection of LLC-PK_1 cells with dominant negative mutant p38 MAPK expressing vectors (Figure 3.11). Thus, TGHQ-induced p38 MAPK pathway activation mediates Hsp27 phosphorylation. The potential significance of Hsp27 phosphorylation was examined by immunostaining of phospho-Hsp27, which was only observed within damaged or dying cells (data shown in Chapter 5, Figure 4.8). Moreover, in post-confluent LLC-PK1 cells lacking Grp78, TGHQ failed to induce Hsp27 phosphorylation, indicating a link between ER stress and the p38 MAPK pathway, and subsequent Hsp27 phosphorylation (Jia *et al.* 2004). We therefore conclude that in preconfluent cells that are actively dividing, Hsp27, another downstream effector of the MAPKs, is phosphorylated by TGHQ through the p38 MAPK pathway, and that this modification is associated with TGHQ-induced oncotic cell death.

In summary, our data indicate that TGHQ induces selective EGFR phosphorylation, leading to the activation of the ERK pathway, and induces EGFR-independent p38 MAPK pathway activation. Both the ERK and p38 MAPK pathways contribute to histone H3 phosphorylation and oncotic cell death. In addition, TGHQ induces Hsp27 phosphorylation via the p38 MAPK pathway. Both histone H3 and Hsp27 phosphorylation have the potential ability to remodel chromatin. Because inappropriate chromatin condensation has been linked to TGHQ-induced cell death, the activation of both p38 MAPK and ERK1/2, and subsequent downstream signaling factors, likely play a key role in ROS-mediated oncotic cell death in renal epithelial cells. The mechanisms of TGHQ induced oncotic cell death are summarized in the cartoon (Scheme 2). The role of p38 MAPK in histone H3 phosphorylation remains to be resolved, as does the functional role of Hsp27 phosphorylation in TGHQ-induced oncotic cell death. Ongoing experiments are addressing these questions. Finally, immunoprecipitation of the EGFR

coupled to western blotting analysis or MALDI-TOF protein sequencing may identify different EGFR binding partners in response to stimulation with either EGF, H_2O_2, or TGHQ.

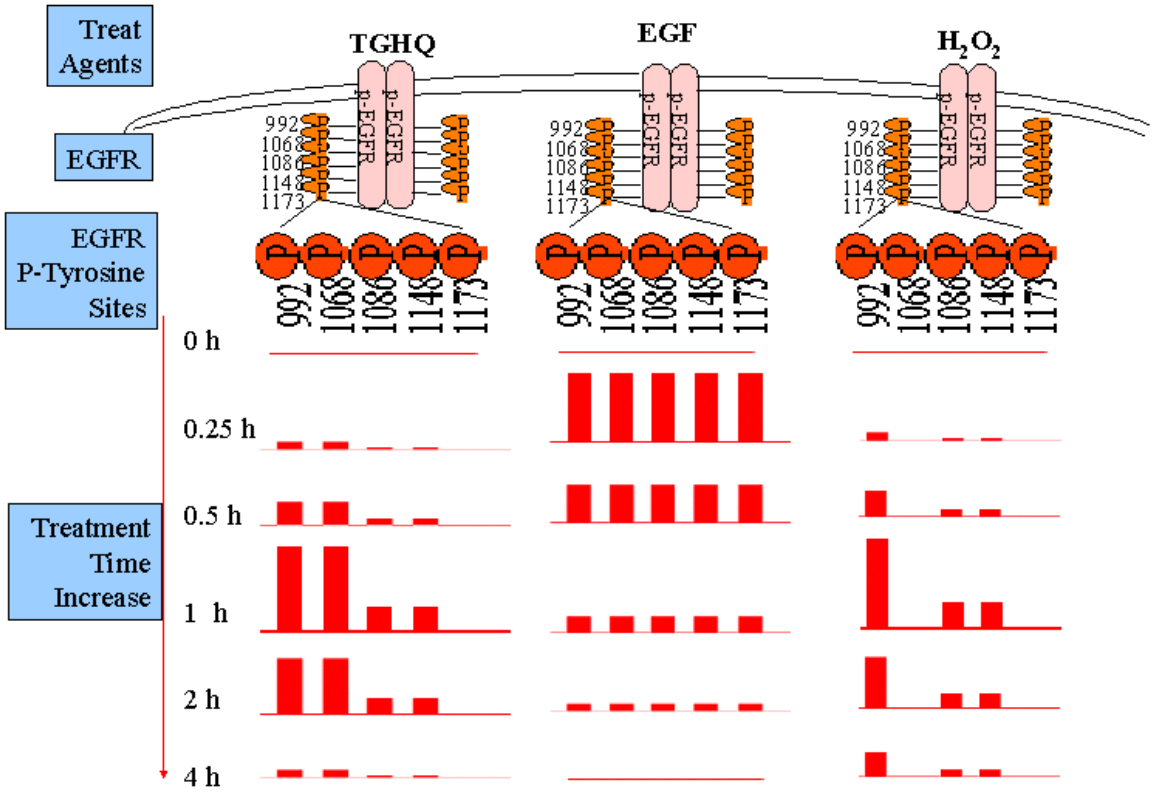

Figure 3.12 Profiles of EGFR tyrosine phosphorylation by TGHQ, EGF, and H_2O_2.

LLC-PK1 cells were treated with TGHQ (200 μM), EGF (50 ng/ml), or H_2O_2 (88.2 μM) for different periods of time (0, 0.25. 0.5, 1, 2, 4 h). Western blot analysis revealed the levels of specific phospho-EGFR at Y992, Y1068, Y1086, Y1148, and Y1173. EGFR tyrosine phosphorylation was determined semi-quantitively by densitometric scanning of each western blot.

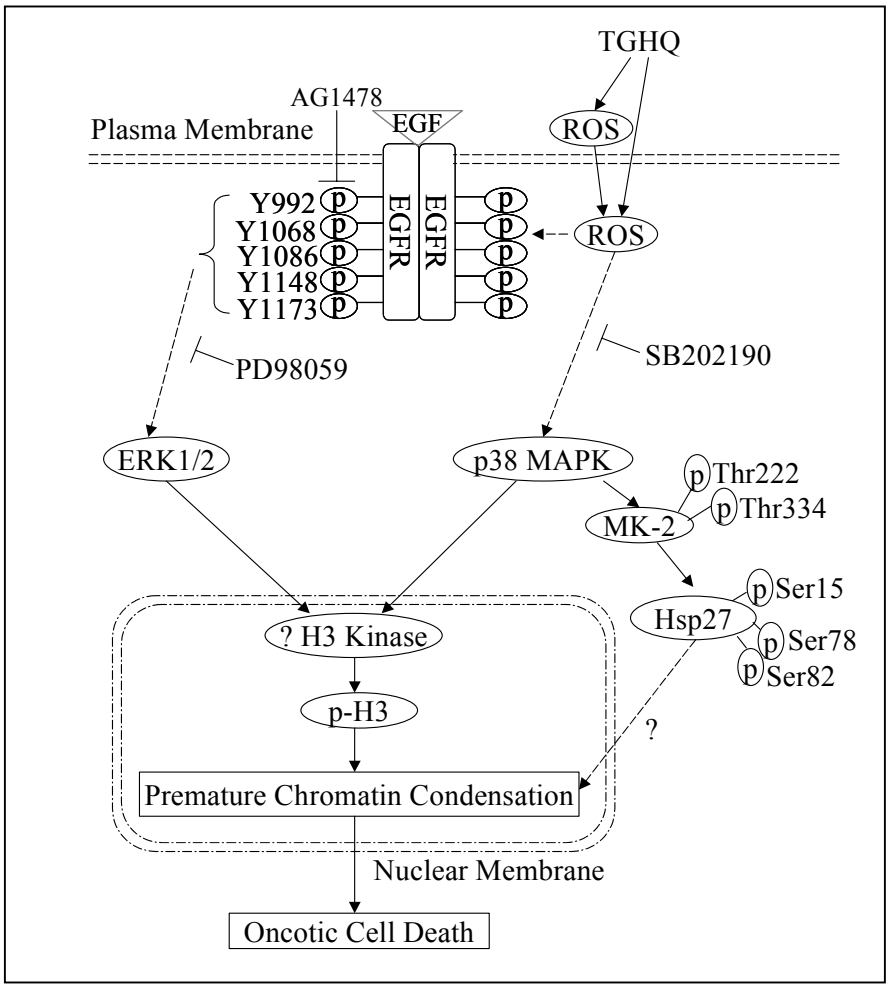

Figure 3.13 Possible signaling pathways that contribute to TGHQ-induced oncotic cell death in LLC-PK$_1$ cells.

TGHQ-generated ROS phosphorylate EGFR tyrosine residues, mainly at Y992 and Y1068, and induce the activation of ERK pathway. ERK1/2 activation leads to histone H3 phosphorylation. TGHQ-generated ROS also induce the activation of p38 MAPK, which phosphorylates MK-2 and Hsp27. p38 MAPK also leads to histone H3 phosphorylation. Inappropriate histone H3 phosphorylation leads to premature chromatin condensation and oncotic cell death. Meanwhile, Hsp27 phosphorylation induced by p38 MAPK activation might also be associated with TGHQ-induced chromatin remodeling, and oncotic cell death. Thus multiple rather than a single pathways contribute to TGHQ-induced oncotic cell death.

Chapter 4: PROTEOMIC STUDIES ON PROTEIN REGULATIONS BY TGHQ IN RENAL EPITHELIAL CELLS

I. INTRODUCITON AND RATIONALE

ROS, including superoxide anion ($O_2^{\cdot -}$), hydrogen peroxide (H_2O_2) and hydroxyl radical ($HO^{\cdot}$) are generated either endogenously as by-products during mitochondrial electron transport or by several oxidoreductases and by the metal-catalyzed oxidation of metabolites, or exogenously by redox-active chemicals. ROS are associated with a variety of human diseases and chemical-induced toxicities (Bolton *et al.* 2000). An increasing number of studies are implicating ROS in key roles in cell signaling (Arnold *et al.* 2001; Irani *et al.* 1997; Rhee 1999). In contrast, ROS may cause direct damage to cellular macromolecules such as lipids, proteins, or nucleic acids, which subsequently induces activation of various stress-response signaling pathways. Renal proximal tubule epithelial cells are particularly susceptible to oxidative stress-induced damage. TGHQ-induced nephrotoxicity in renal epithelial cells is therefore considered a good model for the study of ROS-generating chemical-induced toxicity.

TGHQ is a potent nephrotoxic metabolite of HQ (Lau *et al.* 1988), causes oncotic cell death of renal proximal epithelial cells in a ROS-dependent manner (Ramachandiran *et al.* 2002), and contributes to HQ-mediated nephrotoxicity and nephrocarcinogenicity (Lau *et al.* 1988; Lau *et al.* 2001a; Peters *et al.* 1997). TGHQ induced cell death is ROS-dependent, because catalase is able to completely block TGHQ-mediated cell death. Moreover, TGHQ likely enters renal epithelial cells through the L-amino acid transporter as the corresponding cysteine conjugate, thus providing an intracellular ROS generating source. The one-electron reduced form of a quinol-thioether may react with O_2, yielding

superoxide anion radical, which finally gives rise to hydrogen peroxide and hydroxyl radical (Monks and Lau 1998). These ROS cause extensive DNA damage, as evidenced by the formation of DNA single strand breaks and a rapid growth arrest response (Jeong *et al.* 1996). In the preceding chapter, I discussed the potential signaling pathways that contribute to TGHQ-mediated renal cell death, focusing on the MAPK pathways and histone H3 phosphorylation. Since none of the three inhibitors, or the combination of the inhibitors for the MAPKs, is able to completely block TGHQ-induced renal cell death, activation of some other pathways must also contribute partially to TGHQ-mediated renal cell death. Therefore, using a proteomics approach I intended to reveal additional potential signaling pathways that may play a role in TGHQ-mediated cell death.

The signaling pathways engaged in TGHQ induced oncotic renal cell death are complex. TGHQ induces changes in a complex network of signaling pathways, some of which are initiated as a defensive/buffering response against oxidative stress. Such cell stress responses include initial sacrifice of antioxidants (GSH, Trx, Prx, etc.) and reorganization of the cytoskeleton (actin, etc.), followed by post-translational modification of cell signaling components (MAPK cascades, cell cycle, etc.), and finally, activation of transcriptional factors (AP-1, NF-κB, etc). In our studies using 2-dimensional gel electrophoresis and mass spectrometry, we identified changes in several proteins, either in their overall expression, or as post-translational modifications. Among these proteins, changes to Prxs and Hsp27 were the most significant. Indeed, Prxs are a family of thioredoxin dependent peroxidases, which are believed to be gatekeepers for cell signaling in response to ROS (Wood *et al.* 2003). The 2-Cys Prxs behave as antioxidant enzymes (Hofmann *et al.* 2002), as a peroxynitrite reductase (Bryk *et al.* 2000), and as signaling factors (Fujii and Ikeda 2002). Prxs require two redox-active cysteines to be active as an antioxidant enzyme. Thus, when cells are exposed to very

high levels of ROS, Prxs are oxidized (to sulfenic acid and/or sulfinic acid) (Wagner *et al.* 2002) and consequently lose their antioxidant function. Prxs are also associated with the mitogen activated protein kinases (MAPKs) signaling pathways (Hess *et al.* 2003; Kang *et al.* 2004; Romashko *et al.* 2003; Veal *et al.* 2004), which are all activated by TGHQ very rapidly in LLC-PK1 cells (Ramachandiran *et al.* 2002). Both ERK1/2 and p38 MAPK activation contribute to histone H3 phosphorylation and oncotic cell death. Inappropriate phosphorylation of histone H3 leads to premature chromatin condensation and oncotic cell death in LLC-PK1 cells (Tikoo *et al.* 2001). One downstream substrate of p38 MAPK is the mitogen activated protein kinase activated protein kinase-2, which, upon phosphorylation, phosphorylates its substrate heat shock protein 27 (Hsp27). Hsp27 is a chaperone protein (Rogalla *et al.* 1999), and is associated with actin stabilization (Lavoie *et al.* 1993b; Lavoie *et al.* 1995), and with cell signaling, such as Akt (Rane *et al.* 2003) and IKK (Park *et al.* 2003). Overexpression of Hsp27 in cells provides cytoprotective effects (Kampinga *et al.* 1994; Landry *et al.* 1989; Lee *et al.* 2004; Lewis *et al.* 1999; Park *et al.* 1998), whereas the roles of Hsp27 phosphorylation in ROS-induced cell death remain debatable. On one hand, Hsp27 phosphorylation facilitates actin reorganization and provides a cytoprotective effects (Huot *et al.* 1997; Landry and Huot 1995; Mounier and Arrigo 2002). On the other hand, phosphorylation of Hsp27 could lead to loss in chaperone function, activate/inactivate signaling pathways, or induce actin polymerization and cell blebbing, a typical morphological alteration observed during apoptosis (Huot *et al.* 1996). Unphosphorylated Hsp27, but not phosphorylated Hsp27, also increases cellular GSH levels and protects cells from oxidative stress (Arrigo 1998).

As discussed above, multiple signaling pathways are likely associated with TGHQ-induced renal cell death, each of which may either play a role in cytoprotection or

cell death. Using pharmacological inhibitors or molecular manipulation, we have not been able to identify a single signaling pathway that is solely responsible for TGHQ-induced oncotic cell death. It is likely that the balance of a network of signaling pathways determines the fate of renal epithelial cells. To obtain a more global view of the signaling factors involved in TGHQ-mediated cell signaling at the protein level, we used a high throughput proteomics approach.

II. RESULTS

A. Changes of cellular proteins in TGHQ treated LLC-PK1 cells

After TGHQ (200 μM) treatment for 1, 2, or 4 h, the intensity of eleven spots on the 2-D gel changed compared to that in the untreated cells (Figure 4.1). The changes in spot intensity were first identified manually by two individuals, and then subject to PDQUEST program for analysis and quantitation. Spots with altered intensities after TGHQ treatment were excised out, subject to in-gel digestion, and the proteins in the spots were identified by MALDI-TOF mass spectrometry. Identities of these proteins are listed in Table 4.1, with the percentage of peptide masses matched, key functions of the proteins, and their approximate pIs on the 2-D gel. Among the eleven proteins identified that changed intensity after TGHQ treatment, two pairs of three spots were each recognized as either Prx3 or Hsp27. After TGHQ treatment, the intensity of the spot with more acidic pIs increased, but the intensity of the spot with more basic pI decreased compared to untreated cells (Figure 4.1). Other proteins regulated by TGHQ in LLC-PK1 cells included a rapid increase in the overall expression of annexin I, calreticulin, and an increase followed by a decrease in PDI precursor and nucleophosmin/B23 (Figure 4.1). These proteins are associated with a number of cellular functions such as carcinogenesis, ER stress, calcium regulation, and nuclear shuttling. The changes were quantified by the PDQEST program and summarized (Figure 4.2). Folds of increase in the spot intensity after treatment compared to controls at each time point are illustrated as bars (Figure 4.2). Bars to the left represent decreases in the spot intensity, and bars to the right with increased spot intensity. Annexin I levels increased after TGHQ treatment, as evidenced on the 2-D gel, and confirmed by western blot analysis using a specific antibody for Annexin I (Figure 4.3). The folds of increase after TGHQ treatment compared to controls were quantified by spot-densotometry (Figure 4.3).

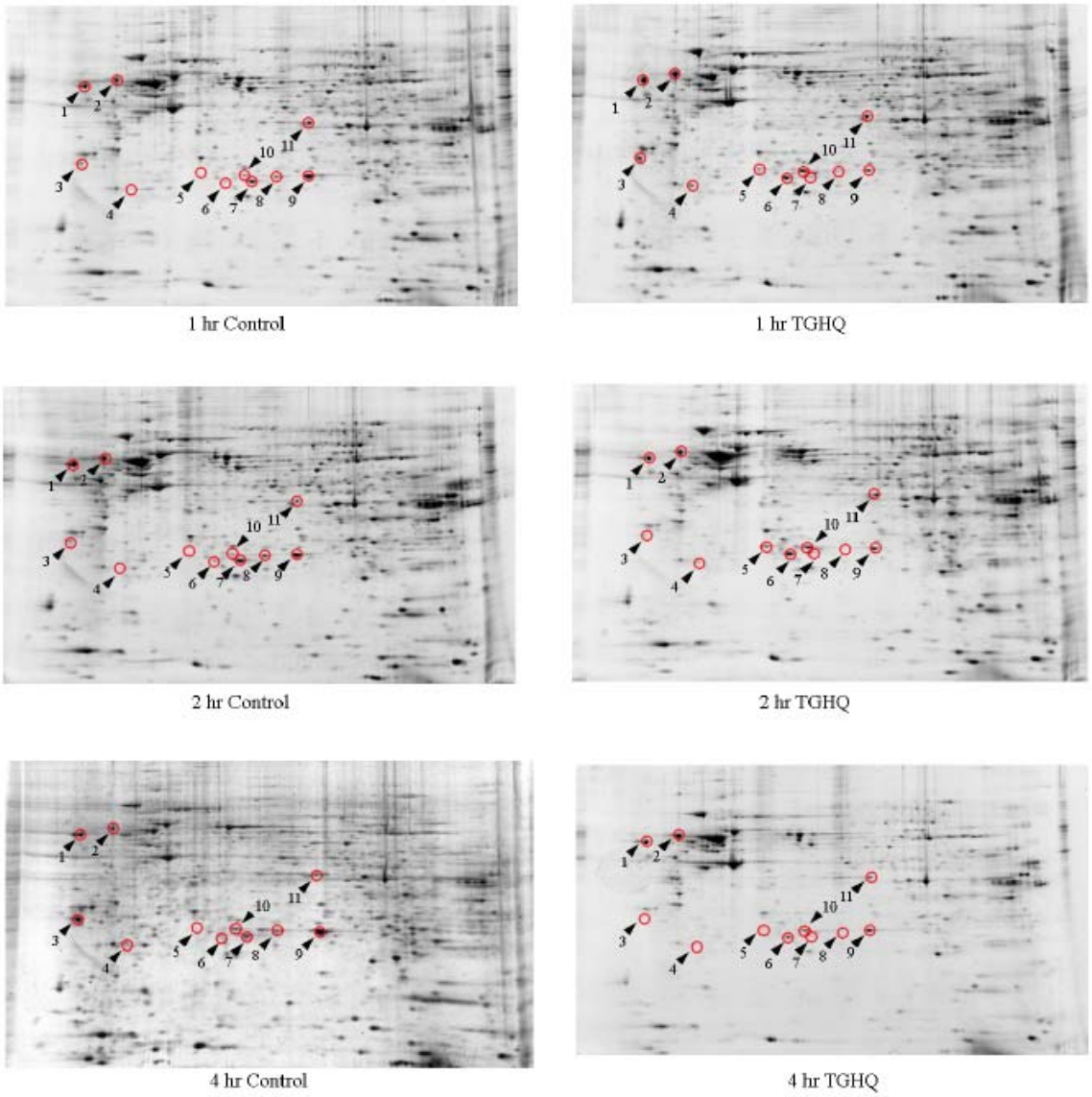

Figure 4.1. 2-D gel analysis of TGHQ induced protein changes in LLC-PK1 cells.
The spots with increased or decreased intensity in TGHQ treated cells compared to controls are circled in red and highlighted with arrows and numbers. The identities of the spots are summarized in Table 4.1. Cells were treated with TGHQ (200 μM) for 1, 2, or 4 h, and were compared to untreated cells at each time point. Changes in the spot intensity were initially identified by at least two individuals, and were subsequently analyzed and quantified by PDQUEST. 1. Calreticulin, 2. Protein disulfide isomerase precursor (PDI), 3. Nucleophosmin/B23, 4. Peroxiredoxin 2, 5 & 9 & 10. Heat shock protein 27 (HSP27), 6 & 7 & 8. Peroxiredoxin 3, 11. Annexin I.

Table 4.1. A summary of the proteins altered by TGHQ.

Identity	**#/% Masses Matched**	**Key Functions**	**~pI**
Calreticulin	8/20 (40%)	Calcium binding protein, protein assembly	4
Protein disulfide isomerase precursor (PDI)	6/20 (30%)	Chaperone, protein folding, regulating cell adhesion	5
Nucleophosmin/B23	2/3 (66%)	Ribosomal assembly/rRNA transport, phophorylated by cdc2 during mitosis	4
Peroxiredoxin 2	5/6 (83%)	Reduce peroxides	5
Heat shock protein 27	5=9=10	Stress resistance actin organization	7
Peroxiredoxin 3	3/5 (60%)	Reduce peroxides	7.5
Peroxiredoxin 3	4/5 (80%)	Reduce peroxides	8
Peroxiredoxin 3	8=6	Reduce peroxides	8.5
Heat shock protein 27	5/11 (45%)	Stress resistance actin organization	9
Heat shock protein 27	10=5=9	Stress resistance actin reorganization	8
Annexin I	7/20 (35%)	Calcium binding protein, cell adhesion, endocytosis/exocytosis, carcinogenesis	9

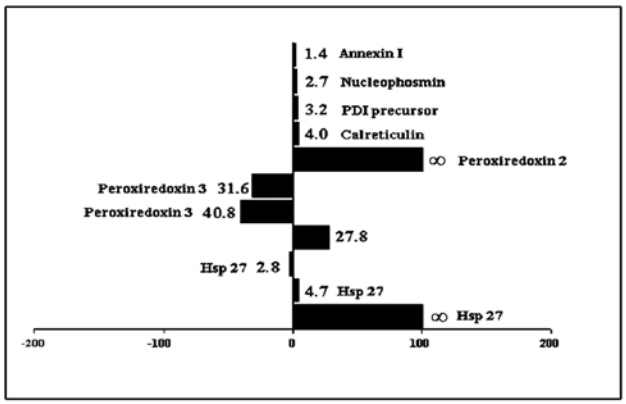

TGHQ 1 hr

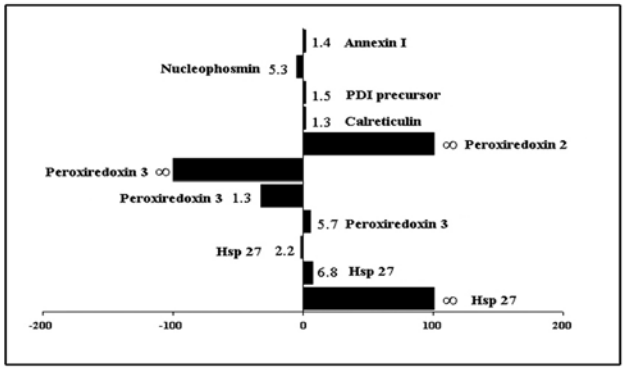

TGHQ 2 hr

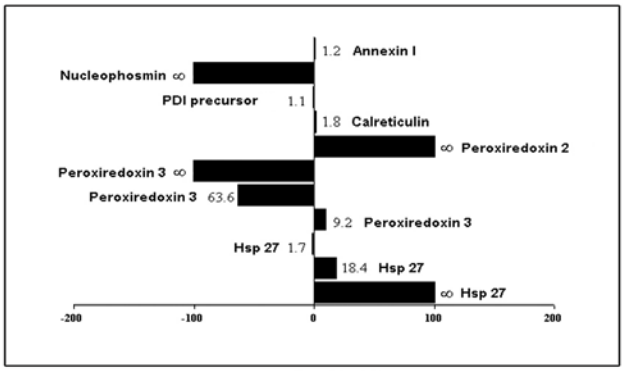

TGHQ 4 hr

Figure 4.2. Quantification of protein changes in TGHQ-treated LLC-PK1 cells.

Spots with altered densities were analyzed using the PDQUEST software package (Bio-Red). Increases or decreases in the intensity of the spots in treated cells compared to controls are illustrated by black bars, along with the fold-increase or decrease. *Note:* '∞' means one of the spots (either in control or in treated) was undetectable on the 2D gel, whereas the counterpart had significant detectable intensity (n=2).

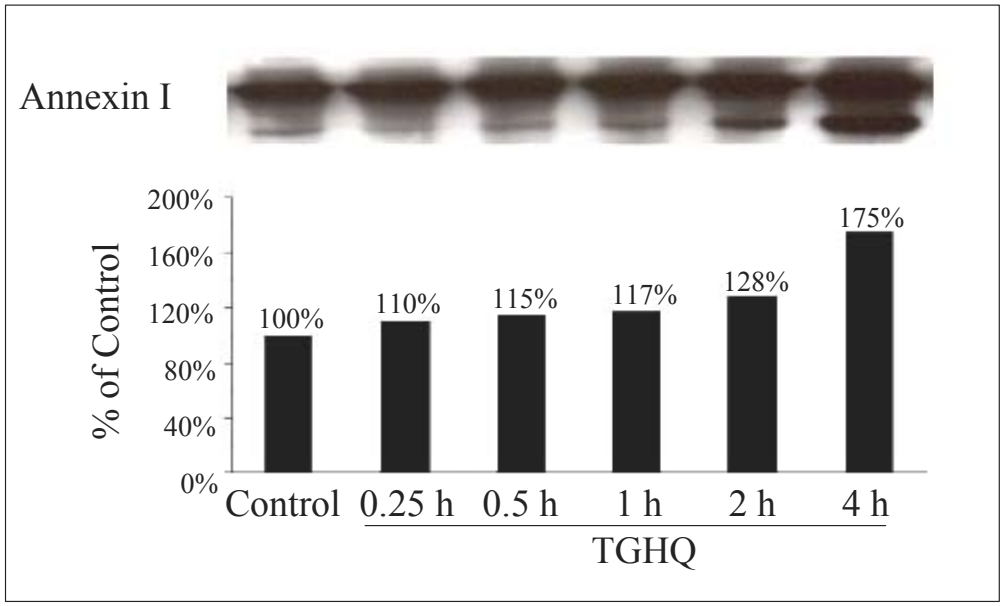

Figure 4.3. Annexin I expression levels increased after TGHQ treatment.

LLC-PK1 cells were treated with TGHQ (200 mM) for 0 to 4 h, and total cellular proteins were extracted and subject to western blot analysis using specific antibody for Annexin I. The intensity of the western bands was quantified by spot-densotometing and shown in the figure (n=1).

B. Prx3 is modified by TGHQ

Three spots on the 2-D gels were identified as Prx3, and the intensity of the spots changed after TGHQ treatment, shifting to a more acidic pI (Figure 4.4). This mode of change is likely due to post-translational modification, for example, oxidation and/or phosphorylation. We used a specific antibody (provided by Dr. Garth Powis, Univ. of Arizona Cancer Center) to examine the total levels of Prx3 before and after TGHQ treatment, and which revealed a decrease in intensity of the Prx3 band (Figure 4.5). A nonspecific staining band serves as an equal loading control for the total proteins. The observed decrease in the Prx3 band intensity is likely due to either a decrease in Prx3 expression levels, or due to a shift of mobility of the protein after TGHQ treatment. Because the western blot analysis was performed under denaturing conditions, which could lead to a reduction of Prx3, we examined the mobility of Prx3 on a native gel under non-denaturing conditions. Native western blot analysis revealed a significant band shift after TGHQ treatment (200 μM, 2 h) (Figure 4.6). Before treatment, a single band was identified as Prx3 and represents the native Prx3 within LLC-PK1 cells. After TGHQ treatment, the intensity of the native Prx3 band decreased significantly, with the concomitant appearance of another band below the native Prx3 band, with a higher mobility on the gel (Figure 4.6). H_2O_2 (88.2 μM, 2 h) was compared with the TGHQ-mediated effects on Prx3, and it produced similar effects as TGHQ, but to a lesser extent (Figure 4.6). This mobility shift is most likely due to oxidation, as reported by others (Rabilloud *et al.* 2002; Woo *et al.* 2003a). To identify the modification of Prx3 after TGHQ treatment, we excised the corresponding band revealed by western blot analysis from the native gel, and digested it with trypsin or chymotrypsin. The peptides, after digestion, were analyzed by LC-MS/MS to identify the modification on Prx3. The band

in the control sample representing the native Prx3 was identified without modification (data not shown), whereas in the TGHQ treated sample we were unable to identify the second band as either Prx3, or the nature of the modification. One spot on the 2-D gel was identified as Prx2 (spot V) (Figure 4.4). The intensity of spot IV increased after TGHQ treatment, which is likely the ROS-modified Prx2, again as supported by the others (Rabilloud *et al.* 2002). Interestingly, Rabilloud *et al.* reported only two spots on 2-D gels as Prx3, including one as the reduced and one as oxidized Prx3 by H_2O_2. However, we identified a third spot as Prx3 (spot III), which has decreased intensity after TGHQ treatment (Figure 4.4). Whether this spot is another modified form of Prx3 or whether it is a sub-isoform of Prx3 invites further investigation.

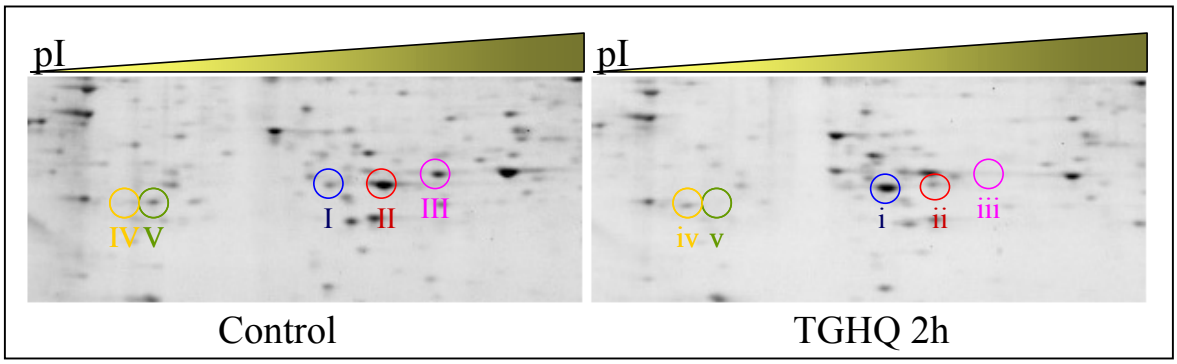

Figure 4.4. TGHQ induced modification of peroxiredoins (Prx) revealed by 2-D gel analysis.

LLC-PK1 cells were treated with TGHQ (200 μM) for 2 h, and the cells were lysed and total proteins were subject to 2-D gel for separation, and finally visualized by fluorescent staining. There are three spots (i, II, III) on the 2-D gel that are all identified as Prx3, one spot (V) identified as Prx2, and one postulated as oxidized Prx2 iv). The corresponding spots on the control or treated samples are marked with the same numbers (capitalized or uncapitalized). Approximate pIs for these spots are listed in Table 4.1.

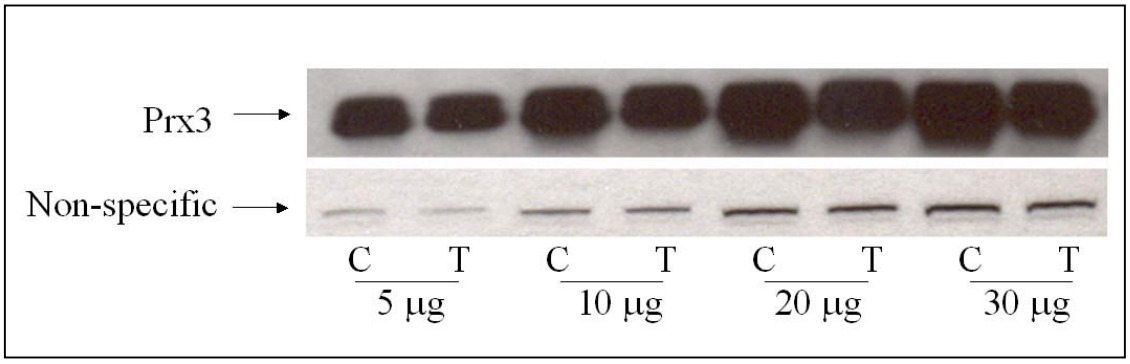

Figure 4.5. TGHQ induced changes in Prx3 revealed by western blot analysis.

LLC-PK1 cells were lysed and subject to western blot analysis under denaturing conditions using a specific antibody for Prx3. Proteins (5-30 μg) were loaded onto SDS-PAGE from either control (C) or TGHQ (200 μM, 2 h) treated samples (T). Nonspecific band are shown here for a verification of equal loading.

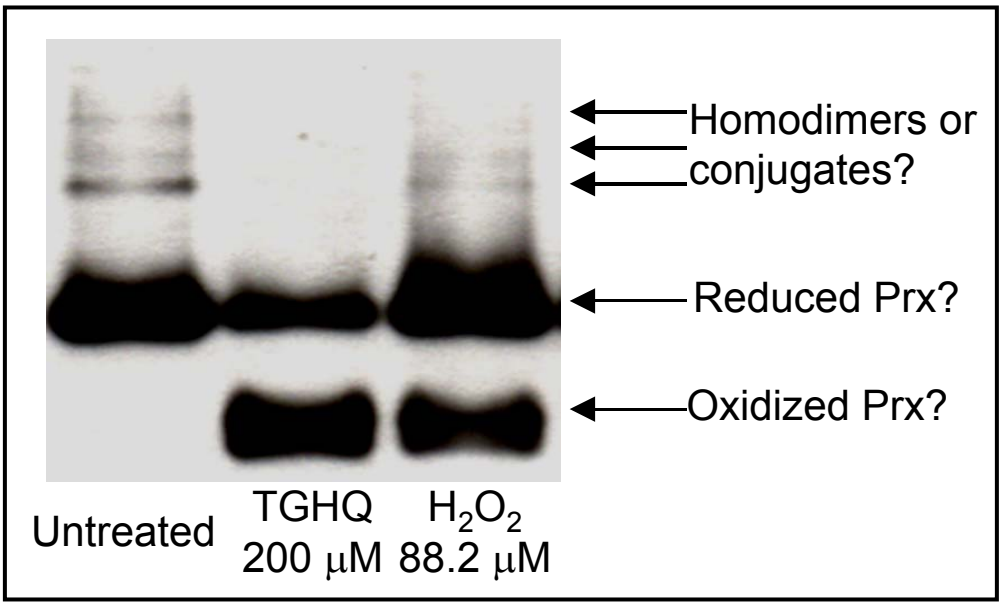

Figure 4.6. TGHQ and H_2O_2 induced a mobility shift of Prx3 revealed by native western blot analysis.

LLC-PK1 cells were treated with TGHQ (200 μM, 2 h), or H_2O_2 (88.2 μM, 2 h), and then lysed and subject to native western blot analysis under non-denaturing conditions. Total proteins (3 μg) were loaded onto the gel and separated.

C. Hsp27 revealed to be modified by TGHQ by 2-D gel analysis

Similar to Prx3, Hsp27 was identified in three spots on 2-D gels that changed intensity after TGHQ treatment (Figure 4.7). The intensity of the spots with more acidic pI increased after TGHQ treatment, whereas the intensity of the spot with a more basic pI decreased after treatment (Figure 4.7). This again implies a post-translational modification of Hsp27 after TGHQ treatment. This was the first time a Hsp27 modification was revealed by 2-D gel analysis. One known modification for Hsp27 is phosphorylation, and there are multiple residues on Hsp27 that may be phosphorylated (Gaestel *et al.* 1991; Landry *et al.* 1992). Using phosho-specific antibodies, we were able to reveal increases in phosphorylation of Hsp27 at S15, S78 and S82 (Figure 3.9). Therefore, the observations on the 2-D gel analysis are most likely due to the phosphorylation of Hsp27 at multiple serine residues. Phosphorylation and oligomerization of Hsp27 are important for its function, as discussed in Chapter 3. Immunocytochemical staining revealed constitutive phospho-Hsp27 (S15) in the untreated cells (Figure 4.8), and an increase in phospho-Hsp27 (S15) after TGHQ treatment (200 μM, 2 h). This observation is consistent with our western blot data on the levels of phospho-Hsp27 (S15) (Figure 3.9). Higher magnification revealed that cells staining positive for p-Hsp27 were mostly those with irregular morphology (Figure 4.8D).

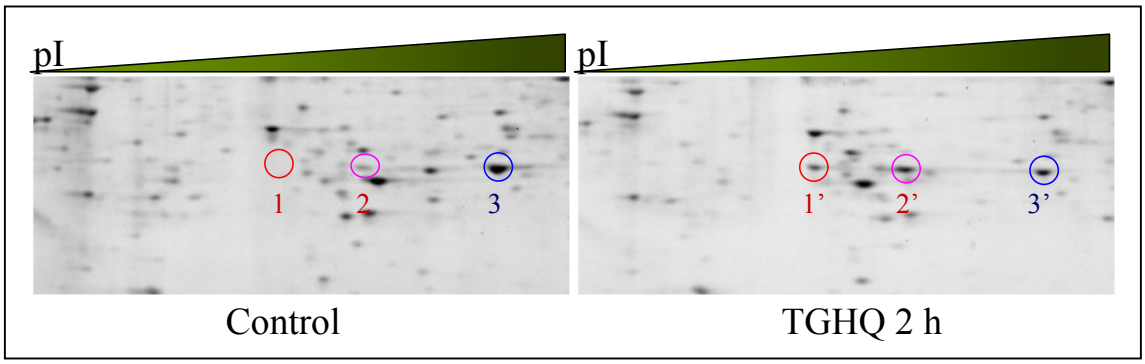

Figure 4.7. TGHQ induced changes of intensity of three spots on 2-D gel, all identified as Hsp27.

LLC-PK1 cells were treated with TGHQ (200 μM, 2 h), lysed, and total protein was subject to 2-D gel separation. Proteins were visualized by fluorescent staining. There are three spots (1', 2', 3) on the 2-D gel that were all identified as Hsp27. The corresponding spots on the control or treated samples are marked with same numbers (capitalized or uncapitalized). Approximate pIs for these spots are listed in Table 4.1.

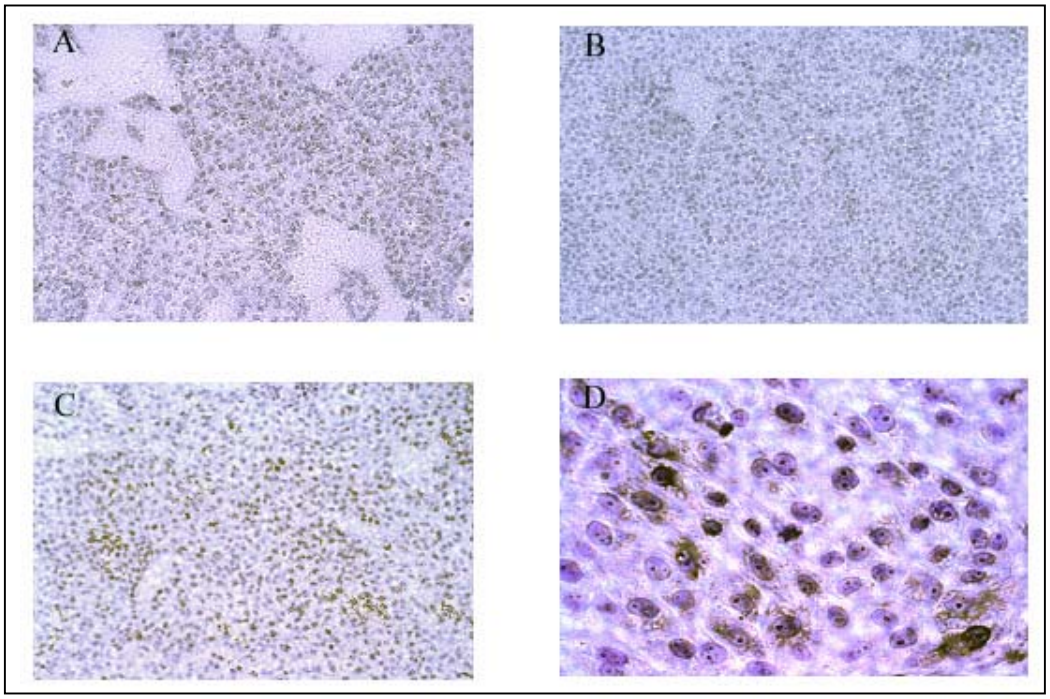

Figure 4.8. Localization of phosphorylated Hsp27 within LLC-PK1 cells after TGHQ treatment.

Untreated or treated LLC-PK1 cells were subject to immunocytochemical staining using phospho-specific antibody for phospho-Hsp27 (Ser15). Cells expressing phospho-Hsp27 (Ser15) stain brown, otherwise, cells stain purple. *A*. untreated; *B*. IgG control; *C&D*. TGHQ treated (200 μM, 2 h). *A&B&C.* ×40; *D*. ×400.

III. DISCUSSION

These experiments were designed to identify additional proteins that modulate ROS-mediated oncotic renal cell death. TGHQ caused consistent changes in the mobility of several proteins upon 2-D gel analysis cells, each with various functions associated with antioxidants, the cytoskeleton, carcinogenesis, ER stress, calcium regulation, and nuclear shuttling. In general, when cells are exposed to ROS, they possess a first line of defensive barrieres to protect themselves against oxidative stress. At the same time, ROS also induce activation of signaling pathways that could either contribute to or protect from cell death. The balance of these two opposing types of signaling pathways determines whether cells survive or die. This balance is dependent on the intensity of the stress that the cells are exposed to. If the amount of stress exceeds the defensive capacity, cell death prevails.

One of the first lines of defense against oxidative stress are the Prxs. Prxs (Hofmann *et al.* 2002) are a family of abundantly expressed peroxidases that provide an initial defense against ROS-mediated cell damage. Other anti-oxidants include GSH, catalase, and SOD. In the presence of a small amount of intracellular ROS, Prxs reduce H_2O_2 and oxidized lipids by the concomitant oxidation of the active cysteine sulfhydryl group to a sulfenic acid (SOH), and subsequently disulfide bond formation with a second active cysteine residue (S-S) (Rhee *et al.* 2001). Oxidation of the cysteine residue is quickly reversed by thioredoxin reductase, and Prxs regain their antioxidant function (Rhee *et al.* 2001). In contrast, in the presence of an overwhelming amount of ROS, additional oxidation of the Prxs cysteine residues to sulfinic (SO_2H) and sulfonic acid (SO_3H) occurs (Rabilloud *et al.* 2002). These oxidation products are not easily reversed and the process of reduction is slow and requires specialized enzymes (Chang *et al.* 2004;

Woo *et al.* 2003a). This super-oxidation of Prxs allows ROS to interact with other cellular constituents and to activate an oxidative stress response. In this respect, superoxidation of Prxs is probably the gateway for ROS-mediated stress signaling activation in cells. We found that Prx3 is modified by TGHQ, as well as by H_2O_2, evidenced by western blot analysis. Others have reported the identification of two spots on a 2-D gel as Prx3, and observed similar phenomenon of spot intensity changes after H_2O_2 treatment (Rabilloud *et al.* 2002). Mass spectrometric analysis of the spots revealed that the spot with a more acidic pI had one cysteine oxidized to sulfonic acid (Rabilloud *et al.* 2002). Therefore, TGHQ-induced Prx3 modification very likely involves oxidation of cysteine residues to sulfinic or sulfonic acid.

Interestingly, Prxs also regulate MAPK activity (Kang *et al.* 2004; Veal *et al.* 2004), and overexpression of Prxs protects cells against oxidative stress induced cell death (Butterfield *et al.* 1999; Nonn *et al.* 2003). Both ERK1/2 and p38 MAPK pathways are activated by TGHQ, and are associated with TGHQ-induced renal cell death. We also know that the activation of ERK1/2 occurs through EGFR activation, whereas p38 MAPK activation is EGFR-independent (Chapter 3). One mechanism by which the stress activated protein kinases (SAPK, p38 MAPK & JNK) are activated is through the dissociation and activation of SAPK, or its upstream kinases, from their binding partners. For example, 14-3-3, a scaffold protein is found to interact with MKK1, 2, or 3 (Fanger *et al.* 1998). Trx binds to Ask1, an upstream kinase of p38 MAPK, and prevents the activation of the p38 MAPK and JNK cascades (Saitoh *et al.* 1998). Trxs have much similarity with Prxs, both functioning as antioxidants, both are activated/inactivated by oxidation, and both are associated with the MAPK pathways. Therefore, oxidation of Prxs by TGHQ may contribute to the activation or inactivation of a number of signaling pathways, especially the MAPK pathways. Native western blot analysis on Prx3 revealed

a band shift after TGHQ and H_2O_2 treatment, most likely due to oxidation. Dithiothreitol treatment was not able to reverse the oxidation (data not shown), indicating that the oxidation of the cysteine residues results in sulfinic or sulfonic acid formation. The bands were excised and analyzed for post-translational modification by LC-MS/MS mass spectrometry. However, the identification of the modification was technically difficult, given that more than one protein were likely present in an excised single band. Further attempts on 2-D gel analysis followed by mass spectrometry has better separation of the proteins but could still not detect the modification. This is probably due to insufficient amount of Prx3 after sample preparation. One way to obtain sufficient sample for mass spectrometric analysis of Prx3 modification would be to pool the samples from several parallel-run 2-D gels. Future functional analysis would probe the cytoprotective effects of Prxs against ROS by overexpressing Prxs in LLC-PK1 cells, and reveal the potential binding partners of Prxs. In contrast to findings from the others, we identified a third spot on the 2-D gel as Prx3, the intensity of which decreased after TGHQ treatment. This spot also had a slower mobility shift on the 2-D gel, either due to a different molecular weight or due to different charges. We have not yet been able to determine the nature of the difference between the spots on the 2-D gels, all identified as Prx3. Because Prxs are abundant and highly conserved proteins, and because MALDI-TOF identification of Prxs relies on only partial peptide sequence match with the theoretical proteins, it is likely that the third spot is an isoform of Prx3. Notably, this spot was also modified by TGHQ.

TGHQ induced a similar pattern of Hsp27 modification upon 2-D gel analysis. The phosphorylation of Hsp27 by TGHQ was confirmed by western blot analysis and was found to be very rapid and intensive. Microscopic analysis revealed an increase in phospho-Hsp27 staining mainly in those cells displaying signs of cellular damage after treatment with toxic doses of TGHQ. Hsp27 lies downstream of the p38 MAPK pathway

(Chapter 3), and has multiple functions. Usually, heat shock proteins are well known for their cytoprotective effects, which are the subject of many studies. However, the consequences of Hsp27 phosphorylation under oxidative stress appear complicated, as evidenced by opposing observations in different systems by different approaches and by investigators (Arrigo 1998; Benndorf *et al.* 1994; Dalle-Donne *et al.* 2001; Ehrnsperger *et al.* 1997; Garrido 2002; Guay *et al.* 1997; Huot *et al.* 1998; Huot *et al.* 1996; Jakob *et al.* 1993; Kato *et al.* 1994; Lavoie *et al.* 1995; Mehlen *et al.* 1996a; Parcellier *et al.* 2003a; Preville *et al.* 1998; Rogalla *et al.* 1999). In summary, unphosphorylated Hsp27 forms large oligomers and functions as a chaperone protein to bind and regulate Hsp27-interacting proteins. Therefore, overexpression of total Hsp27 increases cell viability against ROS challenge. Upon phosphorylation, Hsp27 disaggregates and forms small oligomers or monomers, which lose their chaperoning function. However, phosphorylated Hsp27 can assist in stabilizing cytoskeleton by interacting with actin, providing a cytoprotective effect against ROS. Moreover, only unphosphorylated Hsp27 can increase cellular GSH levels, thereby protecting the cells from oxidative stress. Interestingly, in neutrophils, Akt, p38 MAPK, MK-2, and Hsp27 form a signaling module (Rane *et al.* 2001). Upon activation of p38 MAPK by transient transfection of MKK3 or MKK6 in HEK293 cells, Hsp27 is phosphorylated and dissociates from the module (Rane *et al.* 2001). The association of Hsp27 with Akt is required for the activity of Akt, which is lost due to the dissociation of Hsp27 from Akt (Rane *et al.* 2003). Pivotal experiments showed that LLC-PK1 cells transfected with plasmid expressing mutated Hsp27 (3A), which mimics the fully phosphorylated form of Hsp27 (S15, S78, S82) demonstrated no change in viability compared to the mock-transfected cells (data not shown). Additionally, pretreatment of LLC-PK1 cells with DDM-PGE2 provides protection against TGHQ-induced cytoxicity. However, TGHQ failed to induce Hsp27

phosphorylation and the cytoprotective effects of DDM-PGE2 against TGHQ were lost in post-confluent Grp78 non-inducible LLC-PK1 cells (Jia *et al.* 2004). These data indicate that Hsp27 phosphorylation likely exhibits dual roles in response to TGHQ-induced oxidative stress.

Other proteins that were altered by TGHQ treatment in LLC-PK1 cells could also be associated with TGHQ-induced renal cell death or carcinogenesis. For example, annexin I is a protein typically associated with carcinogenesis, and promotes membrane fusion and is involved in exocytosis (Parente and Solito 2004). Annexin I was induced by TGHQ treatment (Figure 4.1 to 4.3), and is likely involved in TGHQ-mediated signaling activation (PLA2 regulation). PDI and calreticulin are both localized within the endoplasmic reticulum and are closely related to protein refolding and stabilization under stresses (Wilkinson and Gilbert 2004). Nucleophosmin/B23 is a ubiquitously expressed phosphorylatable chaperone protein involved in ribosome assembly/transport, cytoplasmic/nuclear trafficking, regulation of DNA polymerase alpha activity, centrosome duplication, and regulation of p53. NPM continuously shuttles between the nucleus and cytoplasm, and is associated with centrosome and cell division (Okuda 2002). However, changes to these proteins after TGHQ treatment were less apparent than the changes to Prxs and Hsp27. Further studies examining the functional consequences of changes in these proteins would be of a value to our understanding cell response to oxidative stress. Because the pattern of changes in Prxs and Hsp27 on 2-D gels after TGHQ treatment are rapid, significant and highly reproducible, they could also be used as a biomarker for ROS-induced cellular damage.

In summary, I found that TGHQ induced changes in several proteins identified by 2-D gel analysis followed by MALDI-TOF protein identification. These proteins are associated with protection against oxidative stress, carcinogenesis, ER stress response,

calcium regulation, and nuclear shuttling. In particular, Prxs are antioxidants that are oxidized by ROS, and Hsp27 is phosphorylated in response to TGHQ, the consequences of which appear to be context-dependent.

Chapter 5: TGHQ INDUCED ERK & HISTONE H3 PHOSPHORYLATION IN THE KIDNEYS OF TGHQ-TREATED EKER RATS

I. INTRODUCITON AND RATIONALE

Reactive oxygen species (ROS) are associated with a variety of human diseases and toxicity (Bolton *et al.* 2000). Renal proximal tubule epithelial cells are particularly sensitive to oxidative stress-induced damage. However, the molecular mechanisms by which ROS cause injury in renal epithelial cells remain unclear. 2,3,5-Tris-(glutathion-S-yl)hydroquinone (TGHQ) is a potent nephrotoxic metabolite of hydroquinone (HQ). TGHQ causes oncotic/necrotic cell death of renal proximal tubule epithelial cells, and likely mediates HQ-induced nephrotoxicity and nephrocarcinogenicity (Lau *et al.* 1988; Lau *et al.* 2001a; Peters *et al.* 1997). TGHQ maintains the ability to redox-cycle and generate ROS (Towndrow *et al.* 2000; Weber *et al.* 2001), and covalently binds to cellular macromolecules (Kleiner *et al.* 1998a; Kleiner *et al.* 1998b). The one-electron reduced form of TGHQ may react with O_2, yielding superoxide anion radical, which ultimately gives rise to hydroxyl radical and hydrogen peroxide (Monks and Lau 1998). Quinone-thioethers induce rapid ROS-dependent DNA damage, growth arrest, and cell death in a well-established *in vitro* model of porcine renal proximal tubule epithelial cells (LLC-PK1) (Jeong *et al.* 1997a; Jeong *et al.* 1997b; Jeong *et al.* 1996; Mertens *et al.* 1995).

The nephrotoxicity of polyphenolic glutathione (GSH) conjugates is dependent on the high activity of γ-glutamyl transpeptidase (γ-GT) within the brush border membrane of the proximal tubule epithelial cells (Lau *et al.* 1988; Monks and Lau 1998). The

activity of γ-GT is required for the generation of the corresponding cysteine conjugates, which are subsequently transported into cells via the system L-amino acid transport system. ROS generation and covalent binding by the cysteine conjugates and the subsequent activation or inactivation of signaling pathways likely contribute to TGHQ-induced nephrotoxicity. A major signaling pathway that responds to various external stress, including oxidative stress, is the mitogen-activated protein kinase (MAPK) pathway (Martindale and Holbrook 2002). The MAPK family is comprised of three major subfamilies, the extracellular signal-regulated protein kinase (ERK), the c-Jun N-terminal kinases/stress-activated protein kinase (JNK/SAPK), and the p38 MAPK (Cobb 1999). Upon activation, following phosphorylation of the tyrosine and threonine residues, MAPKs subsequently activate a variety of substrates, the majority of which are transcription factors. One indirect downstream substrate of MAPKs is histone H3, which is phosphorylated subsequent to ERK activation, probably through the activation of either 90 kDa ribosomal S6 kinase 2 (RSK2) or mitogen and stress activated protein kinase 1 (MSK1) (Tikoo *et al.* 2001). TGHQ induces the activation of all three major subfamilies of MAPK (Ramachandiran *et al.* 2002) and histone H3 phosphorylation (Tikoo *et al.* 2001) in LLC-PK1 cells. The inappropriate phosphorylation of histone H3 leads to premature chromatin condensation (PCC) and oncotic cell death in LLC-PK1 cells (Tikoo *et al.* 2001). Inhibition of ERK phosphorylation by PD098059, a MAPK kinase (MEK1/2) inhibitor, decreases TGHQ-induced histone H3 phosphorylation (Tikoo *et al.* 2001) and cell death (Ramachandiran *et al.* 2002) in LLC-PK1 cells. Whether similar signaling cascades contribute to the acute nephrotoxicity of TGHQ *in vivo* is not known and was the focus of the current studies.

We utilized the Eker rat (*Tsc-2*$^{EK/+}$) as our animal model with the intent of coupling TGHQ-induced acute nephrotoxicity to the subsequent development of renal

tumors by identifying the early molecular changes that support renal tumor formation. Eker rats carry a germ-line insertion in the tuberous sclerosis tumor suppressor gene (*Tsc-2*), which predisposes the animals to renal tumors (Lau *et al.* 2001a; Walker *et al.* 1992; Walker 2002; Yoon *et al.* 2002; Yoon *et al.* 2001). Overexpression of ERK1/2 is often found in human neoplasia and tumors. For example, constitutive ERK activation was found in 48% of renal carcinomas examined (Oka *et al.* 1995). Moreover, PD184352, an inhibitor of ERK activation, suppressed tumor growth *in vivo* (Duesbery *et al.* 1999; Sebolt-Leopold *et al.* 1999). TGHQ induces an intensive increase in phospho-ERK1/2 expression in LLC-PK1 cells. In addition, both p38 MAPK and JNK/SAPK, which play important roles in inflammation, tummorigenensis and apoptosis (Tian *et al.* 2000), are activated by TGHQ, rapidly and intensively in LLC-PK1 cells (Ramachandiran *et al.* 2002). In the present study I investigated the effects of TGHQ on MAPK activation and histone H3 phosphorylation in Eker rats to identify early molecular changes that may contribute to HQ- and TGHQ-mediated carcinogenicity *in vivo,* and to determine the extent to which the *in vitro* model is predictive of molecular responses *in vivo*.

II. RESULTS

A. Nephrotoxicity of TGHQ

TGHQ (7.5 μmol/kg, *i.v.*) induced nephrotoxicity in the kidneys of Eker rats was confirmed by microscopic examination. By 4 hours after TGHQ administration, morphological damage within proximal tubules located in the OSOM was observed. The brush border became diffuse and the tubular lumen became filled with cellular debris (Figure 5.1). Kidneys of untreated Eker rats appeared unaffected.

B. TGHQ induces ERK1/2 phosphorylation within the outer stripe of outer medulla of Eker rats

ERK1/2 phosphorylation was absent in the proximal tubule of control rat kidneys (Figure 5.1). TGHQ-induced ERK1/2 phosphorylation was time-dependent, appearing as early as 1 h following TGHQ treatment and reaching maximal levels between 4 and 8 h after TGHQ treatment. Levels of phospho-ERK1/2 returned to control levels by 24 h. The staining of phospho-ERK1/2 was found to be specifically localized within the OSOM. Phospho-ERK1/2 was primarily located within the cytoplasm of the proximal tubule epithelial cells at earlier time points after TGHQ administration, although some nuclear staining was also present. Nuclear staining of phospho-ERK1/2 became more intense and prominent at later time points following TGHQ treatment. Additional immunoreactivity was also found in the lumen of the proximal tubules in lesional regions, probably due to the release of the cytoplasmic contents after cell membrane damage. Constitutive staining for phospho-p42/44 MAPK was present in the distal tubules, in both controls and the treated animal kidneys, but did not increase upon TGHQ treatment. The findings suggest that phospho-ERK1/2 translocates from cytoplasm to nucleus, but this initial

interpretation will require confirmation of immunolocalization using confocal microscopy. Western blot analysis, specifically on dissected OSOM tissue, revealed that ERK1/2 phosphorylation changed in a similar pattern to that found with immunohistochemical staining (Figure 5.2).

C. TGHQ induces histone H3 phosphorylation within the outer stripe of outer medulla of Eker rats

Immunohistochemistry revealed increases in phospho-histone H3 (Ser10) 8h following TGHQ treatment, reaching maximal levels between 12h and 24h (Figure 5.3), and returning to control levels by 72h. Western blot analysis was performed on pooled samples from 2-4 animals at each time point, and results confirmed the immunohistochemical findings (Figure 5.4). The presence of phospho-histone H3 within glomeruli likely contributes to the high expression levels in the control western blot analyses, consistent with the immunohistochemical findings. However, the significant increases in phospho-histone H3 levels revealed by western blot analyses, which exhibit the same kinetics as observed by immunohistochemistry, reflects changes occurring specifically within the OSOM, the target of TGHQ-induced toxicity. Thus, *increases* in phospho-histone H3 (Ser10) were found mostly within the OSOM and were associated with tubules exhibiting pathologic features. We also observed that phospho-histone H3 appeared in both nuclei and cytoplasm of the proximal tubule epithelial cells, but most prominently in the nuclei at earlier time points (8 h), with increased intensity of cytoplasmic immunoactivity at later time points (12 h), probably due to the loss of membrane integrity.

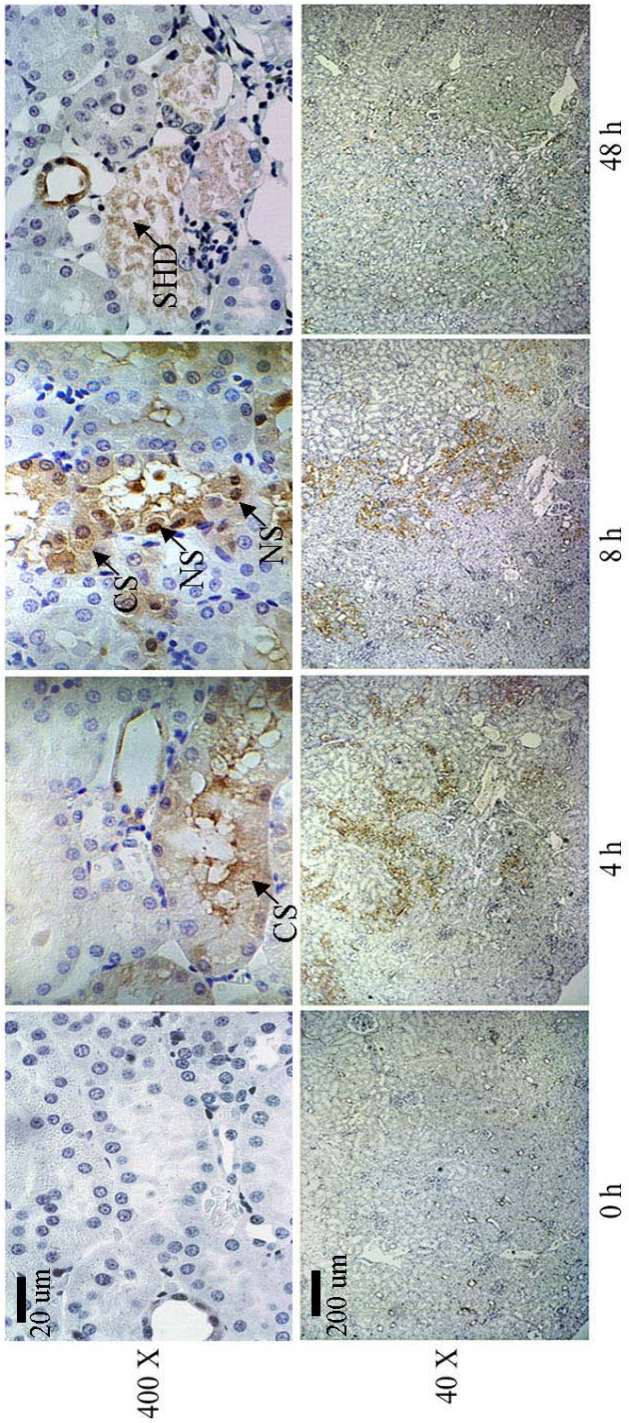

Figure 5.1 Increased ERK1/2 phosphorylation within the OSOM of TGHQ-treated Eker rat kidney:

Cells expressing phospho-ERK1/2 stain brown, phospho-ERK1/2 negative cells stain blue with hematoxylin counterstain. Representative treatment times (0, 4, 8, 24 h) are shown under the photomicrographs, taken under 400 × (Bar = 20 μm) or 40 × (Bar = 200 μm) total magnification. **CS**, cytosolic staining; **NS**, nuclear staining; **SHD**, shedding.

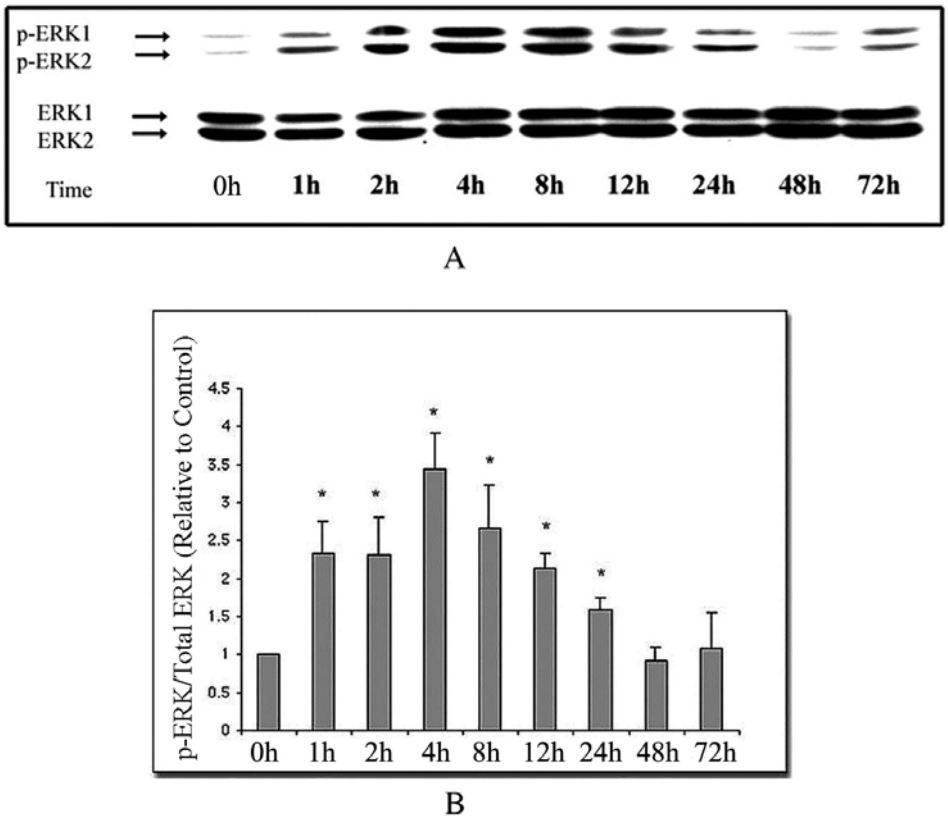

Figure 5.2 Western blot analysis confirms increases in ERK1/2 phosphorylation in OSOM tissue of Eker rat kidneys after TGHQ treatment.

Frozen OSOM tissues of Eker rats (0-72 h) were homogenized, lysed and analyzed by western blot analysis using a phospho-specific antibody for p-ERK1/2. (**A**) ERK1/2 phosphorylation upon TGHQ treatment. p-ERK1/2 (upper two bands), and total ERK1/2 (lower two bands) are shown, and the illustrated blot is typical of at least three independent experiments. (**B**). Statistical analysis on the changes of p-ERK1/2. p-ERK1/2 are compared and normalized to total ERK1/2, at each TGHQ treatment time point, and data are shown as fold-increase compared to untreated controls. Statisticaly significance is at *$p<0.05$ ($n\geq3$).

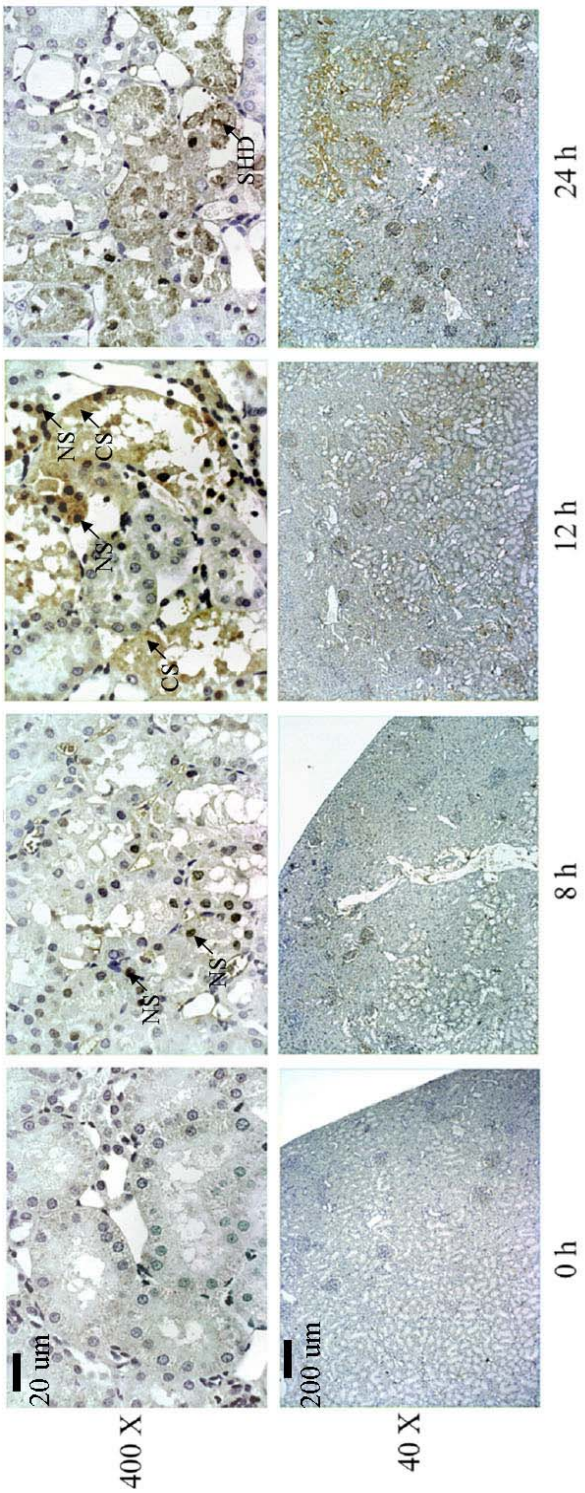

Figure 5.3 TGHQ increases histone H3 phosphorylation at Ser10 within the OSOM of TGHQ treated Eker rat kidneys:

p-Histone H3 (Ser10) expressing cells are stained brown, whereas cells staining negative for p-histone H3 (Ser10) are counter-stained blue with hematoxylin. Time of treatment is shown below the photomicrographs, with meter bar of 200 μm or 20 μm for lower or higher total magnification (40 × or 400 ×). CS, cytosolic staining; NS, nuclear staining; SHD, shedding.

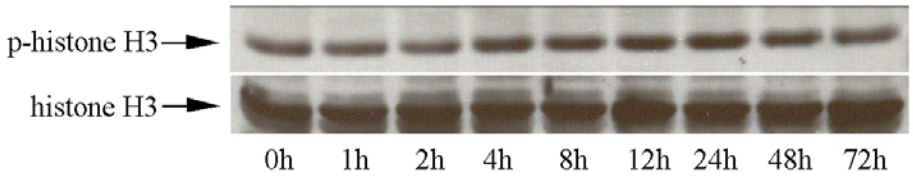

Figure 5.4 Western blot analysis confirms an increase in histone H3 phosphorylation after TGHQ treatment:

Frozen OSOM tissue from untreated or TGHQ-treated Eker rats were homogenized, lysed, sonicated, and analyzed by western blot analysis using a phospho-specific antibody for phospho-histone H3 (Ser10). Lysates from 2-4 animals from each time point (0-72 h) were pooled for analysis. The upper band represents the phospho-histone H3 (Ser10), and the lower band represents the total histone H3.

D. TGHQ induces no increase in phospho-p38 MAPK or JNK1/2 in Eker rats

The phosphorylation status of p38 MAPK (Figure 5.5) and JNK1/2 (Figure 5.6) within the OSOM changed little following TGHQ treatment, compared with the phosphorylation of ERK1/2, as determined by immunohistochemistry. Constitutive staining was observed throughout the kidney, mainly in glomeruli, the outer medulla, the inner medulla, and endothelial cells. We observed a slight increase in phospho-p38 MAPK (Figure 5.5) and phospho-JNK1/2 (Figure 5.6) within the OSOM 12 h after TGHQ administration, but this was observed only within limited loci with much less intensity than that observed for phospho-ERK1/2. Western blot analysis on the OSOM tissues using phospho-specific antibodies confirmed the constitutive phosphorylation of p38 MAPK (Figure 5.7) and JNK1/2 (Figure 5.8) in both untreated and treated animal kidneys, and failed to detect any changes following TGHQ treatment. Preferential phosphorylation of JNK2 compared to JNK1 within OSOM tissue of both untreated and TGHQ-treated Eker rats was observed with a phospho-specific antibody for phospho-JNK1/2. However, the mechanism for the preferential phosphorylation of JNK2 is unclear (Figure 5.8).

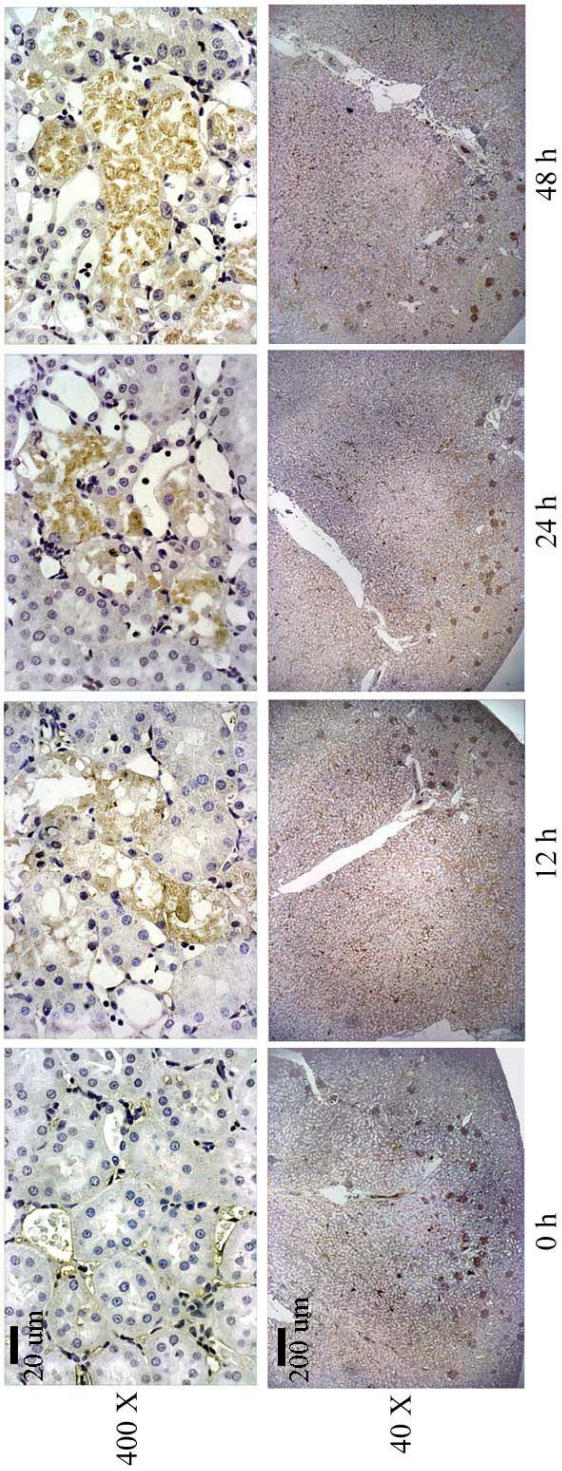

Figure 5.5 TGHQ has little effect on p38 MAPK phosphorylation within the OSOM of Eker rat kidney:

p-p38 MAPK expressing cells are stained brown with DAB, whereas p-p38 MAPK negative cells are counter-stained blue with hematoxylin. Selected treatment times are shown below the pictures. Bar = 200 μm for lower magnification (40 ×); bar = 20 μm for higher magnification (400 ×).

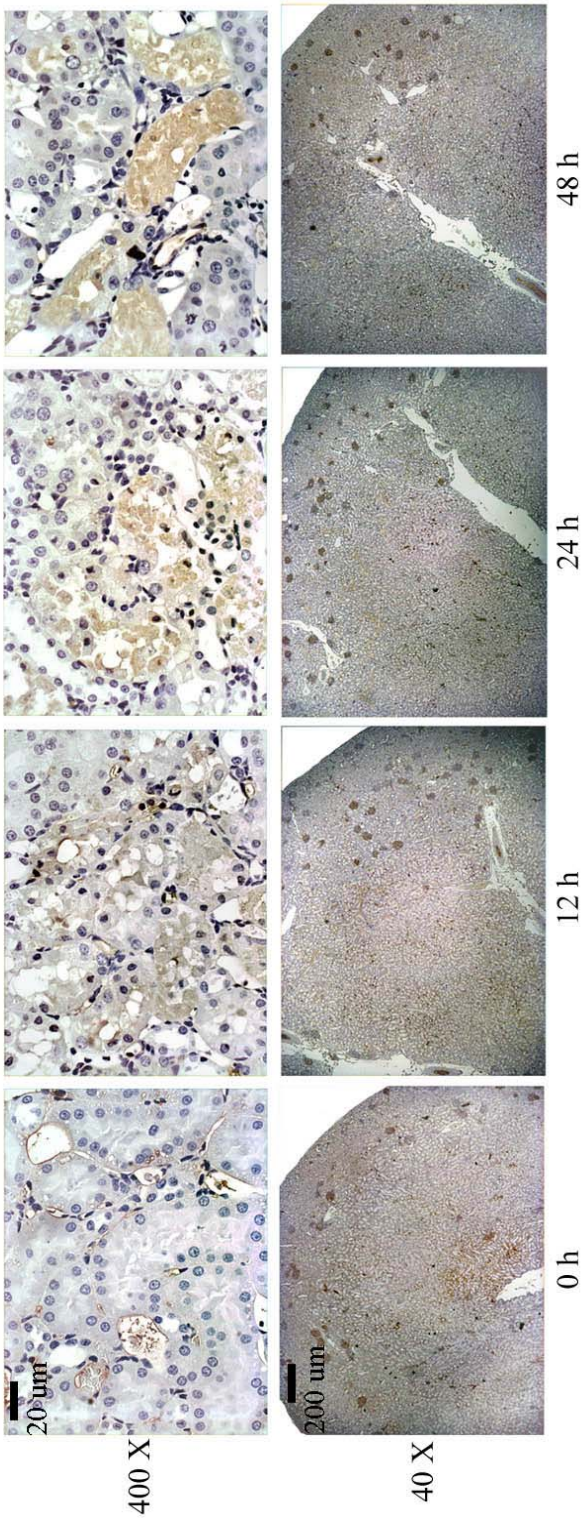

Figure 5.6 TGHQ does not induce significant JNK1/2 phosphorylation within the OSOM of Eker rat kidneys:

In the photomicrographs, p-JNK1/2 expressing cells are stained brown, whereas p-JNK1/2 negative cells are counter-stained blue with hematoxylin. Treatment times are shown below the pictures. Bar = 200 μm for lower magnification (40 ×); bar = 20 μm for higher magnification (400 ×).

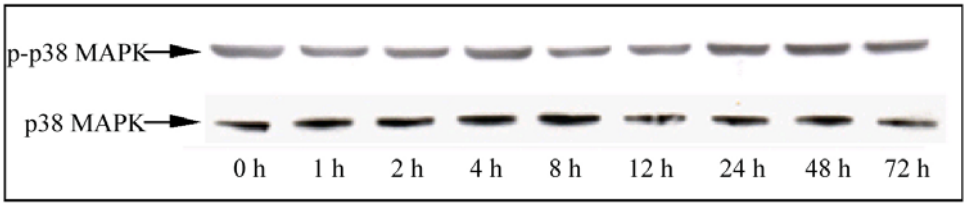

Figure 5.7 Western blot analysis confirms the lack of induction of p38 MAPK phosphorylation after TGHQ treatment:

Frozen OSOM tissue from Eker rats (0-72 h) were homogenized, lysed and analyzed by western blot using a phospho-specific antibody for p-p38 MAPK. The upper band shows unchanged p-p38 MAPK, and the lower band shows unchanged total p38 MAPK. The blot is a representative of at least 3 independent experiments.

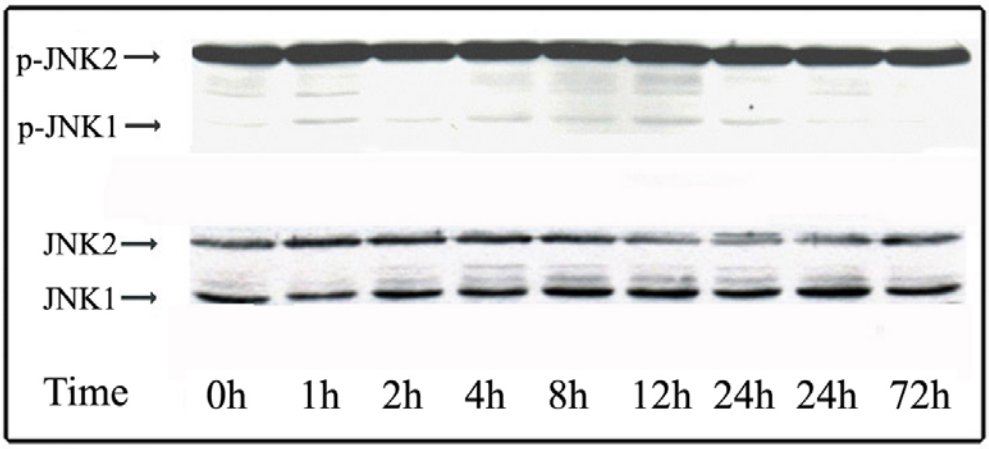

Figure 5.8 Western blot analysis confirms the lack of induction of JNK1/2 phosphorylation after TGHQ treatment:

Frozen OSOM tissue from Eker rat (0-72 h) were homogenized, lysed and analyzed by western blot using a phospho-specific antibody for p-JNK1/2. The upper two bands represent the p-JNK1/2, and the lower two bands represent the total JNK1/2. The blot is a representative of at least 3 independent results.

III. DISCUSSION

In the present study I have shown that TGHQ induces the time-dependent phosphorylation of ERK1/2, followed by the subsequent phosphorylation of histone H3, within the OSOM of Eker rats. More importantly, increases in ERK1/2 phosphorylation precede the morphological findings of acute toxicity, consistent with a role for these phosphorylation events in the toxicity. TGHQ-induced DNA damage precedes nephrotoxicity as determined by immunostaining for 8-oxo-dG, and is maximal 8 h after TGHQ treatment of Eker rats (Habib *et al.* 2003). The acute toxicity of TGHQ is mainly localized to proximal tubule epithelial cells within the OSOM, due to the high concentrations of γ-GT on these cells. Urinary γ-GT levels increase rapidly after administration of renal toxicants, followed by increases in the urinary excretion of cytosolic components, such as glutathione S-transferase (GST). Thus, urinary γ-GT and GST activity serve as predictive indeces of renal toxicity *in vivo*. After TGHQ treatment, urinary γ-GT activity in Eker rats increases as early as 4 h, and rapidly reaches maximum levels at 8 h, and which are sustained for at least 48 h (Habib *et al.* 2003). In contrast, urinary GST activity, an indicator of renal cell shedding into the tubular lumen, increases progressively, and reaches peak levels 24 h after TGHQ treatment (Habib *et al.* 2003). Thus, initial increases in GST occur coincident with increases in histone H3 phosphorylation.

We subsequently performed immunohistochemical experiments to compare Eker rats (possessing a mutation in one allele of the *Tsc-2* tumor suppressor gene) with their wild-type equivalents (Long-Evans), but did not observe any differences in the expression of phospho-ERK1/2 and phospho-histone H3 between the wild type and the mutant Eker rats (data not shown). Consistent with these findings, TGHQ induces

markedly increased cell proliferation and increased ERK activity within the OSOM of the kidneys in both wild type and mutant Eker rats (Yoon *et al.* 2002). Loss of the remaining wild type allele of the *Tsc-2* gene is required for TGHQ induced nephrocarcinogenicity. The Eker rat therefore represents an excellent model with which to examine chemical-induced nephrotoxicity and nephrocarcinogenicity.

Two downstream substrates of ERK1/2 are MSK1 and RSK2, both of which exhibit histone H3 kinase activity (Thomson *et al.* 1999). Consistent with the *in vitro* findings, ERK1/2 phosphorylation preceded histone H3 phosphorylation *in vivo,* suggesting that histone H3 may also be a downstream substrate of phospho-ERK1/2 *in vivo*. However, in contrast to TGHQ-mediated activation of p38 MAPK and JNK1/2 in LLC-PK1 cells, neither of these kinases were significantly altered within the OSOM of Eker rats. Thus, the contribution of p38 MAPK and JNK1/2 to TGHQ-induced nephrotoxicity *in vivo* remains unclear. Western blot analysis of OSOM tissue from TGHQ treated Eker rats confirmed the immunohistochemical findings, and revealed little change in phospho-p38 MAPK and phospho-JNK/1/2 throughout the observed time points. Our data are consistent with the constitutive expression of JNK1/2 and of corresponding JNK1/2 phosphorylation reported in proximal tubules of adult rats (Omori *et al.* 2000).

The roles of the MAPKs in hypertrophy, ischemia/reperfusion-induced injury, chronic renal disease, angiotensinogen gene expression, and in the endoplasmic reticulum stress response have been the subject of many investigations (Hannken *et al.* 2000; Hsieh *et al.* 2002; Hung *et al.* 2003; Khan *et al.* 2001; Park *et al.* 2002). However, relatively less is known with respect to the pattern of activation of the MAPK pathways in kidneys in response to ROS-generating chemicals *in vivo*. The effects of ERK1/2 activation, and the subsequent changes in the phosphorylation status of their substrates are controversial.

Thus, ERK1/2 activation may contribute to both cell proliferation and differentiation. The duration of ERK1/2 activation is also critical for cell signaling decisions in PC12 cells (Marshall 1995); short-term ERK activation leads to proliferation whereas sustained ERK activation leads to differentiation. In the present model, ERK1/2 phosphorylation was maximal 4 h after TGHQ treatment, and returned to control levels by 24 h. The phosphorylation of ERK1/2 and subsequent histone H3 phosphorylation may constitute signals to the proximal tubule epithelial cells to activate the necessary machinery for cell division and proliferation. However, these same cells are simultaneously experiencing extensive DNA damage, with the concomitant activation of growth arrest and DNA damage inducible signals (gadd153 mRNA upregulation, and downregulation of histone mRNA, (Jeong *et al.* 1996). These two conflicting signaling pathways may contribute to premature chromatin condensation and mitotic catastrophe. Moreover, cells that survive the TGHQ-induced ROS-dependent stress by activating specific characteristics/signaling pathways, or by excessive proliferation after tissue damage, may acquire the potential to develop into tumors.

The relationship between TGHQ induced cell proliferation and TGHQ-induced nephrotoxicity and nephrocarcinogenicity has been previously established (Lau *et al.* 2001a; Peters *et al.* 1997; Yoon *et al.* 2002). The mechanism likely involves cytotoxicity and compensatory cell proliferation, accompanied by, in Eker rats, loss of tuberin expression. ERK activation is associated with mitogenesis, and histone H3 (S10/S28) phosphorylation is a marker of cell proliferation. We hypothesize that TGHQ induced DNA damage (Habib *et al.* 2003) increases the frequency of mutations, and perhaps loss of heterozygosity at the *Tsc-2* locus, in the highly proliferate environment that exists in renal proximal tubules in response to tissue injury. In addition, the constitutive phosphorylation of JNK1/2 and p38 MAPK (Figure 5.5 to 5.8) may indicate that Eker

rats, even in the absence of stress, exhibit a unique spectrum of signaling pathways that predispose these animals to the development of spontaneous renal tumors.

The shuttling of MAPKs between the cytoplasm and nucleus plays an important role in regulating MAPKs function (Adachi *et al.* 2000). Activated ERK1/2 usually translocates from the cytoplasm to the nucleus, and inactivated ERK1/2 binds to MEK1/2, and relocalizes to the cytoplasm, assisted by the nuclear export signal on MEK1/2 (Adachi *et al.* 2000). The nuclear export of ERK1/2 is inhibited by leptomycin B, which binds to a component of the nuclear export complex, CRM1, and blocks nuclear export (Adachi *et al.* 2000). Nuclear translocation of activated ERK1/2 may participate in the activation of several targets, mainly transcription factors, and culminate in nuclear histone H3 phosphorylation. Following nuclear export of ERK1/2 to the cytoplasm, or breakdown of the nuclear and/or plasma membranes, phospho-ERK1/2 and phospho-histone H3 are detectable in the cytoplasm and/or within the lumen of the proximal tubules (Figure 5.1), indicating necrotic cell death. With the development of new biological tools, such as leptomycin B, importin antisense, and confocal microscopy, it will be possible to monitor the localization of MAPKs following TGHQ treatment.

In summary, we have shown that TGHQ induces time-dependent phosphorylation of ERK1/2 within the OSOM of Eker rats. Phosphorylation of ERK1/2 and histone H3 are associated with oncotic/necrotic cells. In addition, the nuclear shuttling of both ERK1/2 and histone H3 was observed in response to TGHQ treatment. In contrast, the phosphorylation of p38 MAPK and JNK1/2 remained unchanged after TGHQ treatment.

Chapter 6: CONCLUSIONS AND FUTURE DIRECTIONS

ROS are associated with a number of diseases and toxicities, but also behave as signaling factors in a variety of cellular processes. The roles of ROS in cell signaling have been the subject of many studies, and ROS have been associated with both cell death and cell survival signaling pathways. Although a number of studies have linked ROS-induced signaling pathways to apoptotic cell death, relatively less information is available on the association between ROS-mediated signaling pathways and oncotic cell death. To determine the molecular mechanisms of ROS-mediated cell death, we used a model compound, TGHQ, as a source for ROS generation in cells. TGHQ targets renal proximal tubule epithelial cells, due to the ability of these cells to metabolize TGHQ and to subsequently transport the metabolites into cells. Therefore, TGHQ generates ROS within renal epithelial cells that may activate or inactivate a number of signaling pathways associated with cell fate determination. In addition, TGHQ possesses the ability to alkylate macromolecules and to cause damage to the cells. The ability of TGHQ to generate ROS and to alkylate macromolecules are coupled. Thus, even when TGHQ alkylates macromolecules, it can still generate ROS (Monks and Lau 1998). Therefore, alkylation and ROS generation can be inter-dependent. TGHQ induces oncotic rather than apoptotic renal epithelial cell death. Oncotic cell death and the resulting tissue necrosis frequently elicits an inflammatory response that exacerbates the damage to neighboring cells. During oncotic cell death a number of signaling pathways are also activatied. Studies in this dissertation focused on deciphering the signaling pathways involved in ROS-induced oncotic cell death, with the intent of uncovering ways in which to manipulate this process.

TGHQ induces DNA damage, growth arrest, MAPKs activation, and histone H3 phosphorylation in porcine renal proximal tubule epithelial cells (LLC-PK1). DNA damage inducible histone H3 phosphorylation during oxidative stress likely contributes to premature chromatin condensation, mitotic catastrophe and ultimately cell death. Inhibition of either the ERK or p38 MAPK pathway attenuates TGHQ-induced renal cell death. Activation of the ERK pathway has been coupled to histone H3 phosphorylation. I thereby investigated the molecular mechanisms by which TGHQ induces renal cell death, with the intent of uncovering detailed information on ROS-mediated signaling pathways.

The first question I asked was how ROS generation activates MAPK cascades. TGHQ induces EGFR phosphorylation leading to EGFR-dependent activation of the ERK cascade. In contrast, TGHQ-induced p38 MAPK activation does not occur through EGFR phosphorylation. Instead, at least one of the factors in the p38 MAPK cascade is associated with inhibitory chaperone proteins, the post-translational modification of which leads to the dissociation and activation of the p38 MAPK cascade. The effects of EGF and H_2O_2 on EGFR were compared to TGHQ. Phosphorylation of five tyrosine residues on EGFR was examined, all of which are associated with ERK pathway activation. EGF induced rapid (Max = 15 min) EGFR activation by promoting the phosphorylation of all the tyrosine residues examined (Y992, Y1068, Y1086, Y1148, Y1173), each of which provide binding sites for a variety of signaling factors to initiate disparate signaling cascades. TGHQ induced subtantial EGFR tyrosine phosphorylation at Y992 and Y1068, weak phosphorylation at Y1086 and Y1148, but not at Y1173 (Max = 1 h). H_2O_2, surprisingly, only induced significant increases in tyrosine phosphorylation at Y992, but not Y1068, and weak phosphorylation at Y1086 and Y1148 (Max = 1 h). These observations indicate that the mechanisms of TGHQ-mediated EGFR activation are somehow different from H_2O_2-mediated EGFR activation. EGFR has an excessive

number of tyrosine residues, because many of them may lead to similar responses. However, the different combinatorial and kinetic activation of EGFR tyrosine residues provides a basis for selectivity and differential kinetics of downstream signaling pathway activation. Indeed, the kinetics of ERK1/2 activation by TGHQ and H_2O_2 differed. Total EGFR levels were also different in cells treated with the three agents, with EGF-treated cells exhibiting the most rapid decrease in EGFR expression levels. TGHQ-treated cells responded with less substantial decreases in EGFR expression levels, with no decreases in total EGFR levels in H_2O_2 treated cells. The decrease in total EGFR is probably due to inactivation, or internalization/degradation of EGFR upon phosphorylation of certain EGFR tyrosine residue(s). H_2O_2, however, inhibits EGFR internalization and degradation. It would be interesting to differentiate the recruitments of various binding partners for EGFR tyrosine residues phosphorylated in response to TGHQ, EGF or H_2O_2. Current studies using immunoprecipitation techniques to pull down EGFR and its associated proteins, and analysis of different patterns of recruitment of EGFR binding partners to the EGFR before and after treatment with EGF, TGHQ and H_2O_2 will assist in understanding the mechanisms of EGFR activation and downstream signaling regulation in response to the different agents.

We subsequently endeavored to discover the mechanisms of histone H3 phosphorylation in TGHQ challenged renal cells. Since MAPKs activation has been linked to histone H3 kinase activation, our aim was to determine whether TGHQ-mediated histone H3 phosphorylation results from the activation of MAPKs. Among the MAPKs, both the ERK1/2 and p38 MAPK pathways may lead to histone H3 phosphorylation. Using pharmacological manipulation, we found that both the ERK and p38 MAPK pathways contribute to TGHQ-induced histone H3 phosphorylation. Msk1 and Rsk2 are two histone H3 kinases downstream of ERK1/2 or p38 MAPK. However,

our laboratory has shown that dominant negative Msk1 or pharmacological inhibition of Rsk2 failed to affect TGHQ-induced histone H3 phosphorylation. Therefore, there must be other histone kinases downstream of ERK and p38 MAPK pathways, which contribute to TGHQ-induced histone H3 phosphorylation in LLC-PK1 cells (Cox and Palmer, unpublished data). Future studies will be designed to reveal the kinase(s) responsible for histone H3 phosphorylation induced by TGHQ in renal cells. Moreover, recent finding in the laboratory have revealed that phosphorylation of the conventional phospho-histone H3 residues (S10 and S28) actually decreases after TGHQ treatment, despite overall increase in [^{32}P]-incorparation into histone H3. Therefore, a novel phosphorylation residue(s) on histone H3 must be responsible for the overall increase of histone H3 phosphorylation after TGHQ treatment. One possibility is S31 in histone H3.3. Increases in histone H3 phosphorylation occurs specifically on serine residues, and the increases are limited to the H3.3 isoform, which possesses a serine rather than an alanine residue at position 31, and which is the likely putative phosphoryaltion residue. Current studies involve the construction of vectors containing single or multiple mutations in histone H3, with S10, S28 and S31 being mutated to A10, A28 and A31, which cannot be phosphorylated. These vectors are then transfected into LLC-PK1 cells to study whether S31 phosphorylation is important in TGHQ-mediated cell death.

I further examined roles of the p38 MAPK pathway in TGHQ-mediated renal cell death. p38 MAPK activation leads to the phosphorylation of Hsp27, which acts as a chaperone, and stabilizes the cytoskeleton. TGHQ induces phosphorylation of Hsp27 at S15, S78 and S82 residues (Figure 3.9). Phosphorylation of Hsp27 leads to the break down of large Hsp27 oligomers into smaller oligomers or monomers, which lose their chaperoning functions and their ability to bind to unfolded proteins and to facilitate the efficient refolding of these proteins. Hsp27 also regulates intracellular antioxidant GSH

levels in a manner that protects against oxidative stress. However, this property of Hsp27 is lost upon phosphorylation. In contrast, smaller oligomers or monomers of Hsp27 that form subsequent to phosphorylation assist in stabilizing actin and in protecting cells from oxidative stress induced damage. The roles of Hsp27 phosphorylation in oxidant-induced cell death remain controversial. We speculate that Hsp27 likely acts in both a protective and in a cell death inducing fashion. Total Hsp27 levels provide a cytoprotective effect by providing a larger pool of Hsp27 that function in both a chaperoning function and antioxidant (increases intracellular GSH levels) manner. Once phosphorylated, Hsp27 loses its ability to stabilize damaged proteins (loses its chaperoning properties), and its ability to maintain GSH levels, but it simultaneously acquires the ability to stabilize the actin cytoskeletal network and to maitain cell structure. Moreover, in LLC-PK1 cells that lack the ability for Grp78 induction, the activation of the p38 MAPK pathway and Hsp27 phosphorylation is disrupted, and likely contributes to the loss of DDM-PGE2-mediated cytoprotection against TGHQ-mediated oncotic cell death. The role of Hsp27 phosphorylation in TGHQ-mediated renal cell death clearly requires further investigation. The fraction of unphosphorylated and phosphorylated Hsp27, and the subsequent balance in chaperoning functions, maintainance of GSH levels, and the ability to stabilize the actin cytoskeleton all combined are to determine the overall effect of Hsp27 in ROS stressed cells. I suspect that in the acute toxicity studies (2 h) in preconfluent renal cells, the loss of the chaperoning function and the ability to maintain GSH levels are the key features linking Hsp27 to cell death. In contrast, in DDM-PGE2 pretreated (24 h) or in genetically manipulated post-confluent renal cells (Grp78 antisense), changes in total Hsp27 protein expression and the subsequent phosphorylation are important in stabilizing actin to provide a cytoprotective effects. One approach to further study the roles of Hsp27 would be to overexpress the unphosphorylatable mutants of Hsp27 in renal cells, and to

examine whether blocking of Hsp27 phosphorylation protects or enhances TGHQ-induced renal cell death. More studies using this mutant will help to understand how Hsp27 phosphorylation influences *(i)* the chaperoning function of large unphosphorylatable oligomers *(ii)* GSH levels, and *(iii)* how phosphorylated Hsp27 tetramers and monomers interact with cytoskeletal proteins and their function in cytoprotection. However, as previously discussed, the dual roles of Hsp27 phosphorylation add complexity to this approach, and we should be cautious in interpreting the data acquired.

Because no single or combination of inhibition of TGHQ-induced cell-death-associated signaling pathways can completely block cell death, I hypothesized that there are multiple signaling pathways involved in this process. I therefore investigated global cellular responses to TGHQ in renal epithelial cells using a proteomics approach 2-D gel analysis revealed three spots that were altered in response to TGHQ, all of which were identified by MALDI-TOF as Prx3, and two spots indentified as Prx2 (Figure 4.1, 4.2). After TGHQ treatment, spots with a more acidic pI became more intense. Two spots exhibiting a similar phenomenon of spot intensity shifts on a 2-D gel identified as Prx3 have been similarly observed (Rabilloud *et al.* 2002). Mass spectrometric analysis of the spots revealed that the one with more acidic pI possessed a cysteine residue oxidized to the sulfinic and sulfonic acid. However, no one has yet to report the third spot, identified by us as Prx3, which exhibits a decrease in intensity after TGHQ treatment. Determinating the post-translational modifications of Prxs, and the identity of the third spot found on the 2-D gel is therefore a current priority. We suspect that the third spot, identified as Prx3, is likely a subisoform of Prx3, which shares homology with the peptides altering matched.

Prxs are a family of abundantly expressed peroxidases that provide the first defense barrier against ROS-mediated cellular damage. Other anti-oxidants include GSH, catalse, and SOD. In the presence of small amounts of intracellular ROS, Prxs reduce H_2O_2 and oxidized lipids with the accompanying oxidation of the sulfhydryl group in the active site cysteine residues to the sulfenic acid. Oxidation of the cysteine residue is quickly reversed by thioredoxin reductase and Prxs regain their antioxidant functions. However, in response to excessive amounts of ROS, additional oxidation of Prxs cysteine residues into sulfinic and sulfonic acid, and these oxidative modifications are not readily reversed, the process of reduction being slow. This hyperoxidation of Prxs allows excess ROS to react with additional cellular constituents and yields an oxidative stress response. In this respect, oxidation of Prxs probably represents a gateway for ROS-mediated signaling in cells. Prxs also regulate MAPK activities, and overexpression of Prxs protects cells against oxidative stress induced cell death. Therefore, oxidation of Prxs by TGHQ may contribute to the activation or inactivation of a number of signaling pathways. Native western blot analysis of Prx3 revealed a band shift after TGHQ and H_2O_2 treatment, most likely due to oxidation. The bands were excised and analyzed for post-translational modification by LC-MS/MS mass spectrometry. However, identification of the modification is technically difficult. Although 2-D gel analysis provides improved separation of the proteins, the yield of Prx3 after sample preparation is low. These technical difficulties have limited our ability to study the modification of Prx3 in greater detail. Future studies will attempt to pool the samples to obtain larger amounts of protein for analyses. Studies on the cytoprotective effects of Prxs against ROS can be performed by overexpressing Prxs in renal cells. Current studies are designed to identify potential signaling factors (especially p38 MAPK cascade) associated with Prxs by immunoprecipitation followed by MALDI-TOF protein identification, which will be

confirmed by western blot analysis. Such studies will assist in better understanding the roles of Prxs in ROS induced oncotic renal cell death. Other proteins regulated by TGHQ in LLC-PK1 cells include a rapid increase in the overall expression of annexin I, PDI precursor, calreticulin, and changes in nucleophosmin. These proteins are associated with a number of cellular functions, including carcinogenesis, ER stress, calcium regulation, and nuclear shuttling. We further confirmed increases in annexin I expression levels after TGHQ treatment by western blot analysis. Whether induction of annexin I by TGHQ is associated with nephrotoxicity and nephrocarcinogenicity requires further investigation.

We now have identified a network of signaling pathways that are engaged during TGHQ-induced renal cell death in LLC-PK1 cells (Figure 6.1). Whether these signaling pathways are also activated *in vivo* remains to be examined. Pivotal studies were performed in TGHQ-treated Eker rats in search of the activation of the MAPKs and histone H3 phosphorylation. As shown in Chapter 5, TGHQ induced substantial time-dependent ERK1/2 and histone H3 phosphorylation within the OSOM, the target of TGHQ-mediated nephrotoxicity. Increases in ERK phosphorylation precede indeces of nephrotoxicity, urinary γ-GT and GST excretion. However, constitutive phosphorylation of p38 MAPK within the OSOM of Eker rat kidney obscured any changes that might occur in response to TGHQ. Constitutive p38 MAPK activation might also contribute to the predisposition of these rats to spontaneous renal tumors. *In vivo* mechanistic studies on signaling pathways are much harder to conduct than *in vitro* studies, due to the complexity of the *in vivo* systems in comparison to *in vitro* cell culture. However, *in vivo* evidence is very valuable in predicting human responses and should always be used to confirm the *in vitro* phenomena. Future studies in our laboratory may involve *in vivo* mechanistic studies using TGHQ-sensitive animals. A pharmacological inhibitor of the p38 MAPK pathway (SB202190) is commercially available for *in vivo* studies.

Unfortunately, a similar *in vivo* inhibitor of the ERK pathway is not commercially available because it is patented and in development as an anti-cancer drug. Other *in vivo* mechanistic studies are also possible, such as genetic manipulation of key signaling factors by generating transgenic or knockout animals.

This dissertation describes and discusses my research findings that contribute to an increased understanding of the molecular mechanisms of ROS-induced oncotic renal cell death. It is my wish that these studies and findings would contribute to our overall understanding of quinone-thioethers-mediated toxicities, of signaling pathways involved in ROS-mediated cell death, and assist in identifying potential solutions to manipulate oncotic cell death for therapeutic benefit. Finally, I hope my studies may provoke more innovative experiments.

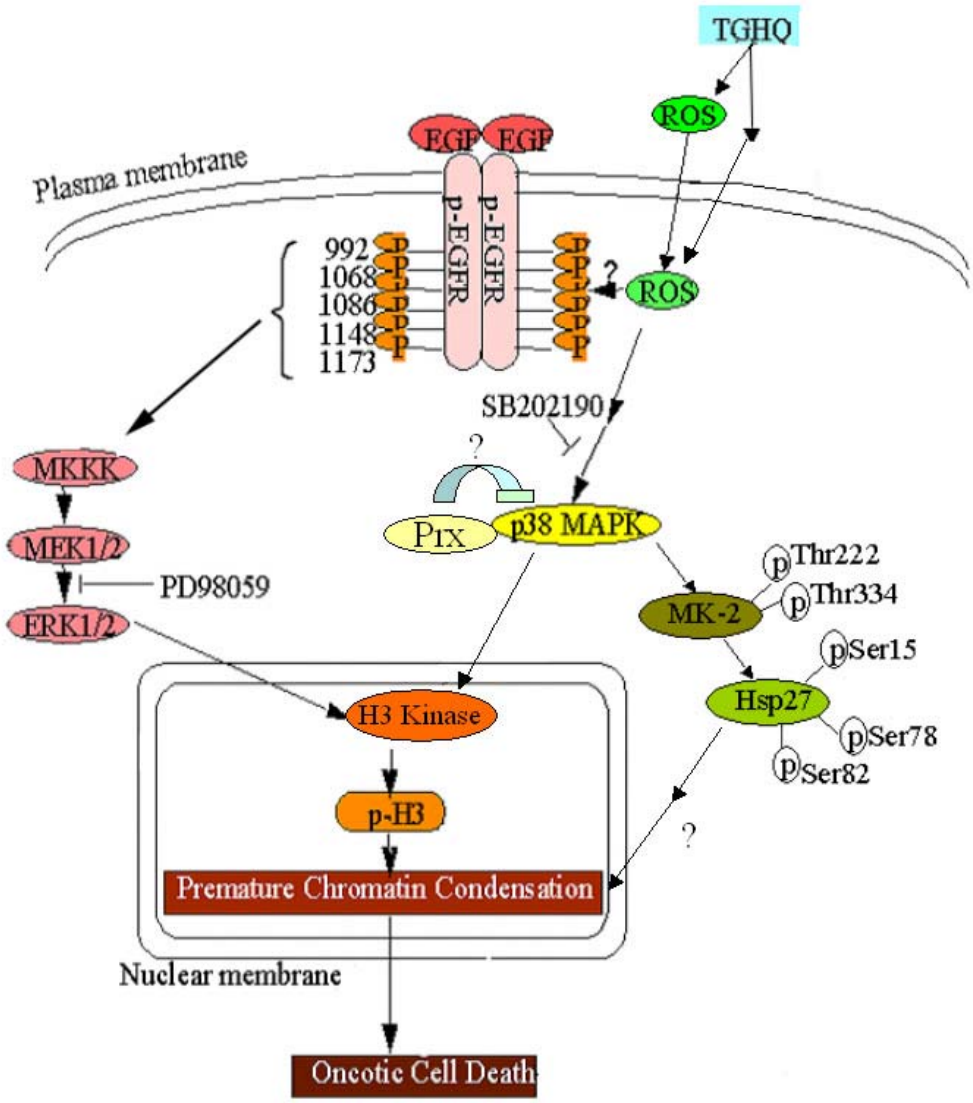

Figure 6.1 Summary of the cell signaling in TGHQ treated renal proximal tubule epithelial cells.

REFERENCES

Adachi, M., Fukuda, M., and Nishida, E. (1999). Two co-existing mechanisms for nuclear import of MAP kinase: passive diffusion of a monomer and active transport of a dimer. *Embo J* **18**, 5347-58.

Adachi, M., Fukuda, M., and Nishida, E. (2000). Nuclear export of MAP kinase (ERK) involves a MAP kinase kinase (MEK)-dependent active transport mechanism. *J Cell Biol* **148**, 849-56.

Alessi, D. R., Cuenda, A., Cohen, P., Dudley, D. T., and Saltiel, A. R. (1995). PD 098059 is a specific inhibitor of the activation of mitogen-activated protein kinase kinase in vitro and in vivo. *J Biol Chem* **270**, 27489-94.

Arnold, R. S., Shi, J., Murad, E., Whalen, A. M., Sun, C. Q., Polavarapu, R., Parthasarathy, S., Petros, J. A., and Lambeth, J. D. (2001). Hydrogen peroxide mediates the cell growth and transformation caused by the mitogenic oxidase Nox1. *Proc Natl Acad Sci U S A* **98**, 5550-5.

Arrigo, A. P. (1998). Small stress proteins: chaperones that act as regulators of intracellular redox state and programmed cell death. *Biol Chem* **379**, 19-26.

Arrigo, A. P., Suhan, J. P., and Welch, W. J. (1988). Dynamic changes in the structure and intracellular locale of the mammalian low-molecular-weight heat shock protein. *Mol Cell Biol* **8**, 5059-71.

Ashkenazi, A., and Dixit, V. M. (1998). Death receptors: signaling and modulation. *Science* **281**, 1305-8.

Bae, Y. S., Kang, S. W., Seo, M. S., Baines, I. C., Tekle, E., Chock, P. B., and Rhee, S. G. (1997). Epidermal growth factor (EGF)-induced generation of hydrogen peroxide. Role in EGF receptor-mediated tyrosine phosphorylation. *J Biol Chem* **272**, 217-21.

Baek, S. H., Min, J. N., Park, E. M., Han, M. Y., Lee, Y. S., Lee, Y. J., and Park, Y. M. (2000). Role of small heat shock protein HSP25 in radioresistance and glutathione-redox cycle. *J Cell Physiol* **183**, 100-7.

Bai, F., Jones, D. C., Lau, S. S., and Monks, T. J. (2001). Serotonergic neurotoxicity of 3,4-(+/-)-methylenedioxyamphetamine and 3,4-(+/-)-methylendioxymethamphetamine (ecstasy) is potentiated by inhibition of gamma-glutamyl transpeptidase. *Chem Res Toxicol* **14**, 863-70.

Bai, F., Lau, S. S., and Monks, T. J. (1999). Glutathione and N-acetylcysteine conjugates of alpha-methyldopamine produce serotonergic neurotoxicity: possible role in methylenedioxyamphetamine-mediated neurotoxicity. *Chem Res Toxicol* **12**, 1150-7.

Barbato, R., Menabo, R., Dainese, P., Carafoli, E., Schiaffino, S., and Di Lisa, F. (1996). Binding of cytosolic proteins to myofibrils in ischemic rat hearts. *Circ Res* **78**, 821-8.

Bennardini, F., Wrzosek, A., and Chiesi, M. (1992). Alpha B-crystallin in cardiac tissue. Association with actin and desmin filaments. *Circ Res* **71**, 288-94.

Benndorf, R., Hayess, K., Ryazantsev, S., Wieske, M., Behlke, J., and Lutsch, G. (1994). Phosphorylation and supramolecular organization of murine small heat shock protein HSP25 abolish its actin polymerization-inhibiting activity. *J Biol Chem* **269**, 20780-4.

Bhat, N. R., and Zhang, P. (1999). Hydrogen peroxide activation of multiple mitogen-activated protein kinases in an oligodendrocyte cell line: role of extracellular signal-regulated kinase in hydrogen peroxide-induced cell death. *J Neurochem* **72**, 112-9.

Biscardi, J. S., Maa, M. C., Tice, D. A., Cox, M. E., Leu, T. H., and Parsons, S. J. (1999). c-Src-mediated phosphorylation of the epidermal growth factor receptor on Tyr845 and Tyr1101 is associated with modulation of receptor function. *J Biol Chem* **274**, 8335-43.

Bishayee, A., Beguinot, L., and Bishayee, S. (1999). Phosphorylation of tyrosine 992, 1068, and 1086 is required for conformational change of the human epidermal growth factor receptor c-terminal tail. *Mol Biol Cell* **10**, 525-36.

Bolton, J. L., Trush, M. A., Penning, T. M., Dryhurst, G., and Monks, T. J. (2000). Role of quinones in toxicology. *Chem Res Toxicol* **13**, 135-60.

Borsch-Haubold, A. G., Pasquet, S., and Watson, S. P. (1998). Direct inhibition of cyclooxygenase-1 and -2 by the kinase inhibitors SB 203580 and PD 98059. SB 203580 also inhibits thromboxane synthase. *J Biol Chem* **273**, 28766-72.

Bratton, S. B., and Cohen, G. M. (2001). Apoptotic death sensor: an organelle's alter ego? *Trends Pharmacol Sci* **22**, 306-15.

Bratton, S. B., and Cohen, G. M. (2003). Death receptors leave a caspase footprint that Smacs of XIAP. *Cell Death Differ* **10**, 4-6.

Bratton, S. B., Lau, S. S., and Monks, T. J. (1997). Identification of quinol thioethers in bone marrow of hydroquinone/phenol-treated rats and mice and their potential role in benzene-mediated hematotoxicity. *Chem Res Toxicol* **10**, 859-65.

Bratton, S. B., Lau, S. S., and Monks, T. J. (2000). The putative benzene metabolite 2,3, 5-tris(glutathion-S-yl)hydroquinone depletes glutathione, stimulates sphingomyelin turnover, and induces apoptosis in HL-60 cells. *Chem Res Toxicol* **13**, 550-6.

Bruey, J. M., Ducasse, C., Bonniaud, P., Ravagnan, L., Susin, S. A., Diaz-Latoud, C., Gurbuxani, S., Arrigo, A. P., Kroemer, G., Solary, E., and Garrido, C. (2000). Hsp27 negatively regulates cell death by interacting with cytochrome c. *Nat Cell Biol* **2**, 645-52.

Bryk, R., Griffin, P., and Nathan, C. (2000). Peroxynitrite reductase activity of bacterial peroxiredoxins. *Nature* **407**, 211-5.

Butt, E., Immler, D., Meyer, H. E., Kotlyarov, A., Laass, K., and Gaestel, M. (2001). Heat shock protein 27 is a substrate of cGMP-dependent protein kinase in intact human platelets: phosphorylation-induced actin polymerization caused by HSP27 mutants. *J Biol Chem* **276**, 7108-13.

Butterfield, L. H., Merino, A., Golub, S. H., and Shau, H. (1999). From cytoprotection to tumor suppression: the multifactorial role of peroxiredoxins. *Antioxid Redox Signal* **1**, 385-402.

Butterworth, M., Lau, S. S., and Monks, T. J. (1998). 2-Hydroxy-4-glutathion-S-yl-17beta-estradiol and 2-hydroxy-1-glutathion-S-yl-17beta-estradiol produce oxidative stress and renal toxicity in an animal model of 17beta-estradiol-mediated nephrocarcinogenicity. *Carcinogenesis* **19**, 133-9.

Camps, M., Nichols, A., and Arkinstall, S. (2000). Dual specificity phosphatases: a gene family for control of MAP kinase function. *Faseb J* **14**, 6-16.

Carvalho, M., Hawksworth, G., Milhazes, N., Borges, F., Monks, T. J., Fernandes, E., Carvalho, F., and Bastos, M. L. (2002). Role of metabolites in MDMA (ecstasy)-induced nephrotoxicity: an in vitro study using rat and human renal proximal tubular cells. *Arch Toxicol* **76**, 581-8.

Castedo, M., Perfettini, J. L., Roumier, T., Andreau, K., Medema, R., and Kroemer, G. (2004). Cell death by mitotic catastrophe: a molecular definition. *Oncogene* **23**, 2825-37.

Chae, H. Z., Chung, S. J., and Rhee, S. G. (1994a). Thioredoxin-dependent peroxide reductase from yeast. *J Biol Chem* **269**, 27670-8.

Chae, H. Z., Robison, K., Poole, L. B., Church, G., Storz, G., and Rhee, S. G. (1994b). Cloning and sequencing of thiol-specific antioxidant from mammalian brain: alkyl hydroperoxide reductase and thiol-specific antioxidant define a large family of antioxidant enzymes. *Proc Natl Acad Sci U S A* **91**, 7017-21.

Chae, H. Z., Uhm, T. B., and Rhee, S. G. (1994c). Dimerization of thiol-specific antioxidant and the essential role of cysteine 47. *Proc Natl Acad Sci U S A* **91**, 7022-6.

Chang, T. S., Jeong, W., Choi, S. Y., Yu, S., Kang, S. W., and Rhee, S. G. (2002). Regulation of peroxiredoxin I activity by Cdc2-mediated phosphorylation. *J Biol Chem* **277**, 25370-6.

Chang, T. S., Jeong, W., Woo, H. A., Lee, S. M., Park, S., and Rhee, S. G. (2004). Characterization of mammalian sulfiredoxin and its reactivation of hyperoxidized peroxiredoxin through reduction of cysteine sulfinic acid in the active site to cysteine. *J Biol Chem*.

Chan-Hui, P. Y., and Weaver, R. (1998). Human mitogen-activated protein kinase kinase kinase mediates the stress-induced activation of mitogen-activated protein kinase cascades. *Biochem J* **336 (Pt 3)**, 599-609.

Chatterjee, S., Berger, S. J., and Berger, N. A. (1999). Poly(ADP-ribose) polymerase: a guardian of the genome that facilitates DNA repair by protecting against DNA recombination. *Mol Cell Biochem* **193**, 23-30.

Chen, K., Vita, J. A., Berk, B. C., and Keaney, J. F., Jr. (2001). c-Jun N-terminal kinase activation by hydrogen peroxide in endothelial cells involves SRC-dependent epidermal growth factor receptor transactivation. *J Biol Chem* **276**, 16045-50.

Chen, W., Martindale, J. L., Holbrook, N. J., and Liu, Y. (1998). Tumor promoter arsenite activates extracellular signal-regulated kinase through a signaling pathway mediated by epidermal growth factor receptor and Shc. *Mol Cell Biol* **18**, 5178-88.

Cho, H. N., Lee, Y. J., Cho, C. K., Lee, S. J., and Lee, Y. S. (2002). Downregulation of ERK2 is essential for the inhibition of radiation-induced cell death in HSP25 overexpressed L929 cells. *Cell Death Differ* **9**, 448-56.

Choi, H. J., Kang, S. W., Yang, C. H., Rhee, S. G., and Ryu, S. E. (1998). Crystal structure of a novel human peroxidase enzyme at 2.0 A resolution. *Nat Struct Biol* **5**, 400-6.

Church, D. F., and Pryor, W. A. (1985). Free-radical chemistry of cigarette smoke and its toxicological implications. *Environ Health Perspect* **64**, 111-26.

Claiborne, A., Mallett, T. C., Yeh, J. I., Luba, J., and Parsonage, D. (2001). Structural, redox, and mechanistic parameters for cysteine-sulfenic acid function in catalysis and regulation. *Adv Protein Chem* **58**, 215-76.

Cobb, M. H. (1999). MAP kinase pathways. *Prog Biophys Mol Biol* **71**, 479-500.

Cochet, C., Gill, G. N., Meisenhelder, J., Cooper, J. A., and Hunter, T. (1984). C-kinase phosphorylates the epidermal growth factor receptor and reduces its epidermal growth factor-stimulated tyrosine protein kinase activity. *J Biol Chem* **259**, 2553-8.

Coco-Martin, J. M., and Begg, A. C. (1997). Detection of radiation-induced chromosome aberrations using fluorescence in situ hybridization in drug-induced premature chromosome condensations of tumour cell lines with different radiosensitivities. *Int J Radiat Biol* **71**, 265-73.

Cohen, P. (1999). The development and therapeutic potential of protein kinase inhibitors. *Curr Opin Chem Biol* **3**, 459-65.

Cuenda, A., Rouse, J., Doza, Y. N., Meier, R., Cohen, P., Gallagher, T. F., Young, P. R., and Lee, J. C. (1995). SB 203580 is a specific inhibitor of a MAP kinase homologue which is stimulated by cellular stresses and interleukin-1. *FEBS Lett* **364**, 229-33.

Curtin, J. F., and Cotter, T. G. (2003). Live and let die: regulatory mechanisms in Fas-mediated apoptosis. *Cell Signal* **15**, 983-92.

Dalle-Donne, I., Rossi, R., Milzani, A., Di Simplicio, P., and Colombo, R. (2001). The actin cytoskeleton response to oxidants: from small heat shock protein phosphorylation to changes in the redox state of actin itself. *Free Radic Biol Med* **31**, 1624-32.

D'Amours, D., Desnoyers, S., D'Silva, I., and Poirier, G. G. (1999). Poly(ADP-ribosyl)ation reactions in the regulation of nuclear functions. *Biochem J* **342 (Pt 2)**, 249-68.

Daum, G., Levkau, B., Chamberlain, N. L., Wang, Y., and Clowes, A. W. (1998). The mitogen-activated protein kinase pathway contributes to vanadate toxicity in vascular smooth muscle cells. *Mol Cell Biochem* **183**, 97-103.

Davies, S. P., Reddy, H., Caivano, M., and Cohen, P. (2000). Specificity and mechanism of action of some commonly used protein kinase inhibitors. *Biochem J* **351**, 95-105.

Davis, R. J. (2000). Signal transduction by the JNK group of MAP kinases. *Cell* **103**, 239-52.

Deak, M., Clifton, A. D., Lucocq, L. M., and Alessi, D. R. (1998). Mitogen- and stress-activated protein kinase-1 (MSK1) is directly activated by MAPK and SAPK2/p38, and may mediate activation of CREB. *Embo J* **17**, 4426-41.

Delaney, A. M., Printen, J. A., Chen, H., Fauman, E. B., and Dudley, D. T. (2002). Identification of a novel mitogen-activated protein kinase kinase activation domain recognized by the inhibitor PD 184352. *Mol Cell Biol* **22**, 7593-602.

Divincenzo, G. D., Hamilton, M. L., Reynolds, R. C., and Ziegler, D. A. (1984). Metabolic fate and disposition of [14C]hydroquinone given orally to Sprague-Dawley rats. *Toxicology* **33**, 9-18.

Dong, J., Ramachandiran, S., Tikoo, K., Jia, Z., Lau, S. S., and Monks, T. J. (2004). EGFR-Independent Activation of p38 MAPK and EGFR-Dependent Activation of ERK1/2 is required for ROS-Induced Renal Cell Death. *Am J Physiol Renal Physiol*.

Duesbery, N. S., Webb, C. P., and Vande Woude, G. F. (1999). MEK wars, a new front in the battle against cancer. *Nat Med* **5**, 736-7.

Eaton, P., Fuller, W., and Shattock, M. J. (2002). S-thiolation of HSP27 regulates its multimeric aggregate size independently of phosphorylation. *J Biol Chem* **277**, 21189-96.

Ehrnsperger, M., Buchner, J., and Gaestel, M. (1998). in Molecular Chaperones in the Life Cycle of Proteins. *Marcel Dekker, New York*, pp. 533-575.

Ehrnsperger, M., Graber, S., Gaestel, M., and Buchner, J. (1997). Binding of non-native protein to Hsp25 during heat shock creates a reservoir of folding intermediates for reactivation. *Embo J* **16**, 221-9.

Eker, R., Mossige, J., Johannessen, J. V., and Aars, H. (1981). Hereditary renal adenomas and adenocarcinomas in rats. *Diagn Histopathol* **4**, 99-110.

Emlet, D. R., Moscatello, D. K., Ludlow, L. B., and Wong, A. J. (1997). Subsets of epidermal growth factor receptors during activation and endocytosis. *J Biol Chem* **272**, 4079-86.

Enslen, H., Raingeaud, J., and Davis, R. J. (1998). Selective activation of p38 mitogen-activated protein (MAP) kinase isoforms by the MAP kinase kinases MKK3 and MKK6. *J Biol Chem* **273**, 1741-8.

Everitt, J. I., Goldsworthy, T. L., Wolf, D. C., and Walker, C. L. (1992). Hereditary renal cell carcinoma in the Eker rat: a rodent familial cancer syndrome. *J Urol* **148**, 1932-6.

Fanger, G. R., Widmann, C., Porter, A. C., Sather, S., Johnson, G. L., and Vaillancourt, R. R. (1998). 14-3-3 proteins interact with specific MEK kinases. *J Biol Chem* **273**, 3476-83.

Fischle, W., Wang, Y., and Allis, C. D. (2003). Histone and chromatin cross-talk. *Curr Opin Cell Biol* **15**, 172-83.

Florin, I., Rutberg, L., Curvall, M., and Enzell, C. R. (1980). Screening of tobacco smoke constituents for mutagenicity using the Ames' test. *Toxicology* **15**, 219-232.

Forman, H. J., and Torres, M. (2002). Reactive oxygen species and cell signaling: respiratory burst in macrophage signaling. *Am J Respir Crit Care Med* **166**, S4-8.

Freshney, N. W., Rawlinson, L., Guesdon, F., Jones, E., Cowley, S., Hsuan, J., and Saklatvala, J. (1994). Interleukin-1 activates a novel protein kinase cascade that results in the phosphorylation of Hsp27. *Cell* **78**, 1039-49.

Frodin, M., and Gammeltoft, S. (1999). Role and regulation of 90 kDa ribosomal S6 kinase (RSK) in signal transduction. *Mol Cell Endocrinol* **151**, 65-77.

Fujii, J., and Ikeda, Y. (2002). Advances in our understanding of peroxiredoxin, a multifunctional, mammalian redox protein. *Redox Rep* **7**, 123-30.

Fukuda, M., Asano, S., Nakamura, T., Adachi, M., Yoshida, M., Yanagida, M., and Nishida, E. (1997). CRM1 is responsible for intracellular transport mediated by the nuclear export signal. *Nature* **390**, 308-11.

Gaestel, M., Schroder, W., Benndorf, R., Lippmann, C., Buchner, K., Hucho, F., Erdmann, V. A., and Bielka, H. (1991). Identification of the phosphorylation sites of the murine small heat shock protein hsp25. *J Biol Chem* **266**, 14721-4.

Gao, Y., and Lenard, J. (1995). Multimerization and transcriptional activation of the phosphoprotein (P) of vesicular stomatitis virus by casein kinase-II. *Embo J* **14**, 1240-7.

Garrido, C. (2002). Size matters: of the small HSP27 and its large oligomers. *Cell Death Differ* **9**, 483-5.

Garrido, C., Bruey, J. M., Fromentin, A., Hammann, A., Arrigo, A. P., and Solary, E. (1999). HSP27 inhibits cytochrome c-dependent activation of procaspase-9. *Faseb J* **13**, 2061-70.

Gocke, E., King, M. T., Eckhardt, K., and Wild, D. (1981). Mutagenicity of cosmetics ingredients licensed by the European Communities. *Mutat Res* **90**, 91-109.

Gocke, E., Wild, D., Eckhardt, K., and King, M. T. (1983). Mutagenicity studies with the mouse spot test. *Mutat Res* **117**, 201-12.

Goto, H., Tomono, Y., Ajiro, K., Kosako, H., Fujita, M., Sakurai, M., Okawa, K., Iwamatsu, A., Okigaki, T., Takahashi, T., and Inagaki, M. (1999). Identification of a novel phosphorylation site on histone H3 coupled with mitotic chromosome condensation. *J Biol Chem* **274**, 25543-9.

Green, A. R., Mechan, A. O., Elliott, J. M., O'Shea, E., and Colado, M. I. (2003). The pharmacology and clinical pharmacology of 3,4-methylenedioxymethamphetamine (MDMA, "ecstasy"). *Pharmacol Rev* **55**, 463-508.

Greenburg, L. (1996). Results of medical examination and clinical tests made to discover early signs of benzol poisoning in exposed workers. *Environ. Health Perspect.* **104 (suppl. 6)**, 1129-1136.

Gross, A., McDonnell, J. M., and Korsmeyer, S. J. (1999). BCL-2 family members and the mitochondria in apoptosis. *Genes Dev* **13**, 1899-911.

Guay, J., Lambert, H., Gingras-Breton, G., Lavoie, J. N., Huot, J., and Landry, J. (1997). Regulation of actin filament dynamics by p38 map kinase-mediated phosphorylation of heat shock protein 27. *J Cell Sci* **110 (Pt 3)**, 357-68.

Guyton, K. Z., Gorospe, M., Wang, X., Mock, Y. D., Kokkonen, G. C., Liu, Y., Roth, G. S., and Holbrook, N. J. (1998). Age-related changes in activation of mitogen-activated protein kinase cascades by oxidative stress. *J Investig Dermatol Symp Proc* **3**, 23-7.

Guyton, K. Z., Liu, Y., Gorospe, M., Xu, Q., and Holbrook, N. J. (1996). Activation of mitogen-activated protein kinase by H2O2. Role in cell survival following oxidant injury. *J Biol Chem* **271**, 4138-42.

Habib, S. L., Phan, M. N., Patel, S. K., Li, D., Monks, T. J., and Lau, S. S. (2003). Reduced constitutive 8-oxoguanine-DNA glycosylase expression and impaired induction following oxidative DNA damage in the tuberin deficient Eker rat. *Carcinogenesis* **24**, 573-82.

Hakura, A., Mochida, H., Tsutsui, Y., and Yamatsu, K. (1995). Mutagenicity of benzoquinones for Ames Salmonella tester strains. *Mutat Res* **347**, 37-43.

Hakura, A., Tsutsui, Y., Mochida, H., Sugihara, Y., Mikami, T., and Sagami, F. (1996). Mutagenicity of dihydroxybenzenes and dihydroxynaphthalenes for Ames Salmonella tester strains. *Mutat Res* **371**, 293-9.

Hannken, T., Schroeder, R., Zahner, G., Stahl, R. A., and Wolf, G. (2000). Reactive oxygen species stimulate p44/42 mitogen-activated protein kinase and induce p27(Kip1): role in angiotensin II-mediated hypertrophy of proximal tubular cells. *J Am Soc Nephrol* **11**, 1387-97.

Helin, K., and Beguinot, L. (1991). Internalization and down-regulation of the human epidermal growth factor receptor are regulated by the carboxyl-terminal tyrosines. *J Biol Chem* **266**, 8363-8.

Hendzel, M. J., Nishioka, W. K., Raymond, Y., Allis, C. D., Bazett-Jones, D. P., and Th'ng, J. P. (1998). Chromatin condensation is not associated with apoptosis. *J Biol Chem* **273**, 24470-8.

Henry, J. A., Jeffreys, K. J., and Dawling, S. (1992). Toxicity and deaths from 3,4-methylenedioxymethamphetamine ("ecstasy"). *Lancet* **340**, 384-7.

Hess, A., Wijayanti, N., Neuschafer-Rube, A. P., Katz, N., Kietzmann, T., and Immenschuh, S. (2003). Phorbol ester-dependent activation of peroxiredoxin I gene expression via a protein kinase C, Ras, p38 mitogen-activated protein kinase signaling pathway. *J Biol Chem* **278**, 45419-34.

Hill, B. A., Kleiner, H. E., Ryan, E. A., Dulik, D. M., Monks, T. J., and Lau, S. S. (1993). Identification of multi-S-substituted conjugates of hydroquinone by HPLC-coulometric electrode array analysis and mass spectroscopy. *Chem Res Toxicol* **6**, 459-69.

Hino, O., Mitani, H., and Knudson, A. G. (1993). Genetic predisposition to transplacentally induced renal cell carcinomas in the Eker rat. *Cancer Res* **53**, 5856-8.

Hirotsu, S., Abe, Y., Okada, K., Nagahara, N., Hori, H., Nishino, T., and Hakoshima, T. (1999). Crystal structure of a multifunctional 2-Cys peroxiredoxin heme-binding protein 23 kDa/proliferation-associated gene product. *Proc Natl Acad Sci U S A* **96**, 12333-8.

Hoeflich, K. P., Yeh, W. C., Yao, Z., Mak, T. W., and Woodgett, J. R. (1999). Mediation of TNF receptor-associated factor effector functions by apoptosis signal-regulating kinase-1 (ASK1). *Oncogene* **18**, 5814-20.

Hofmann, B., Hecht, H. J., and Flohe, L. (2002). Peroxiredoxins. *Biol Chem* **383**, 347-64.

Honda, B. M., Candido, P. M., and Dixon, G. H. (1975). Histone methylation. Its occurrence in different cell types and relation to histone H4 metabolism in developing trout testis. *J Biol Chem* **250**, 8686-9.

Horwitz, J. (1992). Alpha-crystallin can function as a molecular chaperone. *Proc Natl Acad Sci U S A* **89**, 10449-53.

Hsieh, T. J., Zhang, S. L., Filep, J. G., Tang, S. S., Ingelfinger, J. R., and Chan, J. S. (2002). High glucose stimulates angiotensinogen gene expression via reactive oxygen species generation in rat kidney proximal tubular cells. *Endocrinology* **143**, 2975-85.

Hu, M. C., Wang, Y. P., Mikhail, A., Qiu, W. R., and Tan, T. H. (1999). Murine p38-delta mitogen-activated protein kinase, a developmentally regulated protein kinase that is activated by stress and proinflammatory cytokines. *J Biol Chem* **274**, 7095-102.

Hung, C. C., Ichimura, T., Stevens, J. L., and Bonventre, J. V. (2003). Protection of renal epithelial cells against oxidative injury by endoplasmic reticulum stress preconditioning is mediated by ERK1/2 activation. *J Biol Chem* **278**, 29317-26.

Huot, J., Houle, F., Marceau, F., and Landry, J. (1997). Oxidative stress-induced actin reorganization mediated by the p38 mitogen-activated protein kinase/heat shock protein 27 pathway in vascular endothelial cells. *Circ Res* **80**, 383-92.

Huot, J., Houle, F., Rousseau, S., Deschesnes, R. G., Shah, G. M., and Landry, J. (1998). SAPK2/p38-dependent F-actin reorganization regulates early membrane blebbing during stress-induced apoptosis. *J Cell Biol* **143**, 1361-73.

Huot, J., Houle, F., Spitz, D. R., and Landry, J. (1996). HSP27 phosphorylation-mediated resistance against actin fragmentation and cell death induced by oxidative stress. *Cancer Res* **56**, 273-9.

IARC (1977). Monographs on the Evaluation of the Carcinogenic Risk of Chemicals to Man. *World Health Organization, Lyon* **Volume 15**.

IPCS (1993). Benzene / first draft prepared by E.E. McConnell. *Geneva : World Health Organization*.

IPCS, I. P. o. C. S. (1996). Hydroquinone Health and Safety Guide, Health and Safety. *World Health Organization, Geneva* **Guide No. 101**.

Irani, K., Xia, Y., Zweier, J. L., Sollott, S. J., Der, C. J., Fearon, E. R., Sundaresan, M., Finkel, T., and Goldschmidt-Clermont, P. J. (1997). Mitogenic signaling mediated by oxidants in Ras-transformed fibroblasts. *Science* **275**, 1649-52.

Irving, E. A., and Bamford, M. (2002). Role of mitogen- and stress-activated kinases in ischemic injury. *J Cereb Blood Flow Metab* **22**, 631-47.

Jakob, U., Gaestel, M., Engel, K., and Buchner, J. (1993). Small heat shock proteins are molecular chaperones. *J Biol Chem* **268**, 1517-20.

Jeong, J. K., Dybing, E., Soderlund, E., Brunborg, G., Holme, J. A., Lau, S. S., and Monks, T. J. (1997a). DNA damage, gadd153 expression, and cytotoxicity in plateau-phase renal proximal tubular epithelial cells treated with a quinol thioether. *Arch Biochem Biophys* **341**, 300-8.

Jeong, J. K., Huang, Q., Lau, S. S., and Monks, T. J. (1997b). The response of renal tubular epithelial cells to physiologically and chemically induced growth arrest. *J Biol Chem* **272**, 7511-8.

Jeong, J. K., Stevens, J. L., Lau, S. S., and Monks, T. J. (1996). Quinone thioether-mediated DNA damage, growth arrest, and gadd153 expression in renal proximal tubular epithelial cells. *Mol Pharmacol* **50**, 592-8.

Jeong, J. K., Wogan, G. N., Lau, S. S., and Monks, T. J. (1999). Quinol-glutathione conjugate-induced mutation spectra in the supF gene replicated in human AD293 cells and bacterial MBL50 cells. *Cancer Res* **59**, 3641-5.

Jia, Z., Person, M. D., Dong, J., Shen, J., Hensley, S. C., Stevens, J. L., Monks, T. J., and Lau, S. S. (2004). Grp78 Is Essential for 11-Deoxy, 16,16-Dimethyl Prostaglandin E2 Mediated Cytoprotection in Renal Epithelial Cells. *Am J Physiol Renal Physiol*.

Jiang, X., Huang, F., Marusyk, A., and Sorkin, A. (2003). Grb2 regulates internalization of EGF receptors through clathrin-coated pits. *Mol Biol Cell* **14**, 858-70.

Jimenez, L. A., Zanella, C., Fung, H., Janssen, Y. M., Vacek, P., Charland, C., Goldberg, J., and Mossman, B. T. (1997). Role of extracellular signal-regulated protein kinases in apoptosis by asbestos and H2O2. *Am J Physiol* **273**, L1029-35.

Jin, D. Y., Chae, H. Z., Rhee, S. G., and Jeang, K. T. (1997). Regulatory role for a novel human thioredoxin peroxidase in NF-kappaB activation. *J Biol Chem* **272**, 30952-61.

Joazeiro, C. A., Wing, S. S., Huang, H., Leverson, J. D., Hunter, T., and Liu, Y. C. (1999). The tyrosine kinase negative regulator c-Cbl as a RING-type, E2-dependent ubiquitin-protein ligase. *Science* **286**, 309-12.

Jones, D. C., Lau, S. S., and Monks, T. J. (2004). THIOETHER METABOLITES OF MDA AND MDMA INHIBIT hSERT FUNCTION AND SIMULTANEOUSLY STIMULATE DOPAMINE UPTAKE INTO hSERT-EXPRESSING SK-N-MC CELLS. *J Pharmacol Exp Ther*.

Jorissen, R. N., Walker, F., Pouliot, N., Garrett, T. P., Ward, C. W., and Burgess, A. W. (2003). Epidermal growth factor receptor: mechanisms of activation and signalling. *Exp Cell Res* **284**, 31-53.

Jump, D. B., Butt, T. R., and Smulson, M. (1979). Nuclear protein modification and chromatin substructure. 3. Relationship between poly(adenosine diphosphate) ribosylation and different functional forms of chromatin. *Biochemistry* **18**, 983-90.

Kampinga, H. H., Brunsting, J. F., Stege, G. J., Konings, A. W., and Landry, J. (1994). Cells overexpressing Hsp27 show accelerated recovery from heat-induced nuclear protein aggregation. *Biochem Biophys Res Commun* **204**, 1170-7.

Kanda, Y., Nishio, E., Kuroki, Y., Mizuno, K., and Watanabe, Y. (2001). Thrombin activates p38 mitogen-activated protein kinase in vascular smooth muscle cells. *Life Sci* **68**, 1989-2000.

Kang, S. W., Baines, I. C., and Rhee, S. G. (1998a). Characterization of a mammalian peroxiredoxin that contains one conserved cysteine. *J Biol Chem* **273**, 6303-11.

Kang, S. W., Chae, H. Z., Seo, M. S., Kim, K., Baines, I. C., and Rhee, S. G. (1998b). Mammalian peroxiredoxin isoforms can reduce hydrogen peroxide generated in response to growth factors and tumor necrosis factor-alpha. *J Biol Chem* **273**, 6297-302.

Kang, S. W., Chang, T. S., Lee, T. H., Kim, E. S., Yu, D. Y., and Rhee, S. G. (2004). Cytosolic peroxiredoxin attenuates the activation of Jnk and p38 but potentiates that of Erk in Hela cells stimulated with tumor necrosis factor-alpha. *J Biol Chem* **279**, 2535-43.

Kari, F. W., Bucher, J., Eustis, S. L., Haseman, J. K., and Huff, J. E. (1992). Toxicity and carcinogenicity of hydroquinone in F344/N rats and B6C3F1 mice. *Food Chem Toxicol* **30**, 737-47.

Kato, K., Hasegawa, K., Goto, S., and Inaguma, Y. (1994). Dissociation as a result of phosphorylation of an aggregated form of the small stress protein, hsp27. *J Biol Chem* **269**, 11274-8.

Khan, S., Koepke, A., Jarad, G., Schlessman, K., Cleveland, R. P., Wang, B., Konieczkowski, M., and Schelling, J. R. (2001). Apoptosis and JNK activation are differentially regulated by Fas expression level in renal tubular epithelial cells. *Kidney Int* **60**, 65-76.

Kim, J. H., Saito, K., and Yokoyama, S. (2002). Chimeric receptor analyses of the interactions of the ectodomains of ErbB-1 with epidermal growth factor and of those of ErbB-4 with neuregulin. *Eur J Biochem* **269**, 2323-9.

Kim, J. R., Yoon, H. W., Kwon, K. S., Lee, S. R., and Rhee, S. G. (2000). Identification of proteins containing cysteine residues that are sensitive to oxidation by hydrogen peroxide at neutral pH. *Anal Biochem* **283**, 214-21.

Kim, K., Kim, I. H., Lee, K. Y., Rhee, S. G., and Stadtman, E. R. (1988). The isolation and purification of a specific "protector" protein which inhibits enzyme inactivation by a thiol/Fe(III)/O2 mixed-function oxidation system. *J Biol Chem* **263**, 4704-11.

Kleiner, H. E., Jones, T. W., Monks, T. J., and Lau, S. S. (1998a). Immunochemical analysis of quinol-thioether-derived covalent protein adducts in rodent species sensitive and resistant to quinol-thioether-mediated nephrotoxicity. *Chem Res Toxicol* **11**, 1291-300.

Kleiner, H. E., Rivera, M. I., Pumford, N. R., Monks, T. J., and Lau, S. S. (1998b). Immunochemical detection of quinol--thioether-derived protein adducts. *Chem Res Toxicol* **11**, 1283-90.

Knauf, U., Jakob, U., Engel, K., Buchner, J., and Gaestel, M. (1994). Stress- and mitogen-induced phosphorylation of the small heat shock protein Hsp25 by MAPKAP kinase 2 is not essential for chaperone properties and cellular thermoresistance. *Embo J* **13**, 54-60.

Knebel, A., Rahmsdorf, H. J., Ullrich, A., and Herrlich, P. (1996). Dephosphorylation of receptor tyrosine kinases as target of regulation by radiation, oxidants or alkylating agents. *Embo J* **15**, 5314-25.

Konishi, H., Matsuzaki, H., Tanaka, M., Takemura, Y., Kuroda, S., Ono, Y., and Kikkawa, U. (1997). Activation of protein kinase B (Akt/RAC-protein kinase) by cellular stress and its association with heat shock protein Hsp27. *FEBS Lett* **410**, 493-8.

Lander, H. M., Ogiste, J. S., Teng, K. K., and Novogrodsky, A. (1995). p21ras as a common signaling target of reactive free radicals and cellular redox stress. *J Biol Chem* **270**, 21195-8.

Landry, J., Chretien, P., Lambert, H., Hickey, E., and Weber, L. A. (1989). Heat shock resistance conferred by expression of the human HSP27 gene in rodent cells. *J Cell Biol* **109**, 7-15.

Landry, J., Chretien, P., Laszlo, A., and Lambert, H. (1991). Phosphorylation of HSP27 during development and decay of thermotolerance in Chinese hamster cells. *J Cell Physiol* **147**, 93-101.

Landry, J., and Huot, J. (1995). Modulation of actin dynamics during stress and physiological stimulation by a signaling pathway involving p38 MAP kinase and heat-shock protein 27. *Biochem Cell Biol* **73**, 703-7.

Landry, J., Lambert, H., Zhou, M., Lavoie, J. N., Hickey, E., Weber, L. A., and Anderson, C. W. (1992). Human HSP27 is phosphorylated at serines 78 and 82 by heat shock and mitogen-activated kinases that recognize the same amino acid motif as S6 kinase II. *J Biol Chem* **267**, 794-803.

Lau, S. S., Hill, B. A., Highet, R. J., and Monks, T. J. (1988). Sequential oxidation and glutathione addition to 1,4-benzoquinone: correlation of toxicity with increased glutathione substitution. *Mol Pharmacol* **34**, 829-36.

Lau, S. S., and Monks, T. J. (1987). Co-oxidation of 2-bromohydroquinone by renal prostaglandin synthase. Modulation of prostaglandin synthesis by 2-bromohydroquinone and glutathione. *Drug Metab Dispos* **15**, 801-7.

Lau, S. S., Monks, T. J., Everitt, J. I., Kleymenova, E., and Walker, C. L. (2001a). Carcinogenicity of a nephrotoxic metabolite of the "nongenotoxic" carcinogen hydroquinone. *Chem Res Toxicol* **14**, 25-33.

Lau, S. S., Peters, M. M., Kleiner, H. E., Canales, P. L., and Monks, T. J. (1996). Linking the metabolism of hydroquinone to its nephrotoxicity and nephrocarcinogenicity. *Adv Exp Med Biol* **387**, 267-73.

Lau, S. S., Sawalha, A. F., Halpert, J. R., Koop, D. R., and Monks, T. J. (1997). Cytochrome P450 catalyzed oxidation of hydroquinone in rodent and human microsomes. *Toxicologist* **36**, 23.

Lau, S. S., Yoon, H. S., Patel, S. K., Everitt, J. I., Walker, C. L., and Monks, T. J. (2001b). Mutagenicity and carcinogenicity of biological reactive intermediate's derived from a "non-genotoxic" carcinogen. *Adv Exp Med Biol* **500**, 83-92.

Lavoie, J. N., Gingras-Breton, G., Tanguay, R. M., and Landry, J. (1993a). Induction of Chinese hamster HSP27 gene expression in mouse cells confers resistance to heat shock. HSP27 stabilization of the microfilament organization. *J Biol Chem* **268**, 3420-9.

Lavoie, J. N., Hickey, E., Weber, L. A., and Landry, J. (1993b). Modulation of actin microfilament dynamics and fluid phase pinocytosis by phosphorylation of heat shock protein 27. *J Biol Chem* **268**, 24210-4.

Lavoie, J. N., Lambert, H., Hickey, E., Weber, L. A., and Landry, J. (1995). Modulation of cellular thermoresistance and actin filament stability accompanies phosphorylation-induced changes in the oligomeric structure of heat shock protein 27. *Mol Cell Biol* **15**, 505-16.

Leanderson, P., and Tagesson, C. (1990). Cigarette smoke-induced DNA-damage: role of hydroquinone and catechol in the formation of the oxidative DNA-adduct, 8-hydroxydeoxyguanosine. *Chem Biol Interact* **75**, 71-81.

Lee, G. J., Roseman, A. M., Saibil, H. R., and Vierling, E. (1997a). A small heat shock protein stably binds heat-denatured model substrates and can maintain a substrate in a folding-competent state. *Embo J* **16**, 659-71.

Lee, J., Richburg, J. H., Younkin, S. C., and Boekelheide, K. (1997b). The Fas system is a key regulator of germ cell apoptosis in the testis. *Endocrinology* **138**, 2081-8.

Lee, J. C., Kassis, S., Kumar, S., Badger, A., and Adams, J. L. (1999). p38 mitogen-activated protein kinase inhibitors--mechanisms and therapeutic potentials. *Pharmacol Ther* **82**, 389-97.

Lee, Y. J., Cho, H. N., Jeoung, D. I., Soh, J. W., Cho, C. K., Bae, S., Chung, H. Y., Lee, S. J., and Lee, Y. S. (2004). HSP25 overexpression attenuates oxidative stress-induced apoptosis: roles of ERK1/2 signaling and manganese superoxide dismutase. *Free Radic Biol Med* **36**, 429-44.

Lemmon, M. A., Bu, Z., Ladbury, J. E., Zhou, M., Pinchasi, D., Lax, I., Engelman, D. M., and Schlessinger, J. (1997). Two EGF molecules contribute additively to stabilization of the EGFR dimer. *Embo J* **16**, 281-94.

Levinger, L., and Varshavsky, A. (1982). Selective arrangement of ubiquitinated and D1 protein-containing nucleosomes within the Drosophila genome. *Cell* **28**, 375-85.

Levitzki, A., and Gazit, A. (1995). Tyrosine kinase inhibition: an approach to drug development. *Science* **267**, 1782-8.

Levkowitz, G., Waterman, H., Ettenberg, S. A., Katz, M., Tsygankov, A. Y., Alroy, I., Lavi, S., Iwai, K., Reiss, Y., Ciechanover, A., Lipkowitz, S., and Yarden, Y. (1999). Ubiquitin ligase activity and tyrosine phosphorylation underlie suppression of growth factor signaling by c-Cbl/Sli-1. *Mol Cell* **4**, 1029-40.

Levkowitz, G., Waterman, H., Zamir, E., Kam, Z., Oved, S., Langdon, W. Y., Beguinot, L., Geiger, B., and Yarden, Y. (1998). c-Cbl/Sli-1 regulates endocytic sorting and ubiquitination of the epidermal growth factor receptor. *Genes Dev* **12**, 3663-74.

Lewis, S. E., Mannion, R. J., White, F. A., Coggeshall, R. E., Beggs, S., Costigan, M., Martin, J. L., Dillmann, W. H., and Woolf, C. J. (1999). A role for HSP27 in sensory neuron survival. *J Neurosci* **19**, 8945-53.

Lim, Y. S., Cha, M. K., Yun, C. H., Kim, H. K., Kim, K., and Kim, I. H. (1994). Purification and characterization of thiol-specific antioxidant protein from human red blood cell: a new type of antioxidant protein. *Biochem Biophys Res Commun* **199**, 199-206.

Lo, W. S., Trievel, R. C., Rojas, J. R., Duggan, L., Hsu, J. Y., Allis, C. D., Marmorstein, R., and Berger, S. L. (2000). Phosphorylation of serine 10 in histone H3 is functionally linked in vitro and in vivo to Gcn5-mediated acetylation at lysine 14. *Mol Cell* **5**, 917-26.

Ludwig, S., Engel, K., Hoffmeyer, A., Sithanandam, G., Neufeld, B., Palm, D., Gaestel, M., and Rapp, U. R. (1996). 3pK, a novel mitogen-activated protein (MAP) kinase-activated protein kinase, is targeted by three MAP kinase pathways. *Mol Cell Biol* **16**, 6687-97.

Mahadevan, L. C., Willis, A. C., and Barratt, M. J. (1991). Rapid histone H3 phosphorylation in response to growth factors, phorbol esters, okadaic acid, and protein synthesis inhibitors. *Cell* **65**, 775-83.

Majno, G., and Joris, I. (1995). Apoptosis, oncosis, and necrosis. An overview of cell death. *Am J Pathol* **146**, 3-15.

Marnett, L. J. (1999). Lipid peroxidation-DNA damage by malondialdehyde. *Mutat Res* **424**, 83-95.

Marshall, C. J. (1995). Specificity of receptor tyrosine kinase signaling: transient versus sustained extracellular signal-regulated kinase activation. *Cell* **80**, 179-85.

Martindale, J. L., and Holbrook, N. J. (2002). Cellular response to oxidative stress: signaling for suicide and survival. *J Cell Physiol* **192**, 1-15.

McLaughlin, M. M., Kumar, S., McDonnell, P. C., Van Horn, S., Lee, J. C., Livi, G. P., and Young, P. R. (1996). Identification of mitogen-activated protein (MAP) kinase-activated protein kinase-3, a novel substrate of CSBP p38 MAP kinase. *J Biol Chem* **271**, 8488-92.

Mehlen, P., Briolay, J., Smith, L., Diaz-latoud, C., Fabre, N., Pauli, D., and Arrigo, A. P. (1993). Analysis of the resistance to heat and hydrogen peroxide stresses in COS cells transiently expressing wild type or deletion mutants of the Drosophila 27-kDa heat-shock protein. *Eur J Biochem* **215**, 277-84.

Mehlen, P., Hickey, E., Weber, L. A., and Arrigo, A. P. (1997). Large unphosphorylated aggregates as the active form of hsp27 which controls intracellular reactive oxygen species and glutathione levels and generates a protection against TNFalpha in NIH-3T3-ras cells. *Biochem Biophys Res Commun* **241**, 187-92.

Mehlen, P., Kretz-Remy, C., Preville, X., and Arrigo, A. P. (1996a). Human hsp27, Drosophila hsp27 and human alphaB-crystallin expression-mediated increase in glutathione is essential for the protective activity of these proteins against TNFalpha-induced cell death. *Embo J* **15**, 2695-706.

Mehlen, P., Schulze-Osthoff, K., and Arrigo, A. P. (1996b). Small stress proteins as novel regulators of apoptosis. Heat shock protein 27 blocks Fas/APO-1- and staurosporine-induced cell death. *J Biol Chem* **271**, 16510-4.

Merck, K. B., Groenen, P. J., Voorter, C. E., de Haard-Hoekman, W. A., Horwitz, J., Bloemendal, H., and de Jong, W. W. (1993). Structural and functional similarities of bovine alpha-crystallin and mouse small heat-shock protein. A family of chaperones. *J Biol Chem* **268**, 1046-52.

Mertens, J. J., Gibson, N. W., Lau, S. S., and Monks, T. J. (1995). Reactive oxygen species and DNA damage in 2-bromo-(glutathion-S-yl) hydroquinone-mediated cytotoxicity. *Arch Biochem Biophys* **320**, 51-8.

Meves, A., Stock, S. N., Beyerle, A., Pittelkow, M. R., and Peus, D. (2001). H(2)O(2) mediates oxidative stress-induced epidermal growth factor receptor phosphorylation. *Toxicol Lett* **122**, 205-14.

Miller, R. T., Lau, S. S., and Monks, T. J. (1997). 2,5-Bis-(glutathion-S-yl)-alpha-methyldopamine, a putative metabolite of (+/-)-3,4-methylenedioxyamphetamine, decreases brain serotonin concentrations. *Eur J Pharmacol* **323**, 173-80.

Miron, T., Vancompernolle, K., Vandekerckhove, J., Wilchek, M., and Geiger, B. (1991). A 25-kD inhibitor of actin polymerization is a low molecular mass heat shock protein. *J Cell Biol* **114**, 255-61.

Monks, T. J., Highet, R. J., and Lau, S. S. (1988). 2-Bromo-(diglutathion-S-yl)hydroquinone nephrotoxicity: physiological, biochemical, and electrochemical determinants. *Mol Pharmacol* **34**, 492-500.

Monks, T. J., Jones, D. C., Bai, F., and Lau, S. S. (2004). The role of metabolism in 3,4-(+)-methylenedioxyamphetamine and 3,4-(+)-methylenedioxymethamphetamine (ecstasy) toxicity. *Ther Drug Monit* **26**, 132-6.

Monks, T. J., and Lau, S. S. (1994). Glutathione conjugation as a mechanism for the transport of reactive metabolites. *Adv Pharmacol* **27**, 183-210.

Monks, T. J., and Lau, S. S. (1997). Biological reactivity of polyphenolic-glutathione conjugates. *Chem Res Toxicol* **10**, 1296-313.

Monks, T. J., and Lau, S. S. (1998). The pharmacology and toxicology of polyphenolic-glutathione conjugates. *Annu Rev Pharmacol Toxicol* **38**, 229-55.

Monks, T. J., Lau, S. S., Highet, R. J., and Gillette, J. R. (1985). Glutathione conjugates of 2-bromohydroquinone are nephrotoxic. *Drug Metab Dispos* **13**, 553-9.

Morrison, D. K., and Davis, R. J. (2003). Regulation of MAP kinase signaling modules by scaffold proteins in mammals. *Annu Rev Cell Dev Biol* **19**, 91-118.

Mounier, N., and Arrigo, A. P. (2002). Actin cytoskeleton and small heat shock proteins: how do they interact? *Cell Stress Chaperones* **7**, 167-76.

Mu, Z. M., Yin, X. Y., and Prochownik, E. V. (2002). Pag, a putative tumor suppressor, interacts with the Myc Box II domain of c-Myc and selectively alters its biological function and target gene expression. *J Biol Chem* **277**, 43175-84.

Mukherjee, S. P., Lane, R. H., and Lynn, W. S. (1978). Endogenous hydrogen peroxide and peroxidative metabolism in adipocytes in response to insulin and sulfhydryl reagents. *Biochem Pharmacol* **27**, 2589-94.

Nakamura, H., Nakamura, K., and Yodoi, J. (1997). Redox regulation of cellular activation. *Annu Rev Immunol* **15**, 351-69.

Nerland, D. E., and Pierce, W. M., Jr. (1990). Identification of N-acetyl-S-(2,5-dihydroxyphenyl)-L-cysteine as a urinary metabolite of benzene, phenol, and hydroquinone. *Drug Metab Dispos* **18**, 958-61.

New, L., and Han, J. (1998). The p38 MAP Kinase Pathway and Its Biological Function. *Trends Cardiovasc Med* **8**, 220-8.

Nicholl, I. D., and Quinlan, R. A. (1994). Chaperone activity of alpha-crystallins modulates intermediate filament assembly. *Embo J* **13**, 945-53.

Nonn, L., Berggren, M., and Powis, G. (2003). Increased expression of mitochondrial peroxiredoxin-3 (thioredoxin peroxidase-2) protects cancer cells against hypoxia and drug-induced hydrogen peroxide-dependent apoptosis. *Mol Cancer Res* **1**, 682-9.

Nover, L., Scharf, K. D., and Neumann, D. (1983). Formation of cytoplasmic heat shock granules in tomato cell cultures and leaves. *Mol Cell Biol* **3**, 1648-55.

Nowak, S. J., and Corces, V. G. (2004). Phosphorylation of histone H3: a balancing act between chromosome condensation and transcriptional activation. *Trends Genet* **20**, 214-20.

Obrocki, J., Schmoldt, A., Buchert, R., Andresen, B., Petersen, K., and Thomasius, R. (2002). Specific neurotoxicity of chronic use of ecstasy. *Toxicol Lett* **127**, 285-97.

Oka, H., Chatani, Y., Hoshino, R., Ogawa, O., Kakehi, Y., Terachi, T., Okada, Y., Kawaichi, M., Kohno, M., and Yoshida, O. (1995). Constitutive activation of mitogen-activated protein (MAP) kinases in human renal cell carcinoma. *Cancer Res* **55**, 4182-7.

Okuda, M. (2002). The role of nucleophosmin in centrosome duplication. *Oncogene* **21**, 6170-4.

Omori, S., Hida, M., Ishikura, K., Kuramochi, S., and Awazu, M. (2000). Expression of mitogen-activated protein kinase family in rat renal development. *Kidney Int* **58**, 27-37.

Pandey, P., Farber, R., Nakazawa, A., Kumar, S., Bharti, A., Nalin, C., Weichselbaum, R., Kufe, D., and Kharbanda, S. (2000). Hsp27 functions as a negative regulator of cytochrome c-dependent activation of procaspase-3. *Oncogene* **19**, 1975-81.

Parcellier, A., Gurbuxani, S., Schmitt, E., Solary, E., and Garrido, C. (2003a). Heat shock proteins, cellular chaperones that modulate mitochondrial cell death pathways. *Biochem Biophys Res Commun* **304**, 505-12.

Parcellier, A., Schmitt, E., Gurbuxani, S., Seigneurin-Berny, D., Pance, A., Chantome, A., Plenchette, S., Khochbin, S., Solary, E., and Garrido, C. (2003b). HSP27 is a ubiquitin-binding protein involved in I-kappaBalpha proteasomal degradation. *Mol Cell Biol* **23**, 5790-802.

Parente, L., and Solito, E. (2004). Annexin 1: more than an anti-phospholipase protein. *Inflamm Res* **53**, 125-32.

Park, B. S., Kim, G. C., Back, S. J., Kim, N. D., Kim, Y. S., Kim, S. K., Jeong, M. H., Lim, Y. J., and Yoo, Y. H. (2000). Murine bone marrow-derived mast cells exhibit evidence of both apoptosis and oncosis after IL-3 deprivation. *Immunol Invest* **29**, 51-60.

Park, K. J., Gaynor, R. B., and Kwak, Y. T. (2003). Heat shock protein 27 association with the I kappa B kinase complex regulates tumor necrosis factor alpha-induced NF-kappa B activation. *J Biol Chem* **278**, 35272-8.

Park, K. M., Kramers, C., Vayssier-Taussat, M., Chen, A., and Bonventre, J. V. (2002). Prevention of kidney ischemia/reperfusion-induced functional injury, MAPK and MAPK kinase activation, and inflammation by remote transient ureteral obstruction. *J Biol Chem* **277**, 2040-9.

Park, Y. M., Han, M. Y., Blackburn, R. V., and Lee, Y. J. (1998). Overexpression of HSP25 reduces the level of TNF alpha-induced oxidative DNA damage biomarker, 8-hydroxy-2'-deoxyguanosine, in L929 cells. *J Cell Physiol* **174**, 27-34.

Patel, S. K., Ma, N., Monks, T. J., and Lau, S. S. (2003). Changes in gene expression during chemical-induced nephrocarcinogenicity in the Eker rat. *Mol Carcinog* **38**, 141-54.

Paul, A., Wilson, S., Belham, C. M., Robinson, C. J., Scott, P. H., Gould, G. W., and Plevin, R. (1997). Stress-activated protein kinases: activation, regulation and function. *Cell Signal* **9**, 403-10.

Paul, C., Manero, F., Gonin, S., Kretz-Remy, C., Virot, S., and Arrigo, A. P. (2002). Hsp27 as a negative regulator of cytochrome C release. *Mol Cell Biol* **22**, 816-34.

Paulson, J. R., and Taylor, S. S. (1982). Phosphorylation of histones 1 and 3 and nonhistone high mobility group 14 by an endogenous kinase in HeLa metaphase chromosomes. *J Biol Chem* **257**, 6064-72.

Perry, S. J., and Lefkowitz, R. J. (2002). Arresting developments in heptahelical receptor signaling and regulation. *Trends Cell Biol* **12**, 130-8.

Peters, M. M., Jones, T. W., Monks, T. J., and Lau, S. S. (1997). Cytotoxicity and cell-proliferation induced by the nephrocarcinogen hydroquinone and its nephrotoxic metabolite 2,3,5-(tris-glutathion-S-yl)hydroquinone. *Carcinogenesis* **18**, 2393-401.

Peters, M. M., Rivera, M. I., Jones, T. W., Monks, T. J., and Lau, S. S. (1996). Glutathione conjugates of tert-butyl-hydroquinone, a metabolite of the urinary tract tumor promoter 3-tert-butyl-hydroxyanisole, are toxic to kidney and bladder. *Cancer Res* **56**, 1006-11.

Pombo, C. M., Bonventre, J. V., Avruch, J., Woodgett, J. R., Kyriakis, J. M., and Force, T. (1994). The stress-activated protein kinases are major c-Jun amino-terminal kinases activated by ischemia and reperfusion. *J Biol Chem* **269**, 26546-51.

Pramanik, R., Qi, X., Borowicz, S., Choubey, D., Schultz, R. M., Han, J., and Chen, G. (2003). p38 isoforms have opposite effects on AP-1-dependent transcription through regulation of c-Jun. The determinant roles of the isoforms in the p38 MAPK signal specificity. *J Biol Chem* **278**, 4831-9.

Preuss, U., Landsberg, G., and Scheidtmann, K. H. (2003). Novel mitosis-specific phosphorylation of histone H3 at Thr11 mediated by Dlk/ZIP kinase. *Nucleic Acids Res* **31**, 878-85.

Preville, X., Schultz, H., Knauf, U., Gaestel, M., and Arrigo, A. P. (1998). Analysis of the role of Hsp25 phosphorylation reveals the importance of the oligomerization state of this small heat shock protein in its protective function against TNFalpha- and hydrogen peroxide-induced cell death. *J Cell Biochem* **69**, 436-52.

Rabilloud, T., Heller, M., Gasnier, F., Luche, S., Rey, C., Aebersold, R., Benahmed, M., Louisot, P., and Lunardi, J. (2002). Proteomics analysis of cellular response to oxidative stress. Evidence for in vivo overoxidation of peroxiredoxins at their active site. *J Biol Chem* **277**, 19396-401.

Ramachandiran, S., Huang, Q., Dong, J., Lau, S. S., and Monks, T. J. (2002). Mitogen-activated protein kinases contribute to reactive oxygen species-induced cell death in renal proximal tubule epithelial cells. *Chem Res Toxicol* **15**, 1635-42.

Randerath, E., and Randerath, K. (1993). Monitoring tobacco smoke-induced DNA damage by 32P-postlabelling. *IARC Sci Publ*, 305-14.

Rane, M. J., Coxon, P. Y., Powell, D. W., Webster, R., Klein, J. B., Pierce, W., Ping, P., and McLeish, K. R. (2001). p38 Kinase-dependent MAPKAPK-2 activation functions as 3-phosphoinositide-dependent kinase-2 for Akt in human neutrophils. *J Biol Chem* **276**, 3517-23.

Rane, M. J., Pan, Y., Singh, S., Powell, D. W., Wu, R., Cummins, T., Chen, Q., McLeish, K. R., and Klein, J. B. (2003). Heat shock protein 27 controls apoptosis by regulating Akt activation. *J Biol Chem* **278**, 27828-35.

Ravid, T., Sweeney, C., Gee, P., Carraway, K. L., 3rd, and Goldkorn, T. (2002). Epidermal growth factor receptor activation under oxidative stress fails to promote c-Cbl mediated down-regulation. *J Biol Chem* **277**, 31214-9.

Rea, S., Eisenhaber, F., O'Carroll, D., Strahl, B. D., Sun, Z. W., Schmid, M., Opravil, S., Mechtler, K., Ponting, C. P., Allis, C. D., and Jenuwein, T. (2000). Regulation of chromatin structure by site-specific histone H3 methyltransferases. *Nature* **406**, 593-9.

Realini, C. A., and Althaus, F. R. (1992). Histone shuttling by poly(ADP-ribosylation). *J Biol Chem* **267**, 18858-65.

Rhee, S. G. (1999). Redox signaling: hydrogen peroxide as intracellular messenger. *Exp Mol Med* **31**, 53-9.

Rhee, S. G., Chang, T. S., Bae, Y. S., Lee, S. R., and Kang, S. W. (2003). Cellular regulation by hydrogen peroxide. *J Am Soc Nephrol* **14**, S211-5.

Rhee, S. G., Kang, S. W., Chang, T. S., Jeong, W., and Kim, K. (2001). Peroxiredoxin, a novel family of peroxidases. *IUBMB Life* **52**, 35-41.

Rivera, M. I., Jones, T. W., Lau, S. S., and Monks, T. J. (1994). Early morphological and biochemical changes during 2-Br-(diglutathion-S-yl)hydroquinone-induced nephrotoxicity. *Toxicol Appl Pharmacol* **128**, 239-50.

Rogalla, T., Ehrnsperger, M., Preville, X., Kotlyarov, A., Lutsch, G., Ducasse, C., Paul, C., Wieske, M., Arrigo, A. P., Buchner, J., and Gaestel, M. (1999). Regulation of Hsp27 oligomerization, chaperone function, and protective activity against oxidative stress/tumor necrosis factor alpha by phosphorylation. *J Biol Chem* **274**, 18947-56.

Rojas, M., Yao, S., and Lin, Y. Z. (1996). Controlling epidermal growth factor (EGF)-stimulated Ras activation in intact cells by a cell-permeable peptide mimicking phosphorylated EGF receptor. *J Biol Chem* **271**, 27456-61.

Romashko, J., 3rd, Horowitz, S., Franek, W. R., Palaia, T., Miller, E. J., Lin, A., Birrer, M. J., Scott, W., and Mantell, L. L. (2003). MAPK pathways mediate hyperoxia-induced oncotic cell death in lung epithelial cells. *Free Radic Biol Med* **35**, 978-93.

Rossi, J. M., and Lindquist, S. (1989). The intracellular location of yeast heat-shock protein 26 varies with metabolism. *J Cell Biol* **108**, 425-39.

Rouse, J., Cohen, P., Trigon, S., Morange, M., Alonso-Llamazares, A., Zamanillo, D., Hunt, T., and Nebreda, A. R. (1994). A novel kinase cascade triggered by stress and heat shock that stimulates MAPKAP kinase-2 and phosphorylation of the small heat shock proteins. *Cell* **78**, 1027-37.

Sachsenmaier, C., Radler-Pohl, A., Zinck, R., Nordheim, A., Herrlich, P., and Rahmsdorf, H. J. (1994). Involvement of growth factor receptors in the mammalian UVC response. *Cell* **78**, 963-72.

Saitoh, M., Nishitoh, H., Fujii, M., Takeda, K., Tobiume, K., Sawada, Y., Kawabata, M., Miyazono, K., and Ichijo, H. (1998). Mammalian thioredoxin is a direct inhibitor of apoptosis signal-regulating kinase (ASK) 1. *Embo J* **17**, 2596-606.

Sakaguchi, K., Okabayashi, Y., Kido, Y., Kimura, S., Matsumura, Y., Inushima, K., and Kasuga, M. (1998). Shc phosphotyrosine-binding domain dominantly interacts with epidermal growth factor receptors and mediates Ras activation in intact cells. *Mol Endocrinol* **12**, 536-43.

Sakai, M., Yoshida, D., and Mizusaki, S. (1985). Mutagenicity of polycyclic aromatic hydrocarbons and quinones on Salmonella typhimurium TA97. *Mutat Res* **156**, 61-7.

Sassone-Corsi, P., Mizzen, C. A., Cheung, P., Crosio, C., Monaco, L., Jacquot, S., Hanauer, A., and Allis, C. D. (1999). Requirement of Rsk-2 for epidermal growth factor-activated phosphorylation of histone H3. *Science* **285**, 886-91.

Sato, K., Nagao, T., Iwasaki, T., Nishihira, Y., and Fukami, Y. (2003). Src-dependent phosphorylation of the EGF receptor Tyr-845 mediates Stat-p21waf1 pathway in A431 cells. *Genes Cells* **8**, 995-1003.

Schaeffer, H. J., Catling, A. D., Eblen, S. T., Collier, L. S., Krauss, A., and Weber, M. J. (1998). MP1: a MEK binding partner that enhances enzymatic activation of the MAP kinase cascade. *Science* **281**, 1668-71.

Schlessinger, J. (2000). Cell signaling by receptor tyrosine kinases. *Cell* **103**, 211-25.

Schuetzle, D. (1983). Sampling of vehicle emissions for chemical analysis and biological testing. *Environ Health Perspect* **47**, 65-80.

Schuetzle, D., Lee, F. S., and Prater, T. J. (1981). The identification of polynuclear aromatic hydrocarbon (PAH) derivatives in mutagenic fractions of diesel particulate extracts. *Int J Environ Anal Chem* **9**, 93-144.

Sebolt-Leopold, J. S., Dudley, D. T., Herrera, R., Van Becelaere, K., Wiland, A., Gowan, R. C., Tecle, H., Barrett, S. D., Bridges, A., Przybranowski, S., Leopold, W. R., and Saltiel, A. R. (1999). Blockade of the MAP kinase pathway suppresses growth of colon tumors in vivo. *Nat Med* **5**, 810-6.

Shi, Y. (2004). Caspase activation: revisiting the induced proximity model. *Cell* **117**, 855-8.

Shibata, M. A., Hirose, M., Tanaka, H., Asakawa, E., Shirai, T., and Ito, N. (1991). Induction of renal cell tumors in rats and mice, and enhancement of hepatocellular tumor

development in mice after long-term hydroquinone treatment. *Jpn J Cancer Res* **82**, 1211-9.

Shigenaga, M. K., and Ames, B. N. (1991). Assays for 8-hydroxy-2'-deoxyguanosine: a biomarker of in vivo oxidative DNA damage. *Free Radic Biol Med* **10**, 211-6.

Sieg, D. J., Hauck, C. R., Ilic, D., Klingbeil, C. K., Schaefer, E., Damsky, C. H., and Schlaepfer, D. D. (2000). FAK integrates growth-factor and integrin signals to promote cell migration. *Nat Cell Biol* **2**, 249-56.

Snyder, R., Witz, G., and Goldstein, B. D. (1993). The toxicology of benzene. *Environ Health Perspect* **100**, 293-306.

Sorkin, A., Helin, K., Waters, C. M., Carpenter, G., and Beguinot, L. (1992). Multiple autophosphorylation sites of the epidermal growth factor receptor are essential for receptor kinase activity and internalization. Contrasting significance of tyrosine 992 in the native and truncated receptors. *J Biol Chem* **267**, 8672-8.

Stokoe, D., Engel, K., Campbell, D. G., Cohen, P., and Gaestel, M. (1992). Identification of MAPKAP kinase 2 as a major enzyme responsible for the phosphorylation of the small mammalian heat shock proteins. *FEBS Lett* **313**, 307-13.

Stone, D. M., Hanson, G. R., and Gibb, J. W. (1989). In vitro reactivation of rat cortical tryptophan hydroxylase following in vivo inactivation by methylenedioxymethamphetamine. *J Neurochem* **53**, 572-81.

Strahl, B. D., and Allis, C. D. (2000). The language of covalent histone modifications. *Nature* **403**, 41-5.

Subrahmanyam, V. V., Doane-Setzer, P., Steinmetz, K. L., Ross, D., and Smith, M. T. (1990). Phenol-induced stimulation of hydroquinone bioactivation in mouse bone marrow in vivo: possible implications in benzene myelotoxicity. *Toxicology* **62**, 107-16.

Sundaresan, M., Yu, Z. X., Ferrans, V. J., Irani, K., and Finkel, T. (1995). Requirement for generation of H2O2 for platelet-derived growth factor signal transduction. *Science* **270**, 296-9.

Szegezdi, E., Fitzgerald, U., and Samali, A. (2003). Caspase-12 and ER-stress-mediated apoptosis: the story so far. *Ann N Y Acad Sci* **1010**, 186-94.

Tan, Y., Rouse, J., Zhang, A., Cariati, S., Cohen, P., and Comb, M. J. (1996). FGF and stress regulate CREB and ATF-1 via a pathway involving p38 MAP kinase and MAPKAP kinase-2. *Embo J* **15**, 4629-42.

Tavani, A., and La Vecchia, C. (1997). Epidemiology of renal-cell carcinoma. *J Nephrol* **10**, 93-106.

Thomson, S., Clayton, A. L., Hazzalin, C. A., Rose, S., Barratt, M. J., and Mahadevan, L. C. (1999). The nucleosomal response associated with immediate-early gene induction is mediated via alternative MAP kinase cascades: MSK1 as a potential histone H3/HMG-14 kinase. *Embo J* **18**, 4779-93.

Tian, W., Zhang, Z., and Cohen, D. M. (2000). MAPK signaling and the kidney. *Am J Physiol Renal Physiol* **279**, F593-604.

Tice, D. A., Biscardi, J. S., Nickles, A. L., and Parsons, S. J. (1999). Mechanism of biological synergy between cellular Src and epidermal growth factor receptor. *Proc Natl Acad Sci U S A* **96**, 1415-20.

Tikoo, K., Lau, S. S., and Monks, T. J. (2001). Histone H3 phosphorylation is coupled to poly-(ADP-ribosylation) during reactive oxygen species-induced cell death in renal proximal tubular epithelial cells. *Mol Pharmacol* **60**, 394-402.

Torres, M., and Forman, H. J. (2003). Redox signaling and the MAP kinase pathways. *Biofactors* **17**, 287-96.

Towndrow, K. M., Mertens, J. J., Jeong, J. K., Weber, T. J., Monks, T. J., and Lau, S. S. (2000). Stress- and growth-related gene expression are independent of chemical-induced prostaglandin E(2) synthesis in renal epithelial cells. *Chem Res Toxicol* **13**, 111-7.

Trump, B. F., Berezesky, I. K., Chang, S. H., and Phelps, P. C. (1997). The pathways of cell death: oncosis, apoptosis, and necrosis. *Toxicol Pathol* **25**, 82-8.

Tsutsui, T., Hayashi, N., Maizumi, H., Huff, J., and Barrett, J. C. (1997). Benzene-, catechol-, hydroquinone- and phenol-induced cell transformation, gene mutations, chromosome aberrations, aneuploidy, sister chromatid exchanges and unscheduled DNA synthesis in Syrian hamster embryo cells. *Mutat Res* **373**, 113-23.

Ushio-Fukai, M., Alexander, R. W., Akers, M., Yin, Q., Fujio, Y., Walsh, K., and Griendling, K. K. (1999). Reactive oxygen species mediate the activation of Akt/protein kinase B by angiotensin II in vascular smooth muscle cells. *J Biol Chem* **274**, 22699-704.

Van Cruchten, S., and Van Den Broeck, W. (2002). Morphological and biochemical aspects of apoptosis, oncosis and necrosis. *Anat Histol Embryol* **31**, 214-23.

van den Brink, M. R., Kapeller, R., Pratt, J. C., Chang, J. H., and Burakoff, S. J. (1999). The extracellular signal-regulated kinase pathway is required for activation-induced cell death of T cells. *J Biol Chem* **274**, 11178-85.

Veal, E. A., Findlay, V. J., Day, A. M., Bozonet, S. M., Evans, J. M., Quinn, J., and Morgan, B. A. (2004). A 2-Cys peroxiredoxin regulates peroxide-induced oxidation and activation of a stress-activated MAP kinase. *Mol Cell* **15**, 129-39.

Wada, T., Nakagawa, K., Watanabe, T., Nishitai, G., Seo, J., Kishimoto, H., Kitagawa, D., Sasaki, T., Penninger, J. M., Nishina, H., and Katada, T. (2001). Impaired synergistic activation of stress-activated protein kinase SAPK/JNK in mouse embryonic stem cells lacking SEK1/MKK4: different contribution of SEK2/MKK7 isoforms to the synergistic activation. *J Biol Chem* **276**, 30892-7.

Wagner, E., Luche, S., Penna, L., Chevallet, M., Van Dorsselaer, A., Leize-Wagner, E., and Rabilloud, T. (2002). A method for detection of overoxidation of cysteines: peroxiredoxins are oxidized in vivo at the active-site cysteine during oxidative stress. *Biochem J* **366**, 777-85.

Walisser, J. A., and Thies, R. L. (1999). Poly(ADP-ribose) polymerase inhibition in oxidant-stressed endothelial cells prevents oncosis and permits caspase activation and apoptosis. *Exp Cell Res* **251**, 401-13.

Walker, C. (1998). Molecular genetics of renal carcinogenesis. *Toxicol Pathol* **26**, 113-20.

Walker, C., Goldsworthy, T. L., Wolf, D. C., and Everitt, J. (1992). Predisposition to renal cell carcinoma due to alteration of a cancer susceptibility gene. *Science* **255**, 1693-5.

Walker, C. L. (2002). Role of hormonal and reproductive factors in the etiology and treatment of uterine leiomyoma. *Recent Prog Horm Res* **57**, 277-94.

Walles, S. A. (1992). Mechanisms of DNA damage induced in rat hepatocytes by quinones. *Cancer Lett* **63**, 47-52.

Wang, K., and Spector, A. (1996). alpha-crystallin stabilizes actin filaments and prevents cytochalasin-induced depolymerization in a phosphorylation-dependent manner. *Eur J Biochem* **242**, 56-66.

Wang, X., Martindale, J. L., Liu, Y., and Holbrook, N. J. (1998). The cellular response to oxidative stress: influences of mitogen-activated protein kinase signalling pathways on cell survival. *Biochem J* **333 (Pt 2)**, 291-300.

Wang, X., Xu, L., Wang, H., Young, P. R., Gaestel, M., and Feuerstein, G. Z. (2002). Mitogen-activated protein kinase-activated protein (MAPKAP) kinase 2 deficiency protects brain from ischemic injury in mice. *J Biol Chem* **277**, 43968-72.

Waterman, H., and Yarden, Y. (2001). Molecular mechanisms underlying endocytosis and sorting of ErbB receptor tyrosine kinases. *FEBS Lett* **490**, 142-52.

Weber, T. J., Huang, Q., Monks, T. J., and Lau, S. S. (2001). Differential regulation of redox responsive transcription factors by the nephrocarcinogen 2,3,5-Tris(glutathion-S-yl)hydroquinone. *Chem Res Toxicol* **14**, 814-21.

Wei, Y., Mizzen, C. A., Cook, R. G., Gorovsky, M. A., and Allis, C. D. (1998). Phosphorylation of histone H3 at serine 10 is correlated with chromosome condensation during mitosis and meiosis in Tetrahymena. *Proc Natl Acad Sci U S A* **95**, 7480-4.

Wilkinson, B., and Gilbert, H. F. (2004). Protein disulfide isomerase. *Biochim Biophys Acta* **1699**, 35-44.

Wonsey, D. R., Zeller, K. I., and Dang, C. V. (2002). The c-Myc target gene PRDX3 is required for mitochondrial homeostasis and neoplastic transformation. *Proc Natl Acad Sci U S A* **99**, 6649-54.

Woo, H. A., Chae, H. Z., Hwang, S. C., Yang, K. S., Kang, S. W., Kim, K., and Rhee, S. G. (2003a). Reversing the inactivation of peroxiredoxins caused by cysteine sulfinic acid formation. *Science* **300**, 653-6.

Woo, H. A., Kang, S. W., Kim, H. K., Yang, K. S., Chae, H. Z., and Rhee, S. G. (2003b). Reversible oxidation of the active site cysteine of peroxiredoxins to cysteine sulfinic acid.

Immunoblot detection with antibodies specific for the hyperoxidized cysteine-containing sequence. *J Biol Chem* **278**, 47361-4.

Wood, Z. A., Poole, L. B., and Karplus, P. A. (2003). Peroxiredoxin evolution and the regulation of hydrogen peroxide signaling. *Science* **300**, 650-3.

Yamaguchi, S., Hirose, M., Fukushima, S., Hasegawa, R., and Ito, N. (1989). Modification by catechol and resorcinol of upper digestive tract carcinogenesis in rats treated with methyl-N-amylnitrosamine. *Cancer Res* **49**, 6015-8.

Yang, K. S., Kang, S. W., Woo, H. A., Hwang, S. C., Chae, H. Z., Kim, K., and Rhee, S. G. (2002). Inactivation of human peroxiredoxin I during catalysis as the result of the oxidation of the catalytic site cysteine to cysteine-sulfinic acid. *J Biol Chem* **277**, 38029-36.

Yasuda, J., Whitmarsh, A. J., Cavanagh, J., Sharma, M., and Davis, R. J. (1999). The JIP group of mitogen-activated protein kinase scaffold proteins. *Mol Cell Biol* **19**, 7245-54.

Yeung, R. S., Xiao, G. H., Everitt, J. I., Jin, F., and Walker, C. L. (1995). Allelic loss at the tuberous sclerosis 2 locus in spontaneous tumors in the Eker rat. *Mol Carcinog* **14**, 28-36.

Yoon, H. S., Monks, T. J., Everitt, J. I., Walker, C. L., and Lau, S. S. (2002). Cell proliferation is insufficient, but loss of tuberin is necessary, for chemically induced nephrocarcinogenicity. *Am J Physiol Renal Physiol* **283**, F262-70.

Yoon, H. S., Monks, T. J., Walker, C. L., and Lau, S. S. (2001). Transformation of kidney epithelial cells by a quinol thioether via inactivation of the tuberous sclerosis-2 tumor suppressor gene. *Mol Carcinog* **31**, 37-45.

Yoon, H. S., Ramachandiran, S., Chacko, M. A., Monks, T. J., and Lau, S. S. (2004). Tuberous sclerosis-2 tumor suppressor modulates ERK and B-Raf activity in transformed renal epithelial cells. *Am J Physiol Renal Physiol* **286**, F417-24.

Yoshioka, K. (2004). Scaffold proteins in mammalian MAP kinase cascades. *J Biochem (Tokyo)* **135**, 657-61.

Zanella, C. L., Posada, J., Tritton, T. R., and Mossman, B. T. (1996). Asbestos causes stimulation of the extracellular signal-regulated kinase 1 mitogen-activated protein kinase cascade after phosphorylation of the epidermal growth factor receptor. *Cancer Res* **56**, 5334-8.

Zhang, P., Liu, B., Kang, S. W., Seo, M. S., Rhee, S. G., and Obeid, L. M. (1997). Thioredoxin peroxidase is a novel inhibitor of apoptosis with a mechanism distinct from that of Bcl-2. *J Biol Chem* **272**, 30615-8.

Zhong, S., Zhang, Y., Jansen, C., Goto, H., Inagaki, M., and Dong, Z. (2001). MAP kinases mediate UVB-induced phosphorylation of histone H3 at serine 28. *J Biol Chem* **276**, 12932-7.

Zhong, S. P., Ma, W. Y., and Dong, Z. (2000). ERKs and p38 kinases mediate ultraviolet B-induced phosphorylation of histone H3 at serine 10. *J Biol Chem* **275**, 20980-4.

Zhougang, S., and Schnellmann, R. G. (2004). H2O2-induced transactivation of EGF receptor requires Src and mediates ERK1/2, but not Akt, activation in renal cells. *Am J Physiol Renal Physiol* **286**, F858-65.

VITA

Jing Dong was born in Urumqi, Xinjiang Uygur Autonomous Region, China on 09/26/1976. She is the daughter of Aimei Liu and Guangyao Dong. After graduating from Number 1 High School in 1995, she attended the Beijing Medical University (now Peking University, Health Sciences Center) where she got her Bachelor of Science in Pharmacology in 2000. Jing then attended the graduate program in Pharmacology and Toxicology and joined Dr. Monks' laboratory in the University of Texas at Austin in 2000. In the next 3 years, Jing worked as a Graduate Research Assistant in the laboratory of Dr. Monks. She followed Dr. Monks and relocated to University of Arizona in Tucson since 2003, continuing the pursuit of her research and worked as a Senior Research Specialist in his laboratory. Jing received several scholarship and awards during her doctoral training, including the Johnson & Johnson Endowed Graduate Fellowship in Pharmacy in 2002, the Carl C. Smith Award for the third place in the Mechanisms Specialty Section of the 43th Society of Toxicology (SOT) Annual Meeting in 2004, and travel awards to attend the SOT meeting and Gordon Research Conference, Mechanisms of Toxicity in 2004.

Permanent Address: 4175 E. Ft. Lowell, Apt. 3217, Tucson, Arizona 85712.

The author typed this dissertation.